Study of light-duty gasoline vehicle cold climate NOx and particulate number emissions in real-world driving conditions

by

Ali Lotfi

A thesis submitted in partial fulfillment of the requirements for the degree of

Master of Science

Department of Mechanical Engineering
University of Alberta

© Ali Lotfi, 2021

Abstract

Cold climate Nitrogen Oxides(NOx) and Particulate Number(PN) real-world driving emission factors of a gasoline direct injection light-duty vehicle were measured using a portable emission measurement system. The vehicle was driven at the ambient temperature of $-15°C$ in a series of repeated experimentations in an urban route in the city of Edmonton in winter 2020.

The NOx emission factor that was obtained at the cold ambient temperature of $-15°C$ was 466 ± 57 mg/km, to put this number in perspective it is 7.1 times higher than the 65 mg/km Tier2 emission regulation limit for a 2008 model year car. The same car, emitted 56 ± 7 mg/km NOx emissions at ambient temperature of $+15°C$. This increase in cold temperature is attributed to an increase in friction losses, reduced fuel mixing, and catalyst light-off temperature.

The PN emission factor results were obtained at the cold ambient temperature of $-15°C$ at $(1.59 \pm 1) \times 10^{11}$ #/km. The value is 2.3 times higher than PN emission factors at an ambient temperature of $+5°C$ at $(6.8 \pm 2.4) \times 10^{10}$ #/km.

These results show the importance of using real-world driving emissions in a cold climate for NOx and particulate emissions of vehicles. A much larger emission factor obtained in cold ambient temperature and different driving behaviours shows the relative importance of research for future emission regulation fitted to the cold climate of Canadian cities.

Further steady-state driving speed and variation of driving behaviour testing showed that high instantaneous vehicle emissions cause a large sum of total vehicle emissions, although they are produced in a small fraction of driving time.

The experimental results show the NOx emission factors for constant speed test increases with increasing speed. The results show the emission factor of (35 ± 7) mg/km

for 80 km/h, (98 ± 12) mg/km for 90 km/h, (174 ± 9) mg/km for 100 km/h, and (232 ± 24) mg/km for 110 km/h. The correction factor was found that the increase of NOx with speed relates to vehicle speed squared.

Real-world driving NOx emission of the vehicle was also measured using two types of driving behaviour. The behaviour was quantified by the average positive acceleration of the vehicle over the same route. The result shows the engine spike of NOx is sensitive to the transient operating condition of the engine. The NOx increases from (67) mg/km for normal driving behaviour to 12.7 times higher to (856) mg/km for aggressive driving behaviour. The average positive acceleration for the normal driving behaviour and aggressive driving behaviour were 0.78 $(\frac{m}{s^2})$ and 2.92 $(\frac{m}{s^2})$; respectively.

Contents

List of Tables

List of Figures

Acronyms

PEMS Portable Emission Meaasurement System

EPA Environmental Protection Agency

CEPA Canadian Environmental Protection Act

NOx Nitrogen Oxide

PN Particle Number

HC Hydrocarbons

NAAQS National Ambient Air Quality Standards

OBD On-Board Diagnostic

OBE On-Board Equipment

ECM Engine Control and Monitoring

ppm parts per million

GHG Greenhouse Gas

GDI Gasoline Direct Ignition

CAC Criteria Air Contaminant

LD Light Duty

GPF Gasoline Particulate Filter

DF Dilution Factor

Chapter 1

Introduction

1.1 Research Motivation

Emissions of air pollutants decrease air quality and contribute to mortalities [16]. In a comprehensive 2019 study, about 70 million tons of pollution were emitted into the atmosphere in the United States [16]. These emissions contribute to the formation of ozone and particles, the deposition of acids, and visibility impairment[16].

Between 1980 and 2019, gross domestic product increased 182 percent, vehicle miles travelled increased 114 percent, energy consumption increased 28 percent, and the U.S. population grew by 44 percent as shown in Figure 1.1 [7].

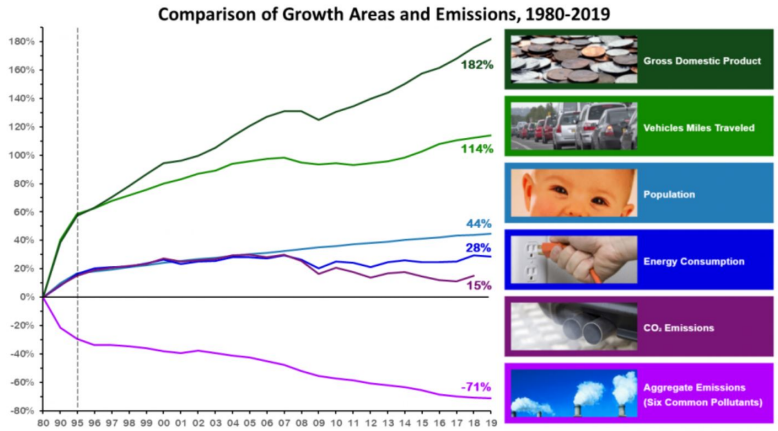

Figure 1.1: Comparison of growth areas and emissions between 1980-2019[7]

Despite great progress in air quality improvement, approximately 82 million people in the USA lived in counties with pollution levels above the primary National Ambient Air Quality Standards(NAAQS) in 2019- see Figure 1.2.

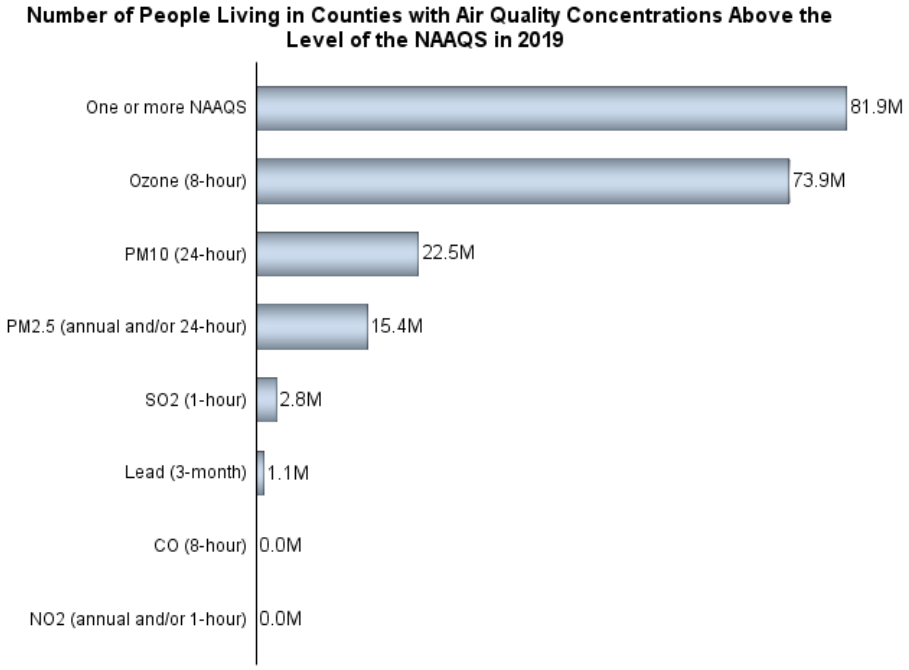

Figure 1.2: Number of people living in countries with air quality concentration above the level of the NAAQS in 2019 [7]

1.1.1 History of air pollution emission inventory in the United states

Air pollution and cars were first linked in the early 1950s by a California researcher who determined that pollutants from traffic were to blame for the smoggy skies over Los Angeles [17]. At the time, typical new cars were emitting nearly 13 grams per mile hydrocarbons (HC), 3.6 grams per mile nitrogen oxides (NOx), and 87 grams per mile carbon monoxide (CO) [18]. Since then, the U.S. Environmental Protection Agency (EPA) has set standards to regulate emissions from other mobile sources of air pollution, such as heavy-duty trucks, agricultural and construction equipment, locomotives, lawn and garden equipment, and marine engines[19].

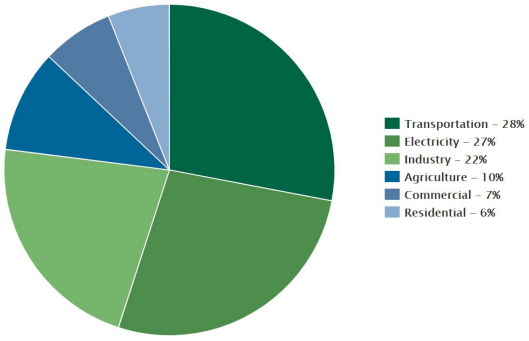

Figure 1.3: Contribution of emission sources to total emissions reported by EPA in 2018[8]

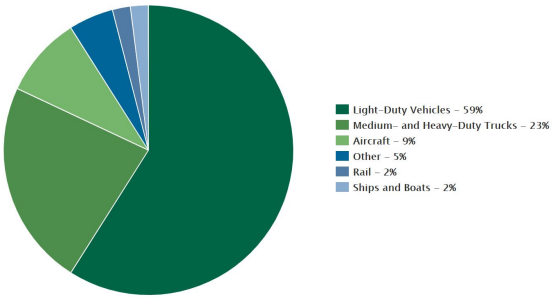

Figure 1.4: Contribution of mobile emission sources to total emissions reported by EPA in 2018[8]

The first step towards informing consumers about the gas mileage of their vehicles was done by EPA in 1971, in this way EPA began testing the fuel economy of cars, trucks, and other vehicles. Later, new cars were required to meet the amended Clean Air Act standards for the first time. In this way three-way catalysts On-board computers and oxygen sensors began to appear in most new cars to optimize the efficiency of the catalytic converter. In 2000, the EPA adopted the final rule that reduces HC and NOx emissions by 70 percent beyond the previous standards[20].

The transportation sector is one of the largest contributors to U.S. greenhouse gas (GHG) emissions as shown in Figure 1.3 and 1.4. According to the inventory of U.S. Greenhouse Gas Emissions and Since 1990–2018 , transportation accounted for the largest portion (28 percent) of total U.S. GHG emissions in 2018. Cars, trucks, commercial aircraft, and railroads, among other sources, all contribute to transportation end-use sector emissions[8]. As shown in Figure 1.5 the contribution of mobile sources in NO production has the largest number of overall emissions.

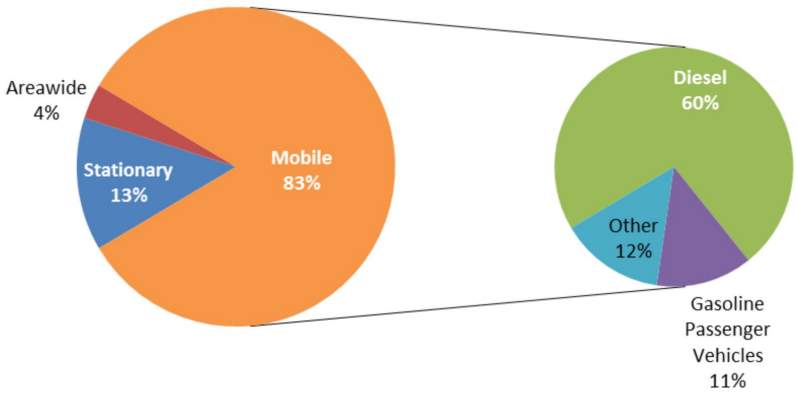

Figure 1.5: Contribution of NO emission sources to total emissions reported by EPA[9]. Right plot shows total siurces contribution of NO emission and left plot shows the contribution of mobile sources in NO emission

1.1.2 Emission inventories in Canada

The agencies charged with implementing exhaust emission standards varies, even in the same country. For example, in the United States, EPA is responsible for this. The authority to regulate emissions from internal combustion engines in Canada rests with Environment and Climate Change Canada and Transport Canada.

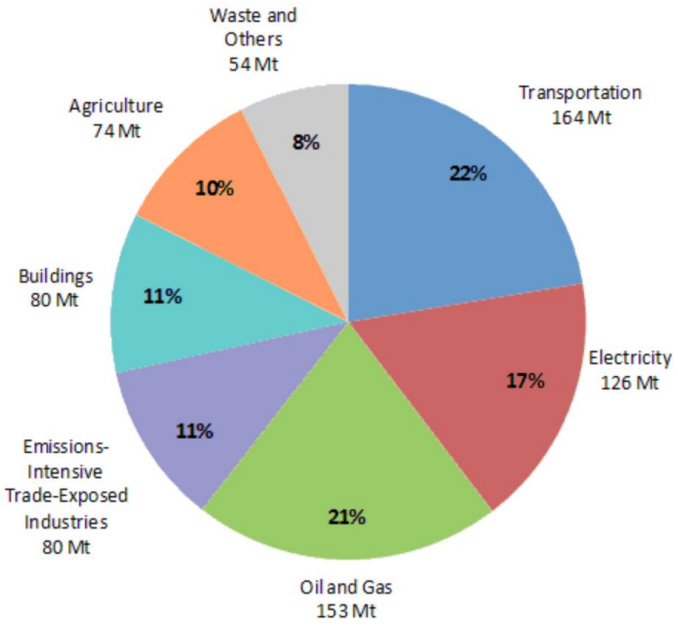

Figure 1.6: Contribution of GHG emission sources to total emissions in Canada reported by Canadian Environmental Protection Act (CEPA) [10]

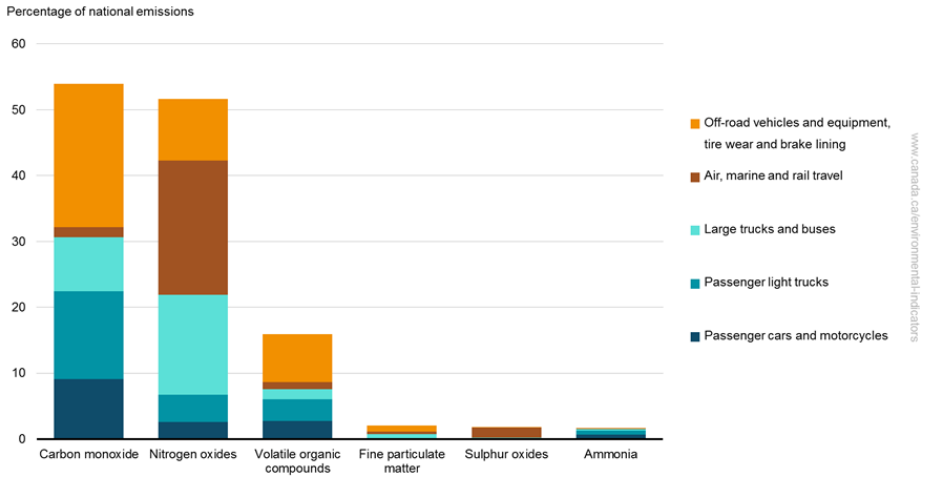

Figure 1.7: Contribution of emission sources to total emissions in Canada reported by Canadian Environmental Sustainability Indicators[11]

Under the Canadian Environmental Protection Act 1999 (CEPA 1999), Environment Canada has the authority to regulate emissions from on-road engines, as well as from most categories of off-road engines. More recently Green House Gas (GHG) have been regulated. As shown in Figure 1.6, 1.7 different sources contribute in GHG emission and the amount of contribution of each sources are shown. Regulations have been adopted to control emissions of criteria air contaminants (CAC) as well as greenhouse gases (GHG)[10].

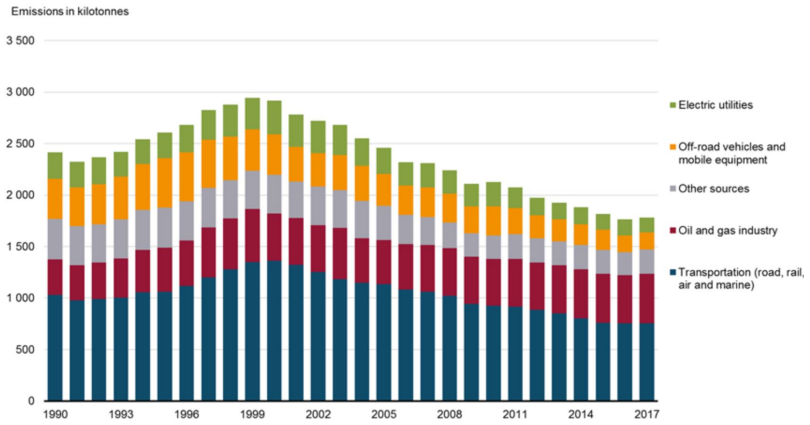

Figure 1.8: Contribution of NOx emission sources to total emissions in Canada reported by Environmental Sustainability Indicators[11]

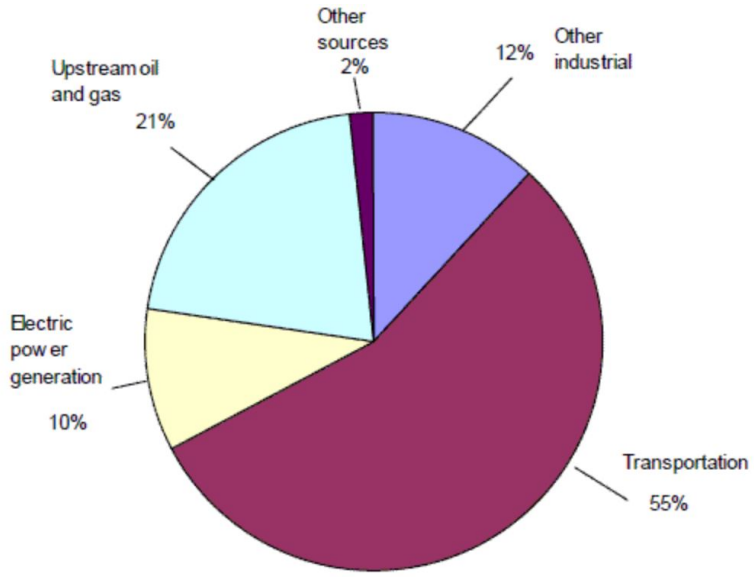

Figure 1.9: Contribution of NOx emission sources to total emissions in Canada reported by CEPA[10]

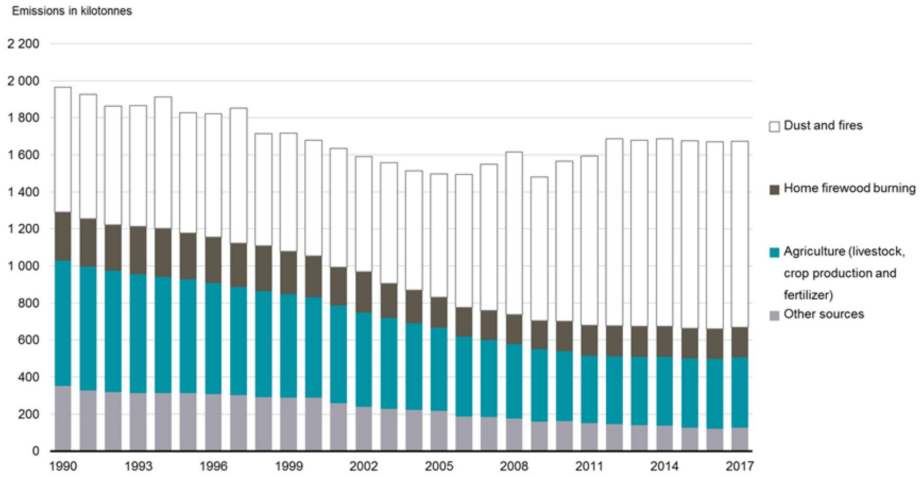

Figure 1.10: Contribution of fine particulate emission sources to total emissions in Canada reported by Environmental Sustainability Indicators[11]

In Figure 1.8 and 1.10, the contribution of NOx and particulate matter emission to total emission is provided. Figure 1.9 shows 55 percent contribution of transportation section to total NOx emission in Canada.

Under CEPA 1999, the legislative authority for controlling on-road vehicle NOx and particulate matter emissions were transferred from transport Canada to Environment Canada. The On-Road Vehicle and engine emission regulations are aligned with US EPA emission standards also which specify emission standards for motorcycles.

1.1.3 North America emission regulation studies

Here, the emission regulations and major developments in vehicular emissions regulations and technologies are discussed. The key regulatory developments, including proposed light-duty (LD) criteria pollutant tightening in the US and Europe, the continuing developments towards real-world driving emissions (RDE) standards are discussed separately with the corresponding regulations.

For example, the EPA provides emission regulations in the USA. Currently, EPA is proposing changes to the test procedures for heavy-duty engines and vehicles to

improve testing accuracy and reduce the testing. The EPA is also proposing other regulatory amendments concerning light-duty vehicles, heavy-duty vehicles, highway motorcycles, locomotives, marine engines, other nonroad engines and vehicles, stationary engines, and portable fuel containers [21].

The rapidly changing and more regulation means that the vehicle industry is faced with challenging and diverse emissions requirements. In addition to the new cutting-edge criteria pollutant regulations being phased-in starting in 2015 in California, large developing countries like China and Brazil are moving forward with their regulations. The EPA emission regulations being used in North America are released in Tiers. Tier 3 refers to a set of fuel and vehicle standards adopted by the EPA in 2014. The Tier 3 program is part of a comprehensive approach to reducing the impacts of motor vehicles on air quality and public health. The program considers the vehicle and its fuel as an integrated system, setting new vehicle emissions standards and a new gasoline sulphur standard beginning in 2017.

The vehicle emissions standards reduce both tailpipe and evaporative emissions from passenger cars, light-duty trucks, medium-duty passenger vehicles, and some heavy-duty vehicles. The gasoline sulphur standard will enable more stringent vehicle emissions standards and will make emissions control systems more effective. After implementation in 2017, these standards immediately reduced toxic air pollution from cars and trucks. Each Tier standards typically affects both fuel manufacturer companies and vehicle manufacturer[22].

Transportation is the largest single source of air pollution in the United States. By reducing transportation-related pollution, the EPA's Tier 3 standards can achieve nationwide public health benefits. According to the EPA's estimates, the Tier 3 standards will prevent up to 2,000 premature deaths, avoid up to 2,200 hospital admissions, and eliminate 19,000 asthma attacks each year by 2030 [23].

To comply with these emission regulations both light-duty and heavy-duty engines

are required to use less fuel and produce fewer emissions. Gasoline engine fuel consumption reductions of up to 30 percent versus the MPI baseline are in development, LD diesel needs to achieve a further 20 percent fuel consumption reduction despite already very efficient existing engines.

Much research and development are ongoing to reach these ambitious targets by 2030. For example, lean NOx systems are being improved and SCR system architecture is improving with better control and system layout [24]. Work on catalyst formulations and designs to achieve the NOx reductions and with a focus on low-temperature performance[25].

The development of particulate filters for diesel engines has resulted in a large reduction in particulate matter emissions [26]. Careful analyses of PM and associated emissions are becoming more difficult because the levels are so low. In applications where a choice of using filters or not using them to meet PM regulations, the PM and PN emissions are significantly lower when the filter is implemented[27].

1.1.4 Using portable emission measurement system (PEMS) for emission measurement

Despite the progress in reducing harmful emissions and CO_2 emissions of vehicles on the road due to strengthening emission regulations, there is still room to achieve even better emissions by altering and managing the vehicle driving cycle. Previous studies have shown that vehicle emission and fuel consumption are highly dependent on driving behaviour, road condition, traffic pattern and metrological conditions[28]. Laboratory to the real driving emission measurement methods can be used to measure the emission of the vehicles for an emission analysis. One of the methods that directly measure on-road emissions is the real driving emission measurement method using a PEMS system.

A PEMS is a vehicle emissions testing device that can be attached to a motor vehicle that is being driven during testing. This differs from traditional certifications done that only simulates real-world driving on the stationary rollers of a chassis dynamometer[29].

Early examples of mobile vehicle emissions equipment were developed and marketed in the early 1990s by Warren Spring Laboratory UK during the early 1990s, which was used to measure on-road emissions as part of the UK Environment Research Program[30].

Governmental agencies like the EPA, European, and various states and private entities have begun to use PEMS to reduce both the costs and time involved in making mobile emissions decisions[31].

Typically production engines, must meet the certification levels when new and tested according to the legislated testing protocols in a laboratory. However, emissions for operating conditions outside of the bounds of the laboratory test procedures are often higher than under the laboratory testing[32].

On-road testings are desirable as they more accurately reflect actual in-use emissions. Also, many more vehicles can be tested under the real driving condition as the testing can take place during the regular operation of the tested vehicles.

To test under normal operating conditions, the PEMS instruments must be small, lightweight, and able to withstand the actual environmental conditions. This emissions data is subject to considerable variances, as real-world conditions are often neither well defined nor repeatable, and significant variances in emissions can exist even among otherwise identical engines[33].

1.1.5 Emission factors difference between lab certifications and real driving emissions

A recent example of PEMS's advantages over laboratory testing is the Volkswagen (VW) Scandal of 2015. The Volkswagen emissions scandal, also known as Dieselgate or Emissionsgate, began in September 2015, when the United States Environmental Protection Agency (EPA) issued a notice of violation of the Clean Air Act to German automaker Volkswagen Group[34].

On-board software that was optimized for the certification test that VW had installed on some diesel passenger vehicles (Dieselgate scandal) were discovered using a PEMS system[35]. The discovery was uncovered using lawsuit, random, on-road evaluation and utilizing a PEMS device[36]. VW paid over US dollar 14 billion in fines and this scandal prompted new regulations in the USA. This also provided an incentive to smaller, lighter, integrated and cost-effective PEMS systems [37].

The agency had found that Volkswagen had intentionally programmed turbocharged direct injection (TDI) diesel engines to activate their emissions controls only during laboratory emissions testing which caused the vehicles' NOx output to meet US standards during regulatory testing, but emit up to 40 times more NOx in real-world driving [12]. The scandal raised awareness over the higher levels of pollution emitted by all diesel-powered vehicles from a wide range of carmakers, which under real-world driving conditions was found much higher than legal emission limits.

A study conducted by International Council on Clean Transportation (ICCT) and Allgemeine Deutsche Automobil-Club (ADAC) showed the biggest deviations from Fiat, Hyundai, Subaru, Renault and Nissan as shown in Figure 1.11, resulting in investigations opening into other diesel emissions scandals[38].

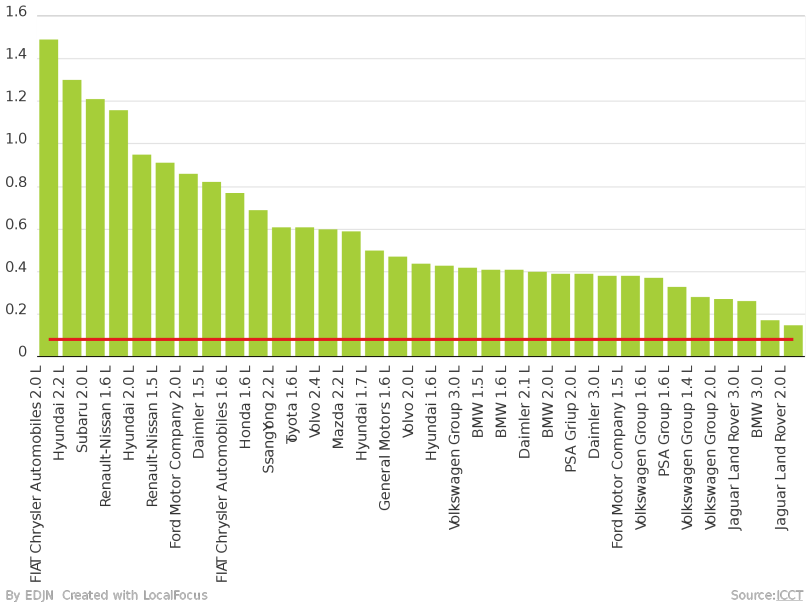

Figure 1.11: Nitrogen oxide (NOx) on-road emissions by manufacturer and capacity. Green bar: Average NOx emission (g/km), Redline: Euro 6 NOx emission limit (g/km) [12]

Since the year 2000, multiple entities have used PEMS data to measured in-use, on-road emissions on hundreds of diesel engines installed in, buses trucks, compressors, locomotives, passenger ferries, and other on-road, off-road and non-road applications. Depending on the application a variety of onboard systems are available, ranging from breadbox sized PEMS to instrumented trailers towed behind the tested truck [39]. Different engine emission components are measured with PEMS systems including hydrocarbons, carbon monoxide, NOx, particulate matter, sulphur oxide and Volatile organic compounds (VOCs) [40].

PEMS tests can also be done in different testing conditions with different goals. The transport sector is an important source of these pollutants and high pollution episodes are often experienced during the cold season. However, vehicle emissions regulation at cold ambient temperature only addresses hydrocarbons and CO vehicular emissions[41]. For that reason, this thesis focuses on the impact that cold ambient

temperatures have on gasoline spark-ignition vehicle emissions using a PEMS system.

1.1.6 Importance of cold climate vehicle emissions

The impact of cold climate on vehicle emissions has been studied by different agencies and in the literature, [42]. One example is the simulator generated by EPA. The EPA open-source MOtor Vehicle Emission Simulator (MOVES2010) is used to estimate national, state, and county-level inventories of criteria air pollutants, greenhouse gas emissions, air toxics, and energy consumption [43].

The MOVES2010 model allows users to import data specific to their unique needs and goals; however, vehicle emission factors during cold ambient conditions are not well established in the model. One study done by using MOVES2010 focuses on temperature and humidity analyzing the changes in emissions from variations of these parameters in isolation and compares the impact of each parameter on emission results by quantifying percent change in emissions[44]. One goal of this thesis is to improve their emission factors to low ambient temperatures (below $-1°C$).

Actual driving behaviour and ambient conditions strongly influence the vehicle emissions and thus, users must be knowledgeable of the input parameters and their relative sensitivity to emissions so as to accurately model them. Relevant input parameters include meteorology, vehicle population, age distributions, vehicle miles travelled (VMT), average speed distributions, road type distributions, ramp fractions, fuel supply, and I/M program parameters[45].

Ambient temperature and humidity are known to have a significant impact on most pollutant processes for on-road vehicles. In MOVES2010 simulation, temperature and humidity affect emissions mainly through temperature adjustment on emission rates[46].

For example MOVES2010 simulation, ambient temperature is varied in increments of

$10°F$ from $-40°F$ to $+120°F$ at a national scale while keeping all parameters constant except for temperature. NOx and PM result for this test is shown in Figure 1.12.

The results show that cold temperature has a substantial impact on MOVES2010 estimates of emissions. This analysis addresses the degree to which MOVES2010 estimates of emission are affected by temperature and humidity, indicating, the importance of accurately estimate these parameters in the emissions inventory when using MOVES2010. The analysis emphasizes the importance of obtaining accurate local meteorological data when using MOVES2010 [13].

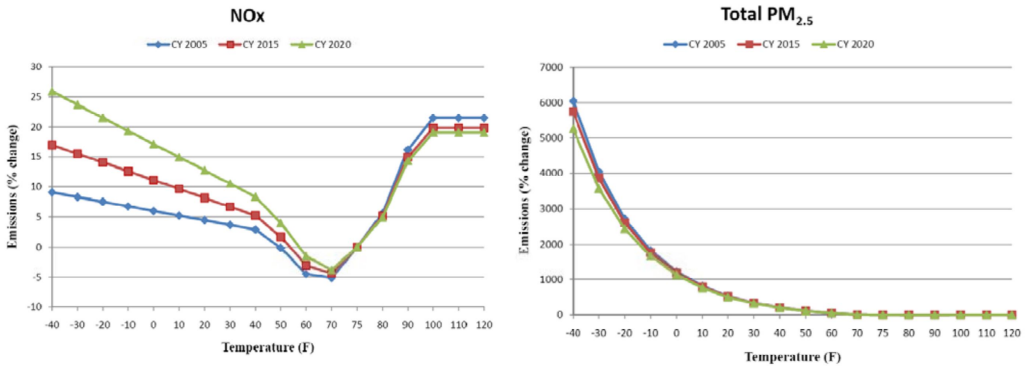

Figure 1.12: Emission change (NOx and $PM_{2.5}$) concerning temperature for gasoline vehicles in model years 2005, 2015, and 2020 done in MOVES2010 emission model. (a) NOx emission change in respect to temperature, (b) PN emission change in respect to temperature [13]

Air quality in the winter is typically associated with a higher number of pollution episodes [47]. Recent seasonal studies have shown that in some urban areas the highest levels of NOx, NH_3, CO and PN occur in the cold season which is due to higher vehicle emission and atmospheric conditions.[48]. The only emissions that are currently regulated at cold temperature are hydrocarbon and CO[49].

1.1.7 Using emission data in connected vehicles

Driving style is known to affect fuel economy and emissions [50]. The fuel consumption and atmospheric pollution emissions of vehicles depending on driving conditions, the characteristics of the driver and the vehicle. The influence of driving style on the environmental footprint of a car journey has been investigated. Driver characteristics can be determined by a Driver Behaviour Questionnaire and the observed acceleration and deceleration behaviour of the vehicle [51].

Recent studies have shown that in certain situations the driver's driving style can result in differences in terms of fuel consumption (and therefore CO_2 emissions) as much as 40 percent between a normal driver and an aggressive one [52].

Driving behaviour can vary from aggressive to normal driving style. Aggressive driving behaviour takes many forms. Typical aggressive driving behaviours include speeding, driving too close to the car in front, not respecting traffic regulations, improper lane changing or weaving.

Individual driving behaviour can strongly affect emission and GHG [53]. Eco-driving is a driving style developed since the mid-'90s and has been the subject of some initiatives and projects at the European level to define it precisely[54].

Although research projects are ongoing to update the eco-driving rules the basic characteristics of eco-driving remain the same. Investigating the effect of speed and driving style on vehicle emission using a PEMS system is also performed in this thesis. Since driving style can adversely influence emissions and fuel economy there is interest in removing the driver effect by using connected vehicle technology. Connected vehicles refer to applications, services, and technologies that connect a vehicle to its surroundings. A connected vehicle includes different communication devices (embedded or portable) present in the vehicle, which enable in-car connectivity with other devices present in the vehicle and/or enable connection of the vehicle to external de-

vices, networks, applications, and services. The introduction of new ITS technologies including wireless communication technologies, connected vehicle technologies, smart vehicle technologies, and distributed and cloud computing technologies allow a variety of new connected vehicle applications [55].

Applications of connected vehicles include everything from traffic safety and efficiency, infotainment, parking assistance, roadside assistance, remote diagnostics, and telematics to autonomous self-driving vehicles and global positioning systems (GPS). Typically, vehicles that include interactive advanced driver-assistance systems (ADASs) and cooperative intelligent transport systems (C-ITS) can be regarded as connected. Connected-vehicle safety applications are designed to increase situation awareness and mitigate traffic accidents through vehicle-to-vehicle (V2V) and vehicle-to-infrastructure (V2I) communications[56].

The current transportation system is built upon the interaction between humans and technologies. Technologies not only promote new ways of observing, monitoring, and managing transportation systems but also have the ability to change the basic characteristics of transportation in a system fundamental way. The ability to use connected automated vehicle technology to not only optimize criteria such as congestion and trip time but also emissions is important for urban air quality. The emission studies done by the PEMS system can be used to improve the emission factor of the vehicle in cold weather which in there can be used in simulation with connected vehicle systems.

Incorporating accurate emission data when using EPA air quality emission model MOVES2010 to study the correlation between drivers' driving behaviour and the distribution of the OpMode ID during each scenario [57]. Results show that the DSAS was able to induce drivers to accelerate smoothly, keep longer headway distance and stop earlier when a hazardous situation in the work zone, these driving behaviours result in a statistically significant reduction in vehicle emissions for almost all studied air pollutants [57].

1.2 Research objectives

The objective of this research is to investigate the effect of cold weather conditions and driving style on the PN and NOx emission in the real driving condition by using the PEMS system. An emission factor for the GDI engine vehicle which is accurate for ambient condition and driving conditions is obtained.

There is a lack of vehicle emission regulations for cold ambient temperature conditions and regulations only considered a limited set of emissions and do not include some important emissions like NOx and PN at cold temperatures. Current vehicle emissions regulation at cold ambient temperature only addresses hydrocarbons and CO vehicular emissions [49]. This lack of regulations means that there is also a lack of PEMS measurement at cold temperature relevant to winter conditions below $-7°C$

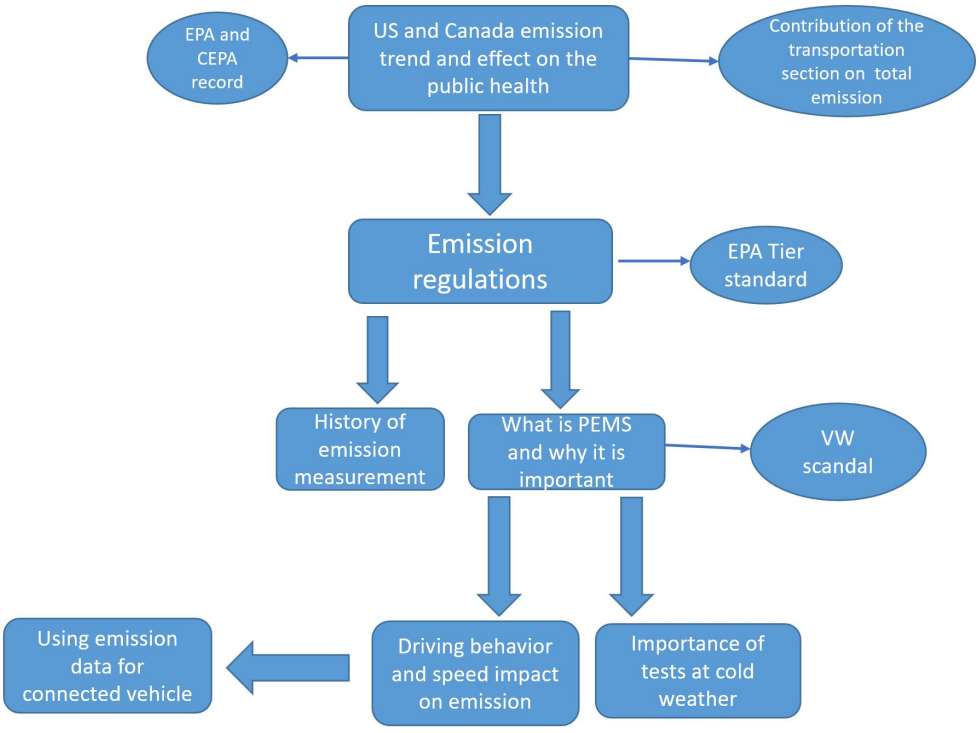

Figure 1.13: Research elements shows the motivation and objectives of this research

In the literature very limited emission tests below $-7°C$ were found. Here, tests down to $-15°C$ were performed. Tests up to $+15°C$ were also performed to investigate how the cold temperature affects vehicle emissions.

The effect of the cold ambient temperature on the emissions is known. Step one of this research is collecting data in cold weather (outside the requirement of the regulations) and comparing the results to the emission regulations.

There is a lack of research for NOx and PN emissions in cold weather as many studies focus on CO and CO_2 [49]. Recent studies indicate that NOx and PN emissions affect human health through air quality. Thus, in this research, the focus is on measuring NOx and PN data using real driving emissions by a PEMS system. However, emissions change for different, ambient temperatures are investigated.

The effect of speed and driving style on the emissions is also investigated. For these, different speeds and driving styles tested in this research the vehicle and emission data is collected by the vehicle and PEMS systems.

1.3 Thesis outline and contribution

In this research, a PEMS system is used to measure on-road vehicle emissions for various conditions. This thesis has five chapters. This chapter reviews the relevant background and motivation and provides an introduction to the PEMS system and real driving emission tests. The method and motivation are described.

In the second chapter, a literature review including the PEMS system is provided. Studies related to the effect of ambient temperature and driving style measuring NOx and PN emission are also provided. The experimental setup is given in chapter 3. The experimental setup is described in detail and a schematic of the testing PEMS system is provided. The integration and data synchronization of the devices is given

and an example of data calculation for NOx and PN is given. The error analysis and uncertainty are also detailed in chapter 3.

In chapter 4, experimental results are provided. The results are divided into these three different parts: which very the following: (1) ambient temperature; (2) vehicle speed and (3) driving behaviour. Vehicle emissions and vehicle data are collected. To understand test variation, each set of tests are repeated and a discussion of the results is given.

Finally, chapter 5 summarizes the main conclusions of this work and possible future works that are beyond the scope of this research are briefly discussed. The contribution of this thesis is the use of the PEMS system to measure emissions at cold temperatures. In particular, a laboratory-grade PN system was used in a vehicle along with a production NOx sensor.

Real driving emission tests are reported at colder temperature conditions than previously reported in the literature. The emission tests were done down to $-15°C$ ambient temperature and results for cold ambient temperature showing measured emissions provide a motivation to consider emission regulation for this kind of weather to reduce emissions.

Finally, NOx and PN emission factors for the tested car at different temperatures and driving conditions were obtained. This can be compared with existing emission regulations and air quality models to improve their parameterization for cold ambient conditions.

Chapter 2

Literature Review

Increasing the number of vehicles driving in the streets makes the fact of studying the precise amount of exhaust emission more important. Recently lots of studies are done in decreasing harmful emissions and CO_2 footprint of vehicles on the road, however, there is still room to even achieve better emissions by studying the emission especially NOx and PM/PN more accurately and measuring the emission and in real driving conditions [58, 59].

Recent investigations demonstrated that real-world emissions usually exceed the levels achieved in the laboratory-based type approval processes[29, 60]. This shows a difference between results achieved by laboratory and RDE tests. This leads to the real driving emission(RDE) tests and using a PEMS device to obtain the exact amount of emission data about a vehicle in real driving conditions [61].

Many factors may impact the emission data collected during PEMS/RDE tests. Doing tests in the real driving condition provides a wide range of opportunities for emission tests. In this chapter, research on PEMS/RDE is discussed.

2.1 Studies on the effect of ambient temperature on the vehicle's emission

One of the conditions of the PEMS tests is investigating the effect of ambient temperature on exhaust emissions. Tests have been done in different cities with different weather conditions, done. The temperature range for these tests was limited to $-7°C$ to $+23°C$.

The impact that cold ambient temperatures have on Euro 6 diesel and spark ignition is studied in [49]. In this paper, it is discussed that EU vehicle emissions regulation at cold ambient temperature only addresses hydrocarbons (HC) and CO vehicular emissions. However, HC, CO, NOx, NH_3, N_2O, CO_2 and particulate matter emissions affect air quality, global warming and human health. For that reason, the impact that cold ambient temperatures on Euro 6 diesel and spark ignition vehicle emissions using the World-harmonized Light-duty Test Cycle at $-7°C$ and $+23°C$ was investigated [49]. Results showed that emissions disproportionally increased when vehicles were tested at cold ambient temperature ($-7°C$). High solid particle number (SPN) emissions were measured from gasoline direct injection (GDI) vehicles and gasoline port fuel injection vehicles. However, only diesel and GDI SPN emissions are currently regulated. Results show the need for a new, technology-independent, procedure that enables the authorities to assess pollutant emissions from vehicles at cold ambient temperatures.

To investigate the effect of ambient temperature, regulated and non-regulated pollutants were measured over different test cycles and ambient temperatures in the laboratory and different on-road routes driven[62]. In this study regulated and non-regulated pollutants were measured over different test cycles and ambient temperatures ($+23°C$ and $-7°C$) in the laboratory and different on-road routes are driven normally or dynamically and up to 1100 m altitude. The results showed that under

certain conditions high emissions of some pollutants were measured (total hydrocarbons emissions at $-7°C$, high CO during dynamic RDE tests and high NOx emissions in one dynamic RDE test). The particle number emissions, even including those with a particle size below 23 nm, were lower than 6×10^{10} (#/km) under all laboratory test cycles and on-road routes, which are less than 10 percent of the current laboratory limit (6×10^{11} #/km)

In [63] it is discussed that performing emissions testing outside a laboratory setting immediately raises the question of the impact of ambient conditions, especially temperature, on the results. In the spirit of RDE legislation, a wide range of ambient temperatures are permissible, with a correction of the results only permissible for ambient temperatures. Within the standard range of temperatures, $0°C$ to $+30°C$, no correction for temperature is applied to emissions results and the applicable emissions limits have to be met.

The recent trends in cold-start emissive behaviour with the impact of changes in ambient temperature over the advanced technology GDI and PFI vehicles are studied in [64]. This research surveys the approaches taken to reduce engine-out emissions and tailpipe emission challenges during cold-start and transient operation using new technology. It was found that ambient temperature had a significant influence on cold start emissions. The result showed some exhaust emissions increased by 10 times as the temperature varied from $+30$ °C to $-7°C$ and fuel consumption increased as well.

The emission characteristics of light-duty vehicles in real-road driving Conditions in Korea are investigating [65]. The driving cycles of the US or Europe have been used in emission certification for Korean light-duty vehicles, despite the fact that it is not known how well these driving cycles reflect real driving patterns in Korea. This provides motivation to estimate vehicle emissions based on the real road driving conditions to raise the effectiveness of vehicle emission regulation in Korea. Real driving emission measurements were conducted for three Korean light-duty vehicles

with PEMS. The driving routes consisted of urban, rural and motorway in Seoul and Incheon. The data were analyzed with various averaging methods including a moving averaging windows method and compared to emission limits set with emission certification modes applied to tested vehicles.

The nitrogen dioxide (NO_2) pollution in urban areas of Europe is partially attributed to the increasing market penetration of diesel cars that show higher distance-specific nitrogen oxides (NOx) emissions than gasoline cars[66, 67]. The European Commission intends to also introduce PEMS based procedures to ensure that emissions are regulated based on [68]

2.2 Studies on the effect of driving behaviour/cycles on the emission

One of the factors that impact the amount of emission is the driving cycle. PEMS system gives us this opportunity to study these driving methods in real driving conditions.

In [69] a comprehensive study focusing on the events of high instantaneous NOx emissions produced under real driving is presented. Additionally, the relationships of these events with different parameters measured using PEMS were determined. Three Euro 6b diesel passenger cars with exhaust gas recirculation (EGR), lean-burn NOx trap (LNT) and selective catalytic reduction (SCR) were tested based on the real driving emissions (RDE) regulation. The results show that high instantaneous NOx emissions represent a large fraction of total NOx emissions, although they are produced during a small percentage of driving time. Somehow eliminating these high NOx emissions could reduce emissions by 30-82 percent. The emission of high instantaneous NOx emissions are related to characteristic speed modes of urban, rural and

motorway sections, and are primarily produced in a narrow engine speed in engine transients conditions. In general, the probability of producing high instantaneous NOx emissions increases as the engine speed, the exhaust gas temperature or the vehicle speed is increased.

A comparison of the NOx emissions from light-duty diesel vehicles measured from on-road tests was detailed in [70]. Real-driving NOx emissions using PEMS were measured under the urban, rural and motorway road traffic conditions. On-road tests were repeated in the summer, fall and winter seasons with an accumulated driving distance of more than 1,200 km per each vehicle. Route average NOx emission factors were compared among nine route-season combinations. The emission characteristics of each combination were investigated using time series mass emission rates and vehicle operation-based emission rates and activities. It was concluded that the emission rates and activities under low speed operating conditions should be managed to reduce urban-summer NOx. From a NOx control strategy perspective.

In a similar study [71], the differences in NOx emissions between standard and non-standard driving and vehicle operating conditions are quantified, and the amount of NOx emissions was estimated to see how much they exceed the legislative emission limits under typical Korean road traffic conditions. Twelve Euro 3–5 light-duty diesel vehicles (LDDVs) manufactured in Korea were driven on a chassis dynamometer over the standard New European Driving Cycle (NEDC) and a representative Korean on-road driving cycle (KDC). NOx emissions, average speeds and accelerations were calculated for each 1-km trip segment so-called averaging windows. The results suggest that the NOx emissions of the tested vehicles are more susceptible to variations in the driving cycles than to those in the operating conditions.

In [72] an analysis of exhaust emissions in vehicles with gasoline engines according to current RDE test procedures is presented. The compliance of test parameters (on chosen test routes) was evaluated against the requirements of the standard and dynamic

parameters were determined characterizing the trips (among others – the product of speed and positive acceleration). Time ranges of respective trips were analyzed in coordinates – vehicle's speed vs acceleration; based on that a matrix was developed that allows for comparing trips not only based on averaged parameters (e.g. average speed, stoppage time, etc.) but also all conditions of the vehicle's operation during the road test.

2.3 Use of PEMS to measure particle number

Recently, real-driving emissions (RDE) test procedures have been introduced in the EU to evaluate particulate number (PN) emissions from passenger cars during on-road operation[73, 74]. These tests procedures apply to passenger cars powered by diesel, gasoline, Liquefied Petroleum Gas (LPG), Compressed Natural Gas (CNG) and hybrid-electric powertrains vehicles[75]. The goal is to reduce both emission and fuel consumption[76]. These are a broad range of experimental test conditions that may affect exhaust emissions such as road conditions[77] are possible to make the RDE test reflect real driving.

The effect of particulate filters is also studied in PEMS tests. In [78] the on-road gaseous and particulate emissions from three current technology gasoline direct injection (GDI) PEMS were assessed. Two vehicles were also retrofitted with catalyzed gasoline particulate filters (GPFs). All vehicles were tested over four routes with different topological and environmental characteristics, representing urban, rural, highway, and high-altitude driving conditions. The results showed strong reductions in particulate mass (PM), soot mass, and particle number when fitted with the particulate filters.

PN assessment was performed in several ways including using RDE/PEMS system [79]. In Europe, PEMS testing is currently applicable to gaseous emissions only, but

the introduction of solid particle number (SPN) PEMS is under discussion for heavy-duty vehicles. Although SPN PEMS testing is required for light-duty vehicles, the robustness and the accuracy of the systems for the different conditions of heavy-duty vehicles. These tests were conducted by heavy-duty vehicle manufacturers in Europe which the results showed that the PEMS measure within 40–65 percent of the laboratory standards with only minor robustness issues [79].

For many urban centers, PN is studied to assess air quality. One of these cities is Stockholm [80] where a three-dimensional dispersion model for the urban area of Stockholm (35×35 km) is used to assess the spatial distribution of number concentrations of particles in the diameter range of 3–400 nm. A typical background number concentrations in Stockholm is 10000 cm^3, while levels three times higher close to a major highway outside the city and seven times higher within a high traffic street canyon site in the city center are observed.

Although heavy-duty Vehicles (HDVs) represent a small part of the overall vehicle population they have been identified as one of the most important contributors to air pollution [81]. This is one of the reasons why HDV emissions regulations are becoming more and more stringent worldwide. For example, Europe introduced the Euro VI standard which includes more stringent emission limits for hydrocarbons, PM and NOx, and for the first time a limit for solid PN emissions was set. Research of five HDVs, including four trucks and one bus, were tested on-road under typical driving conditions [82]. A breakdown of the emissions to low, medium, and high-speed conditions was also performed to investigate the performance of aftertreatment systems under different speed conditions. In a similar study, the PN emissions of a diesel vehicle on the road and in the laboratory were measured by considering the condition of using regeneration events[83].

2.4 Use of PEMS to measure NOx

Despite the strengthening of vehicle emissions standards and test methods, nitrogen oxide (NOx) emissions from on-road mobile sources are not being notably reduced [84]. The introduction of RDE regulations is expected to reduce the discrepancy between emission regulations and actual air pollution. A focus on analyzing the effect of different data measurement and analysis methods (i.e. cold-operation, road grade, trip selection and driving style) on CO2 and nitrogen oxides (NOx) emissions based on RDE tests are essential [84, 85].

It is mentioned in [86] that a portable emission measurement system (PEMS) was applied to carry out CO and NOx emissions test on conventional roads for a light-duty gasoline vehicle (Toyota Levin) and a heavy-duty diesel vehicle (KING LONG bus) in Nanjing to provide an RDE basis for the formulation of China automotive test cycle (CATC). The results showed that in terms of NOx emission rate, as the vehicle speed increased, the NOx emission rates increased. The CO and NOx emission factors showed similar patterns.

CO2 and NOx emissions from 149 Euro 5 and 6 diesel, gasoline and hybrid passenger cars were compared using a PEMS [87, 88]. The vehicle models used represent 56 percent of all passenger cars sold in Europe in 2016. It is found that gasoline vehicles had CO2 emissions 13–66 percent higher than diesel.

Simultaneous measurements of fuel consumption, driving patterns, and CO2, CO, and NOx emission factors for diesel passenger buses under real operating conditions in high-altitude cities and mountainous regions with an average road grade of 4 percent is reported in [89]. These measurements were obtained using a PEMS monitoring a sample of 15 buses during eight months of daily operation.

On-road tests were conducted in real traffic conditions, within and outside the boundary conditions of the regulated European RDE test in [90]. NOx, PN, CO, HC, and

CO_2 emission factors were developed considering the whole cycles, sub-cycles, and the first 300s of each test to assess the cold start effect.

2.5 Emission regulation using PEMS

The recently introduced RDE light-duty vehicle emissions regulation requires testing with PEMS during vehicle type approval and in-service conformity [91]. An inter-laboratory correlation PEMS of systems took place in Italy in 2017. Eight laboratories measured exhaust emissions from a Euro 6 gasoline vehicle with a PEMS installed in it. In addition, the individual PEMS also were compared to the regulated laboratory method (bags from the dilution tunnel).

The solid particle number method was introduced in the European Union (EU) light-duty legislation for diesel vehicles to ensure the installation of the best available technology for particles [92–94]. RDE testing on the road with PEMS for particle number (and NOx) during type approval and in-service conformity testing was recently (in 2017) introduced for light-duty vehicles. This is also under discussion for heavy-duty vehicles in-service conformity testing so it is required to understand existing legislation regarding solid particle number and discuss the on-going activities at the EU level.

To strengthen emissions regulations to minimize the differences between on-road and laboratory emission levels in some cases, PEMS testing, including solid particle number (SPN), was introduced for the type-approval of light-duty vehicles in Europe in 2017 and for in-service conformity in 2019 [95]. The heavy-duty evaluation phase at a single lab and later at various European laboratories revealed higher measurement differences due to the small particle size of the generated particles and their high charge at elevated temperatures. This issue, along with robustness at low ambient temperatures, was addressed by the instrument manufacturers bringing the measure-

ment uncertainty to the 50 percent levels.

In the future assessment of 10-nm PN, PEMS for regulations will be considered[96]. EU regulation also includes a PEMS based test at type approval, followed by in-service conformity (ISC) testing [97]. There, the Euro VI emission standards for heavy-duty vehicles (HDVs) introduce limits for PN and NH_3 emissions. EU regulation also includes a PEMS based test at type approval, followed by in-service conformity (ISC) testing. The analyses revealed that up to 85 percent of the NOx emissions measured during the tests performed are not taken into consideration if the boundary conditions for data exclusion set in the current legislation are applied [97].

2.6 Studies on the effect of cold start using PEMS

Cold-start operation is an important factor affecting vehicle emissions from gasoline direct injection (GDI) and port fuel injection (PFI) vehicles[64]. The analysis of the cold start emissions level is particularly important because it typically occurs mainly in urban areas in the immediate vicinity of people[98].

In [99], two independent analyses that were conducted to support the inclusion of cold-start emissions in the RDE test procedure are documented. First, the results of a scoping review on cold-start frequencies and trip distances in Europe are presented. Then a scenario analysis that aims to quantify the impact of modifications in the RDE data pre-processing and evaluation on the calculated NOx emissions over the urban part of an on-road test is discussed.

2.7 Discussion of literature review

Cold climate vehicular emissions have not been comprehensively studied. Several vehicle studies were done in mild to low climate temperature [49]. Many more have

focused on cold start emissions but not necessarily on cold ambient conditions [64]. Current emission regulations have a minimum climatic temperature test in a controlled laboratory environment that goes down to $+20°F$ or $-7°C$. However, many cities around the world have a colder ambient temperature for a significant fraction of the year. Additionally, both EU and US emission regulations for cold climate laboratory tests have typical requirements of HC, CO, CO_2 emissions [49]. However, NOx and fine particulate are also important in a cold climate [62]. While particulate mass has consistently appeared in all diesel vehicle emission regulations both in EU and US, particulate number limit values were just recently added to EU regulations for Euro 6 diesel and Euro 6 GDI engines.

While chassis dynamometer controlled laboratory tests have been widely used for emission testing, the VW scandal [35] and many other studies show that there are large discrepancies between laboratory defined-cycles emission testing and real-world driving emissions [12]. For this the same reason, RDE testing is now part of EU regulations. The above review of the relevant literature showed a knowledge gap in cold climate NOx and PN testing of vehicles using the PEMS-RDE method. The unique location of the University of Alberta in the City of Edmonton at moderate altitude, cold climate, and a population of more than 1 million provides an opportunity to study RDE emission for use in future air quality models.

Chapter 3

Experimental Setup

In this chapter, the experimental setup used in this research is described in detail.

3.1 General setup

A PEMS system consisting of a NOx sensor, particle number sensor for exhaust emissions while vehicle engine operating data from OBD and GPS is obtained. The data is synchronized by programs written for this thesis. All the equipment is installed in the 2008 Toyota highlander car.

The PEMS system used in this research is not a commercial system. It is a custom-made system with a system schematic shown in Figure 3.1. This system measures NOx, and particulate. GPS and OBD variables during the real driving tests on the road are also measured.

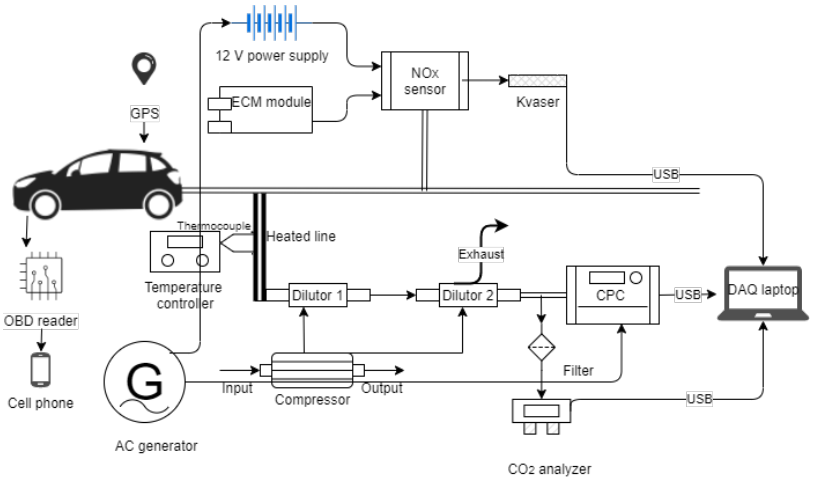

Figure 3.1: Schematic of custom made PEMS that shows sampling line, sensors and power systems. GPS and OBD reader also shown.

Figure 3.2: A picture of experimental setup inside 2008 Toyota highlander car

A custom PEMS system shown in Figure 3.2 used in combined several components that are put together and require more space than a commercial system. The setup consists of four main parts which are: the NOx sensor, the particle measurement, the ECU and the GPS. The components needed and the measured values for these

four components are summarized in Table 3.1. Next, the details of the four parts are given.

Table 3.1: PEMS four main parts: measured values and components

System features	**PN**	**NOx**	**GPS**	**OBD**
Measured values	Particle number concentration	NOx concentration	Position, speed	Mass air flow rate, Engine torque, Speed, Engine RPM, Fuel/Air ratio
Components	CPC device, Compressor CO_2 sensor, Heated line, Temperature controller, Two stages of dilution	Power supply, ECM, Kvaser CAN interface	OBU device	Vepeek OBD device

The tested vehicle used in this research shown in Figure 3.3 is a Toyota highlander model 2008 with a GDI engine and TWC and EGR in the exhaust without GPF. The engine of this car is a 3.5l V6 gasoline engine with 270 hp at 6200 rpm power and a four-wheel-drive drivetrain. The transmission of this car is a 5-speed automatic transmission with manual mode. This vehicle belongs to Transport Canada and is used by the Centre for Smart Transportation (CST) at the department of civil engineering at the University of Alberta. The mileage of this vehicle is about 30,000 km.

Figure 3.3: Toyota highlander model 2008 used in this research

The particle measurement system shown in Figure 3.1 includes a CPC device which uses 120V power and is directly connected to the generator. To collect emission from exhaust CPC is required to be connected to a heated line and sample emission through heated line which connects to exhaust through a hole made on exhaust shown in Figure 3.4. This is because of the requirement of eliminating water from the exhaust sample and import dry air to the CPC to be able to measure particles. The heated line temperature is controlled by a temperature controller and the temperature is set to $+200°C$.

The other part of the particle measurement system is the dilution system which includes 2 stages of dilution that provide around 100 times dilution factor. The dilution factor depends on the diluter pressure and is a time series value which is calculated in Section 3.4. To calculate dilution factor CO_2 before and after dilution. To measure CO_2 after dilution a CO_2 analyzer is used after heated line and a fraction of emission sample goes to CPC and the other fraction goes to the filter and then to CO_2 analyzer.

The NOx sensor shown in Figure 3.1 includes a module that controls the sensor. This

module needs 12V power which is provided by a power supply that is connected to the generator. The sensor collects data from the exhaust through the sampling access that is made on the exhaust shown in Figure 3.4 For logging data from NOx sensor to the laptop Kvaser CAN interface is used that connects to laptop through USB and logs data.

A GPS and Vehicle On-Board Equipment (OBE) device is used and connected to the vehicle and uses 12V power and logs data to the laptop through wi-fi. Also for OBD reading a Vepeek OBD reader is used that is connected to the OBD port of the vehicle and logs data to the cell phone through Bluetooth.

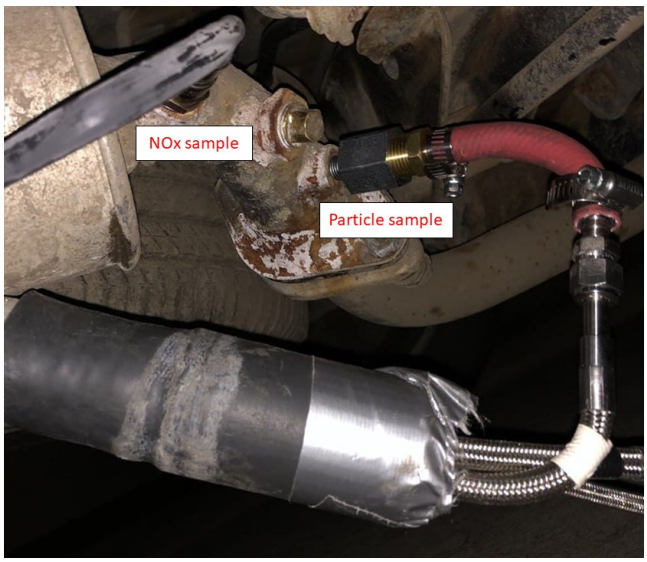

Figure 3.4: Tailpipe of the Toyota highlander car and holes mounted on it for emission collection

3.1.1 PN measurement system

Particle number measurement system includes condensation particle counter device, dilution system, CO_2 sensor and the heated line which is described in detail here.

CPC (condensation particle counter):

Magic 200 WCPC device has been used to measure particle number and is a mod-

erated aerosol growth with an internal water cycling device. The MAGIC-200 is a self-sustaining, water-based condensation particle counter that utilizes a three-stage "moderated" condensational growth system, with a continuous wick.

As in all condensational particle counters, the MAGIC-200 enlarges ultrafine particles through condensation and then detects them optically. Unlike conventional counters, the MAGIC-200 has no internal water reservoirs, and thus it tolerates tipping and vibration. Once the wick is wetted it operates using water that is extracted from the sampled air stream or is recovered internally within the wick. If operated with the Inlet Humidifier, it will sustain many weeks of operation without servicing [1].

In this device, the condensational growth is provided by the growth tube which consists of a single, wet-walled channel with laminar flow passing through three temperature regions. During operation, the sampled aerosol is first cooled and humidified by the initial conditioner stage. Flow then passes into the warm, wet-walled initiator stage where it becomes supersaturated, initiating condensational growth. This supersaturation is created due to the diffusive transport of water vapour from the warm, wet initiator walls, which occurs more rapidly than the flow warms.

The higher the temperature difference between the initiator and conditioner stages the higher the supersaturation, and the smaller size of particle size that may be activated. Condensational growth continues in the subsequent cooler moderator stage, which removes both water vapour and heat while maintaining the supersaturated conditions.

Provided the Inlet Humidifier is attached, MAGIC 200 can be operated in a fully self-sustaining mode through control of the moderator temperature. MAGIC 200's moderator temperature is controlled based on the measured input dew point, which deliberately errors on the side of letting slightly more water vapour escape with the exiting flow than enters with sample flow. In this mode, the wick will run wet and the MAGIC 200 has a small solenoid pump to remove excess wick water.

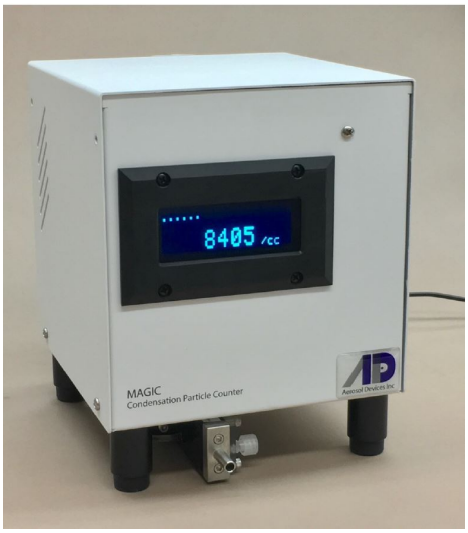

Figure 3.5: Magic 200 WCPC device[1]

In figure 3.5 the Magic 200 WCPC is shown and in Table 3.2 the specification of this device is provided.

Table 3.2: Magic 200 WCPC module specifications[1]

Power supply	12 VDC
Measured parameter	Airborne particle number concentration
Particle size range	5 nm to 2.5 μm
Sample flow rate	Nominal 300 cm^3/min
Averaging time	User selectable between 1 second to 30 minutes
Operating fluid	Distilled water
Communications	RS-232 and USB, digital pulse BNC
On board data storage	125000 records, approximately 1 week of 5-s averaged data
Orientation	Insensitive to tipping, shock or vibration. Upright orientation recommended for long-term operation
Weight	2.4 kg, with humidifier and power supply.
Dimensions	LWH 18.5 cm $\times$ 16.5 cm $\times$ 21 cm

Heated line and dilution system:

As the CPC device requires a dry air to be imported in and measure the particle, it is required to use a heated line that connects to the exhaust and the sample emission come through a heated line that removes all water exists in the sample emission comes from exhaust. This heated line has almost 2m length and is controlled by a temperature controller that keeps the temperature of heated line to a constant value. For this research the temperature is set to $+200°C$, the power used by heated line is as high as 1kW.

The other component of this particle measurement system is dilution system. As the allowable range that can be measured by CPC is lower than the range of the exhaust particle, it is required to use dilution that brings the exhaust particle in the range of CPC device. The diluter model used in this research is Dekati DI-1000 shown in Figure 3.6. The specification of this diluter is given in Table 3.3. To provide gauge pressure for this dilutor a compressor that generates 2 bar gauge pressure is connected to input port of dilutor.

Figure 3.6: Dekati DI-1000 dilutor schematic [2]

Table 3.3: Dekati DI-1000 dilutor specification [2]

Sample aire flow (inlet)	7 lpm
Diluted sample flow(outlet)	45 lpm
Dilution factor	1:8 (Available up to 1:50)
Dilution air pressure	2 bar gauge
Sample temperature tange	$0 - 450°C$
Weight	2.8 kg

In this research two stages of dilution are used that provide approximately a 100 times dilution factor. After the dilution, the diluted emission goes to the CPC to measure particle number.

To calculate the dilution factor, the CO_2 concentration before and after dilution is used. Before the dilution upstream CO_2 is obtained from the combustion equation which will be described in section 3.4.

To measure CO_2 after dilution a CO_2 analyzer is used after heated line and one part of emission sample goes to CPC and the other part goes to the filter and then to CO_2 analyzer. The CO_2 analyzer used in this research is LI-COR 850 gas analyzer shown in Figure 3.7. The specification of this gas analyzer is given in Table 3.4.

Figure 3.7: LI-COR CO_2 analyzer device [3]

Table 3.4: LI-COR CO_2 analyzer specification [3]

Measurement range	0 to 20,000 ppm
Accuracy	Within 1.5
Lower limit of detection	1.5 ppm
Output rate	Up to 2 measurements per second
Measurement principle	Non-Dispersive Infrared
Measurement principle	Non-Dispersive Infrared
Pressure compensation range	50 to 110 kPa
Maximum gas flow rate	1 liter/min
Input voltage	1.2 A @ 12 VDC (14 W) maximum

This gas analyzer connects to laptop with USB and the data is recoreded through the specific software designed by LI-COR company. The configuration of this software is shown in Figure 3.8.

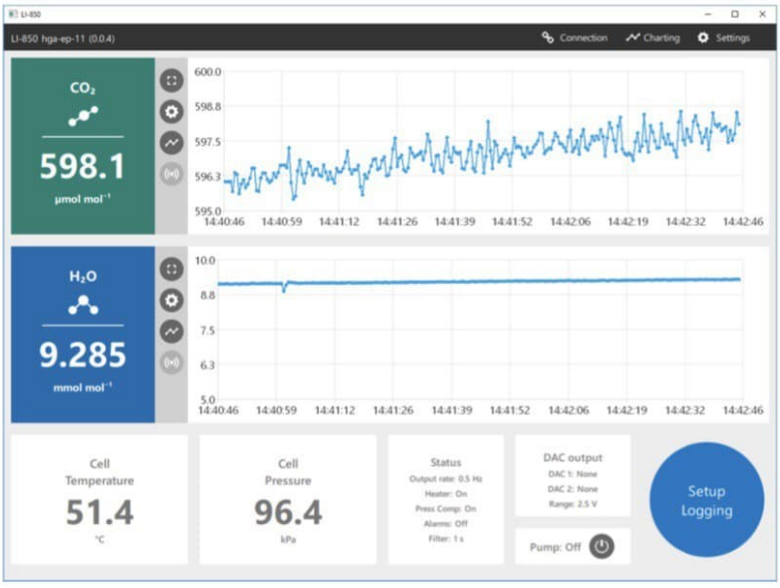

Figure 3.8: LI-COR CO_2 analyzer configuration tool [3]

3.1.2 NOx setup

NOx system includes ECM NOxCANt sensor, power supply and Kvaser CAN interface which is described in detail here.

ECM NOx sensor

The ECM NOxCANt, Type T Module (NOxCANt) is an integrated NOx, and O2 measurement module for the development of all engines, combustion systems, and their after-treatment systems.

The NOxCANt uses a ceramic NOx sensor that is mounted in the exhaust and is a production Bosch NOx sensor. The sensor is connected via a CAN to the ECM measured system and through the CAN port. The sensor is shown in Figure 3.9 and the module specification of this sensor is given in Table 3.5.

The CAN node identification can be programmed by the user allowing multiple NOx modules on the same bus. Fuel H:C, O:C, and N:C ratios can be programmed. NOx sensors used with the module have memory chips in their connector where calibration information is stored. This allows the sensors to be recalibrated (zero, span) by using a standard gas flow bench [14]. PC software to set-up, control, calibrate, and view outputs and sensor parameters is included (requires CAN adapter, not included).

Figure 3.9: ECM NOxCANt sensor [4]

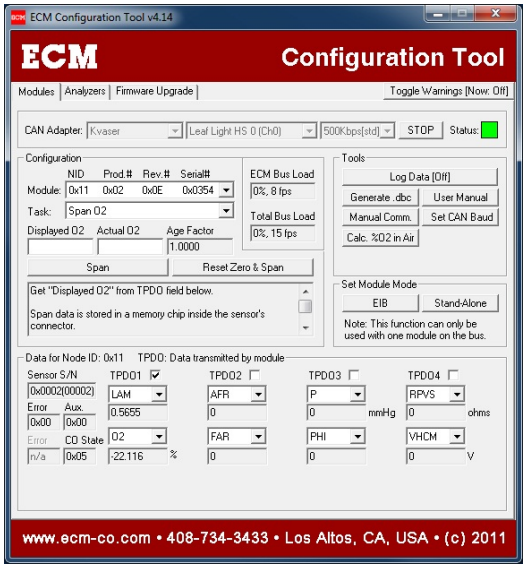

Figure 3.10: ECM NOx sensor configuration tool [4]

Table 3.5: ECM-NOxCANt module specification [4]

Input	ECM Amperometric Nox sensor
Ranges	NO_x: 0 to 5000 [ppm], λ (Lambda): 0.40 to 25, AFR: 6.0 to 364, O_2: 0 to 25 [%]
Accuracies	NO_x: 5 [ppm] (0 to 200 [ppm]), 20 [ppm] (200 to 1000 [ppm]), 2.0 % (elsewhere)
Response Time	Less than 1 s for Nox. Less than 150 ms for , AFR, O_2
Fuel Type	Programmable H:C, O:C, N:C ratios
CAN	High Speed according to ISO 11898
Configuration	Via CAN Bus with Configuration Software. Programmable Node ID.
Module	145mm 120mm 40mm, Environmentally Sealed
Environmental	-55 to $+125^oC$ for the module, 950^oC (maximum continuous) NO_x sensor
Power	11 to 28 VDC, 1.2A at 12V (steady-state), 4A at 12V for 30s (start-up)

The ECM Configuration tool, shown in Figure 3.10 is used to set-up the sensor, view output variables, calibrate the sensor and change the sensor operating parameters. The sensor controller module is connected to a PC via Kvaser Light HS CAN interface shown in Figure 3.11. The interface is connected to the DAQ laptop which is ASUS Zenbook CORE i7 through a USB port.

Figure 3.11: Kvaser Light HS CAN interface[14]

3.1.3 GPS setup

GPS system includes OBE device which is installed in the vehicle

Location and speed

The GPS test platform includes OBE, Roadside Equipment (RSE), Traffic Signal Controller (TSC) and mobile devices. OBE device shown in Figure 3.12 is capable of obtaining its vehicle status data in real-time and broadcasting continues to be used for collecting speed and location data from the vehicle.

As a display terminal, the mobile device is connected to the OBE through a Wi-Fi network and displays valuable information acquired by the OBE on the screen. In this research OBE, which is mainly used, is an intelligent device developed by China Huali Smart Ways Technology Company. The connection of notebook computers and OBE through the network line can realize real-time data transmission and storage.

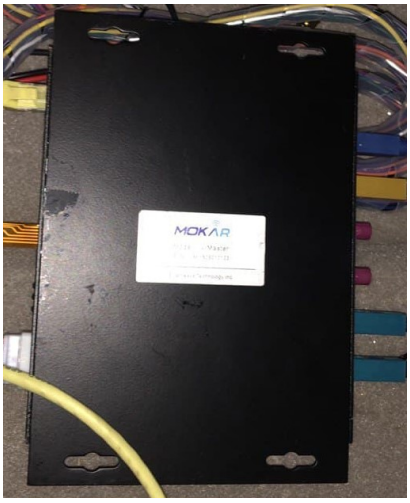

Figure 3.12: A picture of GPS module and I/O ports used in this research

3.1.4 On-board diagnostic(OBD) System

OBD reader system includes Veepeak OBDCheck BLE which plugs in the OBD port of the vehicle that is described in detail here.

Veepeak OBDCheck BLE

The OBDCheck BLE directly plugs into the vehicle and connects to an OBD II App on the iOS or Android device via Bluetooth to log data.

The advantage of Bluetooth over WiFi is much lower power consumption while allowing you to have access to the internet for other apps via your cellular data without a complex setting. The Veepeak OBDCheck specification is shown in Table 3.6.

Table 3.6: Veepeak OBDCheck specification [5]

Communication Method	Bluetooth LE for iOS and Classic Bluetooth for Android
Supported Devices	iOS device with Bluetooth 4.0 or above, Android phone and tablet
Operating Voltage	9 16V
Operating Current	Max 45mA
Operating Temperature	-40 - 85°C
Dimension	4.07×4.98×2.20 cm

Diagnostic and monitoring:

The provided app allows reading and clear check engine light trouble codes (both generic and manufacturer-specific), reset check engine light, prepare smog test, view real-time sensor readings, create a customized dashboard and estimate fuel economy.

Universal vehicle compatibility:

The OBDcheck BLE is compatible with OBD2 compliant cars and light trucks, vehicles since the year 1996 are supported including light-duty diesel pickup trucks, hybrid and many electric vehicles, no brand limitation and supports all five OBD-II protocols.

3.2 Methodology

The data collection method and data processing is described in this section. The custom PEMS system is used to collect real driving emission data from a 2008 Toyota

highlander and to collect data from different devices and DAQ systems are used with details below.

To power the heated line and the various measurement components a 2kW Honda (EU 20i) gasoline generator is used to generate 120V AC power. This generator is mounted on a trailer hitch rack model behind the vehicle shown in Figure 3.13.

Figure 3.13: 2kW Honda EU 20i generator used in this research [15]

3.2.1 Detailed experimental procedure

To collect data, all the measurement equipment and sensor, installed in the Toyota Highlander car. This consists of: installing sensors to the exhaust, doing the required preparation for each device to get ready for the main test, running programs and software in the laptop for DAQ, and starting generator and car to drive in designated route for collecting data. Here each of these steps is described.

The first step experimental procedure is bringing all the instruments and putting them in the back of the vehicle in the place that is considered for each of them. As some systems like particle measurement systems include different components that

need to be connected, they must be connected.

The connections and fitting required significant set up in this research as each of the devices come from different places and they were not designed to work with each other.

The next step is connecting sensors to the exhaust to sample data. In this way, suitable fittings are used as shown in Figure 3.4 to connect sensors to the exhaust.

Before starting to collect data, some devices required preparation to be ready for the test. For example, the heated line needed to reach $+200°C$ to be hot enough for the test. For this purpose, the heated line was first connected to the building power to reach the designated temperature then for doing the test it was brought to the car and connected to the generator. Also, the CO_2 analyzer must reach $+40°C$ before test setup. These steps, plus testing checking each device to make sure it is working properly were repeated before each test.

After making sure that each device is connected and working properly, the DAQ part starts and all devices are connected to the laptop and programs are run on the laptop to do DAQ. Each software application is required to be started and initiated by setting the required information including serial port, baud rate, frequency and saving location of each of them.

After these steps the test can be started. Here vehicle and generator are started at the ambient temperature inside the mechanical engineering building of the university of Alberta, the test then starts outside after about 5 minutes. The temperature inside building is $+18°C$. Also all devices and power supplies are connected. Then the devices are connected to the laptop. Everything is checked again to make sure all systems are working properly. Then, each program and software is started one by one to start collecting data from each device. After this immediately the test is started and the vehicle is driven in the testing route.

This switching between each program and device to run and start collecting data is

time-consuming and causes a time shift between the start of the collected data from each device. This time differenced needs to be synchronized to remove this delay for all sets of data and is described in section 3.3.

After making sure the data collecting is working, the vehicle is driven over the designated route and continue until data collection continues the route is completed.

At the end of the test, the data collecting programs and software are stopped. Then each device is disconnected from power and the generator is turned off. Next initial check of all the collected data is performed to make sure there was no obvious error during the data collection.

3.2.2 Defining testing routes used in this research

Three different driving routes each for a purpose were chosen. As three types of tests are done in this research a specific route is chosen to be compatible with the purpose of each type of test. These routes include urban and highway areas.

In Figure 3.14 the test routes are shown and the properties of each of them are described.

The tests are done in this research divided into three main types of (a) Ambient temperature, (b) Constant speed, (c) Driving behaviour tests. As these are different types of tests and each has a specific objective a specific route is selected for each of them.

Figure 3.14a shows the route chosen for the ambient (cold) temperature test. This route is around the University of Alberta's north campus in an urban area. The maximum permitted speed in this route is 60 (km/h) and the length of the route is 3.6 km.

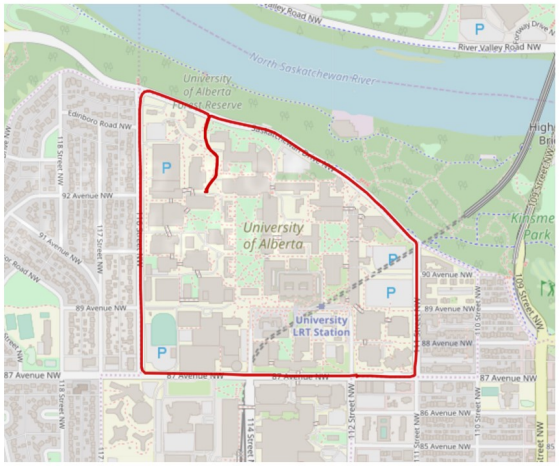

(a)

(b)

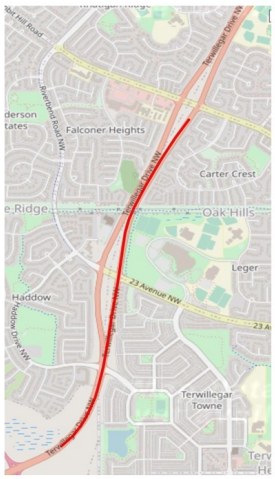

(c)

Figure 3.14: Driving route used in the city of Edmonton (a) Ambient temperature driving route: Route A, (b) Constant speed driving route: Route B, Driving behaviour driving route: Route C

Figure 3.14b shows the route chosen for the constant speed test. This route is on Terwillegar road near the Edmonton airport in the highway area. The maximum permitted speed in this route is 110 (km/h) and the length of the route is 12.43 km. As in this type of test, the effect of speed on the emission is studied, it is required to have a wide range of high speeds which leads to choosing a highway area for this test. Figure 3.14c shows the route chosen for the driving behaviour test. This route is on Terwillegar road near Edmonton airport in the highway area. The maximum permitted speed in this route is 110 (km/h) and the length of the route is 2.36 km. As in this type of test, the effect of driving behaviour on the emission is studied, it is required to choose a route to drive with quick acceleration and deceleration which leads to choosing a highway area for this test.

3.2.3 Data processing method

All the measurement data collected are transferred to the DAQ laptop synchronized and analyzed. Each device has data formatted differently requiring specialized data transfer and analysis. The NOx sensor measurement is through CAN protocol that by and Kvaser CAN interface the CAN data is converted and transferred to the laptop through USB. The ECM NOxCANt sensor also communicates through CAN to ECM configuration software installed on the computer as shown in Figure 3.10. The sample rate of the device and data that needs to be collected including NOx and oxygen can be set on this configuration tool. In this research, the sample rate is set to 1s. A sample of NOx data is provided in Table 3.7.

Table 3.7: NOx sensor output data sample

Date & Tim	Elapse Tim	Elapse Time (sec)	NOX(ppm)	VP2(V)	VH(V)	IP2(uA)	IP1(mA)	VP1P(V)	VS(V)	RPVS(ohms	Error Code	Aux Error	CO State
43:48.7	00:00.5	19.506	11.423	0.449	8.874	-0.0236	-0.00555	3.984	0.423	252	0x00	0x00	0x05
43:49.7	00:01.5	20.51	20.37	0.448	8.914	-0.01006	-0.00317	3.984	0.423	252	0x00	0x00	0x05
43:50.7	00:02.5	21.51	17.8242	0.448	8.954	-0.02553	-0.00594	3.984	0.423	252	0x00	0x00	0x05
43:51.7	00:03.5	22.512	18.3337	0.448	8.914	-0.02399	-0.00594	3.984	0.423	251.667	0x00	0x00	0x05
43:52.7	00:04.5	23.512	11.6781	0.449	8.874	-0.02321	-0.00555	3.984	0.423	251.333	0x00	0x00	0x05
43:53.7	00:05.5	24.516	13.4645	0.449	8.914	-0.0205	-0.00555	3.984	0.423	252	0x00	0x00	0x05
43:54.7	00:06.5	25.514	14.9958	0.449	8.914	-0.01818	-0.00555	3.984	0.423	252.333	0x00	0x00	0x05

The CPC device, the measurement data is in serial format. This allows data logging adding sample rate and data processing parameters, adjust data reporting interval, and change system operating.

Serial communications are established collected through the RS-232 serial communication on the back panel of the instrument.

On the PC side a terminal emulator called Real-Term which is capable of serial communication is used. Serial communications settings for CPC are listed in Table 3.8:

Table 3.8: CPC serial communication settings properties [1]

Baud rate	115200
Bits	8
Stop bits	1
Parity	None
Flow Control	None

The data output record is comma-separated ASCII contains both particle concentrations and various operating parameters including temperatures, flows, particle counts and dead time. Data may be streamed to the serial port or saved to internal flash at a user-settable interval of 1 to 2000 seconds. The reported concentrations, counts, flows, live time and dead time are average values over the reported interval, but the temperatures and pressures are the value during the last second of the interval. The OBE GPS device is connected to the DAQ laptop through the wi-fi. Then by using the MobaXterm software the data from GPS will transfer to the laptop and will be analyzed. The data format exported from GPS is .nmea which a sample of that is shown in Figure 3.15. The data format is the National Marine Electronics Association which is a standard for GPS data. The data is analyzed using GPS-Visualizer which is on the web tool to convert to comma-separated ASCII .csv which is shown in Table 3.9.

```
$GPZDA,050703.30,09,03,2020,00,00*6E
$GPGGA,050703,5331.6838,N,11331.6088,W,1,07,1.69,730.06,M,-19.786,M,,*70
$GPRMC,050703,A,5331.6838,N,11331.6088,W,0.1065,36.611,090320,,*01
$GPGSA,A,3,2,5,21,194,68,69,84,,,,,3.6,1.7,3.2*05
$GPGBS,050703,12.93,M,27.08,M,2299.77,M*0B
$GPZDA,050703.40,09,03,2020,00,00*69
$GPGGA,050703,5331.6838,N,11331.6088,W,1,07,1.69,730.05,M,-19.786,M,,*73
$GPRMC,050703,A,5331.6838,N,11331.6088,W,0.0897,12.973,090320,,*08
$GPGSA,A,3,2,5,21,194,68,69,84,,,,,3.6,1.7,3.2*05
```

Figure 3.15: A snapshot of GPS raw data

Table 3.9: GPS output converted to location and speed values used in this research

type	time	latitude	longitude	altitude (m	speed (km/	course	sat	hdop	eos	name
T	37:27.9	53.52811	-113.527	710.3	0.2		12	0.8		
T	37:28.9	53.52811	-113.527	710.2	0.4		12	0.8		
T	37:29.9	53.52811	-113.527	710	0.2		12	0.7		
T	37:30.9	53.5281	-113.527	709.8	0.3		12	0.7		
T	37:31.9	53.5281	-113.527	709.7	0.1		12	0.7		
T	37:32.9	53.5281	-113.527	709.5	0.1		12	0.7		
T	37:33.9	53.5281	-113.527	709.3	0.2		12	0.8		
T	37:34.9	53.52809	-113.527	709.2	0.4		12	0.8		
T	37:35.9	53.52809	-113.527	709	0.2		12	0.8		

For the data processing of the OBD device, the Veepeak OBDCheck BLE is connected through wi-fi. The OBD Fusion app (on the iOS phone) is used to convert the data to .csv format. This is transferred to the DAQ laptop for data analysis. A sample of OBD data is provided in Table 3.10.

Table 3.10: OBD output data sample

Time (sec)	Latitude (c	Longitude	Vehicle spe	Fuel rate (l	Engine RPI	Intake air t	Mass air fl	Absolute t	Engine Pov	Engine Tor
15.603	53.52755	-113.527	0	0	772.5	27	4.82	16.07843	5.733026	53.58003
16.585	53.52755	-113.527	0	0	775.75	27	4.93	16.07843	5.863863	54.57322
17.609	53.52756	-113.527	0	0	785	27	4.87	16.07843	5.792497	53.27381
18.599	53.52757	-113.527	0	0	776.5	27	4.76	16.07843	5.66166	52.64049
19.598	53.52757	-113.527	0	0	792	27	4.93	16.07843	5.863863	53.4535
20.592	53.52758	-113.527	0	0	771	27	4.81	16.07843	5.721131	53.5729
21.592	53.52758	-113.527	0	0	776.5	27	4.89	16.07843	5.816286	54.07815
22.6	53.52758	-113.527	0	0	775	27	4.82	16.07843	5.733026	53.4072
23.588	53.52759	-113.527	0	0	778.75	27	4.75	16.07843	5.649766	52.37813
24.581	53.52759	-113.527	0	0	778.75	27	4.78	16.07843	5.685449	52.70894
28.572	53.5276	-113.527	0	0	778	27	4.79	16.07843	5.697343	52.87013
29.609	53.5276	-113.527	0	0	778.75	27	4.89	16.07843	5.816286	53.92191

3.3 Time synchronization and Integration

Since the data is collected on multiple systems the data must be synchronized in time. Data synchronization is the process of establishing consistency among data from a source to a target data storage. It is also the ongoing process of synchronizing data between two or more devices and updating changes automatically between them to maintain consistency within systems.

The data is collected from four different devices at four sampling times. This means the time axis must be aligned on synchronized. Once the data is time-synchronized it can be integrated for the data analysis.

3.3.1 Time synchronization

To do the synchronization features in the OBD data are used to see the relation between the change of that value with the change of values of other devices.

For example, when the engine throttle opens, the mass airflow rate goes up the use of fuel and emissions are increased. By analyzing the change of the mass air flow rate and NOx emission the OBD and NOx devices are synchronized.

The unsynchronized mass airflow rate and NOx sensor data plotted versus time are shown in Figure, 3.17. The sample rate differs for different devices so for the data with lower sample rate interpolation between data is done to have interpolated data from all devices at the highest sample rate. As mentioned change in mass airflow rate increases the engine load which results in a shift in the NOx values. Putting these values together leads to synchronized data shown in Figure, 3.17. MATLAB software is used to align the two peak values of the mass airflow rate and NOx together to have a synchronized set of data.

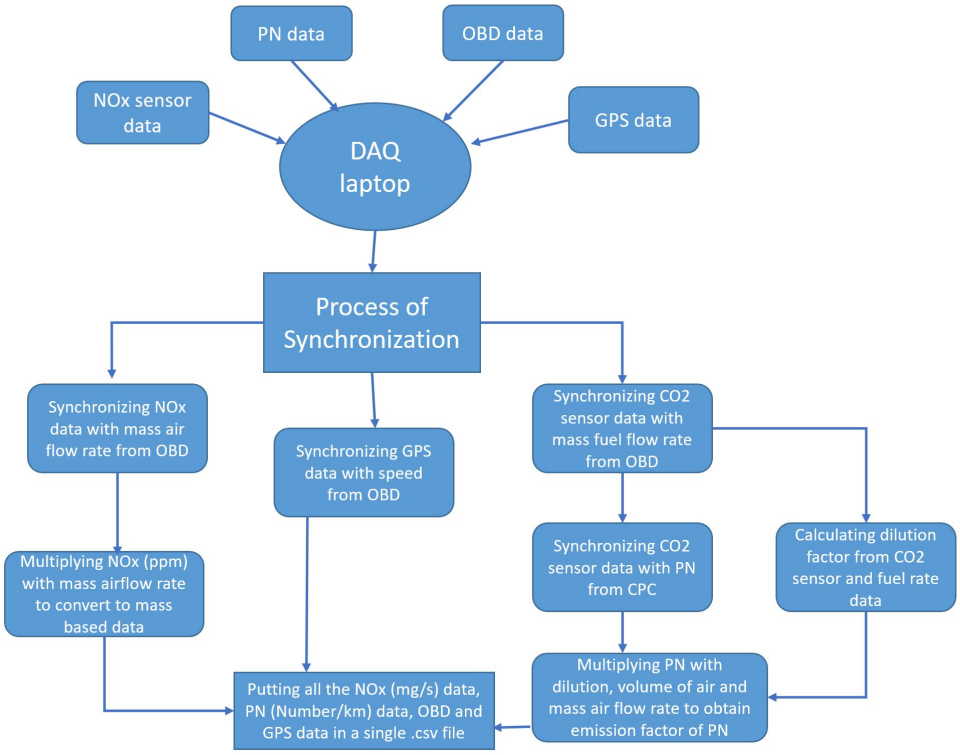

Figure 3.16: Process of the synchronization of each data from each device and conversion to mass

This kind of synchronization is called timestamp synchronization [100]. In this case, all changes to the data are marked with timestamps. The synchronization proceeds by transferring all data with a timestamp later than the previous synchronization.

The timestamp method are the most useful general technique for efficient synchronization. The technique involves tracking the last time that each user synchronized, and using this information to control the rows downloaded to each remote database [100].

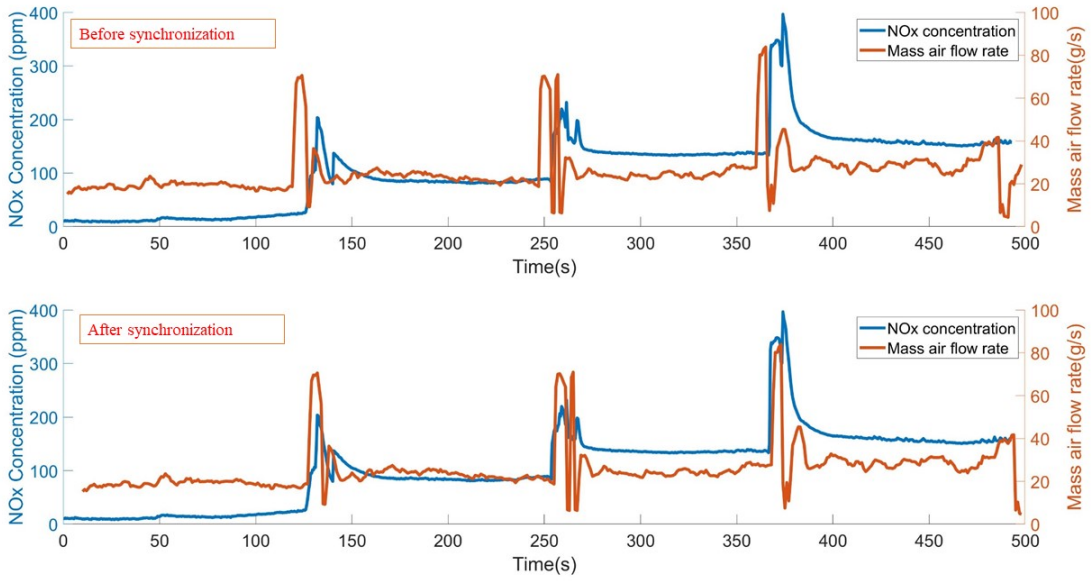

Figure 3.17: The NOx and ODB data synchronization using mass air flow rate and NOx data. Data before synchronization (Upper plot), Data after synchronization(Lower plot)

As it is seen in Figure 3.17 the time delay of NOx and OBD data is around 12(s). As the NOx sensor is a fast responding sensor this delay, as described in section 3.2.1, is due to the starting time for each software and program. As starting each software and switching between them to run separately takes some time it is reasonable to have this time delay between two sets of data. In other words, this 12(s) is not only the delay of sensor responding and a big part of that includes the time required to run each data collecting program on the laptop. For PN and GPS, the same method for synchronization is used. For PN same as NOx, the OBD mass airflow rate is used to synchronize particle data from CPC.

For the GPS data since vehicle speed is measured in both OBD and GPS, the GPS data can be synchronized to OBD speed. To validate the synchronization process, the root means square value(RMS) of each signal for each test before and after the

synchronization is calculated using Equation 3.1.

$$RMS = \sqrt{mean[\frac{X_i}{max(X)} - \frac{Y_i}{max(Y)}]^2} \tag{3.1}$$

Where X and Y are two sets of data that should be synchronized. For example, X is NOx concentration and Y is the mass airflow rate from OBD.

By doing the process of synchronization this RMS value should decrease to show synchronization process works properly. This RMS value for each test is provided in Table 3.11.

Table 3.11: Root mean square value for the tests before and after synchronization

Test ID	**NOx RMS before synch.**	**NOx RMS after synch.**	**PN RMS before synch.**	**PN RMS after synch.**	**GPS speed RMS before synch.**	**GPS speed RMS after synch.**
CA.1	0.783	0.316	0.762	0.325	0.612	0.095
CA.2	0.845	0.287	0.724	0.329	0.587	0.086
MA.1	0.732	0.347	0.757	0.325	0.512	0.094
MA.2	0.849	0.314	0.836	0.327	0.627	0.075
WA.1	0.773	0.297	-	-	0.542	0.083
WA.2	0.761	0.323	-	-	0.584	0.081
SS.1	0.632	0.194	-	-	0.521	0.072
DB.1	0.876	0.316	-	-	0.653	0.114

The considerable reduction of RMS value before and after synchronization for both NOx and PN shows the validity of the synchronization process. However, because the nature of two values(for example, NOx and OBD mass airflow rate) are not the same, it is not expected that they match perfectly. The process of synchronization for the same parameter of speed from GPS and OBD in the last column of Table 3.11 shows RMS for the same data type approaches to zero as expected from the synchronization process.

3.4 Data processing

The data collected from each device is in a raw data format that must be converted to physical units value for analysis. In a commercial PEMS, a mass flow meter is installed on the exhaust. In this research, engine OBD data provides the air mass flow rate which is used as the basis to convert concentration of NOx from ppm to emission factor mg/km. Also, the same thing is done for PN and the mass airflow rate from OBD and ideal gas law is used to have the exhaust values for PN data conversion to emission factor #/km. A summary of the calculation is provided here.

3.4.1 NOx Calculation

The data that is measured from the NOx sensor is $NO_x(ppm)$ which is concentration-based data. For analysis conversion to a mass flow (mg/s) is needed.
To do this, the basic gasoline combustion equation is used as:

$$\mathrm{C_8H_{18}} + 12.5\,[(\mathrm{O_2}) + (3.76\,\mathrm{N_2})] \longrightarrow 8\,(\mathrm{CO_2}) + 9\,(\mathrm{H_2O}) + 47\,(\mathrm{N_2}) \tag{3.2}$$

Ideal complete combustion of C_8H_{18} was assumed for stochiometric combustion of gasoline.

$$MW_{exh} = \sum y_i Mw_i \tag{3.3}$$

In Eq. 4.1 y_i is the mole fraction of the exhaust species i and Mw_i is molar mass of exhaust species i. After calculation the molar mass of exhaust will be: $MW_{exh} = 28.86\frac{g}{mol}$. Finally to convert ppm to mass based data for NO we will have:

$$\dot{M}_{NO} = Y_{NO} \times \frac{MW_{NO}}{MW_{exh}} \times \dot{m}_{exh} \tag{3.4}$$

In Eq. 3.4 Y_{NO} is the NO molar fraction in the exhaust which is the same as volume concentration measurement with NOx sensor for the mixed ideal gas.

$$\dot{m}_{exh} = \dot{m}_{air} + \dot{m}_{fuel} \tag{3.5}$$

In Eq. 3.5 $\dot{m}_{air}$ is obtained from OBD data. As OBD data shows a value of $\lambda = 1$ for all collected data values and according to Eq. 3.2 it was assumed $\dot{m}_{fuel} = \frac{1}{14.7} \times \dot{m}_{air}$. Hence, this calculation shows the fuel mass flow rate is around 6 percent of the mass airflow rate.

3.4.2 PN data analysis

The raw PN data is obtained from the CPC. This device has a saturation limit of one million particles per cm^3 since the amount of particles emitted from the exhaust exceeds this amount, it was necessary to use two stages of dilution and account for the dilution when calculating the actual particle number.

PN Conversion to emission factor:

The data that is collected from CPC is $(\frac{\#}{cm^3})$ which should be converted to $(\frac{\#}{km})$ to obtain the emission factor.

The first step is to calculate the actual amount of PN in the exhaust during one cycle of driving. To do this, the dilution factor is multiplied with measured PN concentration. This number is per volume of exhaust gas then the volume concentration is multiplied by the total volume of exhaust gas that is emitted during the driving cycle. This calculation is done every second which is the PN measurement sample rate. This is the total number of PN during this trip.

How to calculate the volume of the emitted products is discussed next.

To calculate the exhaust density, the ideal gas law is used and in the ideal gas equation,

temperature and pressure at the end of the exhaust are assumed to be in equilibrium with ambient conditions. This is approximate, a sensitivity analysis shows $10°C$ difference in approximation creates less than 1 percent error in PN calculation. By solving this equation v which is $(\frac{m^3}{g})$ will be obtained.

Then the exhaust flow rate will be multiplied with PN, then multiplied by (v) that is obtained from the last step is multiplied to it, so the PN data will be $(\frac{\#}{s})$. The equation is:

$$PN(\frac{\#}{s}) = PN(\frac{\#}{m^3}) \times v(\frac{m^3}{g}) \times \dot{m}_{exh}(\frac{g}{s}) \tag{3.6}$$

By integrating the PN $(\frac{\#}{s})$ versus the time plot the total PN number is calculated.

Dilution factor(DF) calculation:

To calculate the dilution factor, the CO_2 concentration before and after dilution are used and the ratio of these two numbers is the dilution factor.

To measure the dilution after the two stages of dilution there is a LICOR CO_2 sensor which measures the concentration of CO_2 is used. Upstream CO_2 concentration is calculated using the complete combustion equation of CO_2, exhaust temperature T, pressure P and mass air flow rate from OBD. According to Eq. 3.2 the upstream CO_2 concentration ratio is 0.125. The dilution factor formula is:

$$DF = \frac{CO_{2,up}}{\mathrm{CO_{2,down}}} \tag{3.7}$$

Figure 3.18 shows the diluted values of PN concentration, dilution factor and corrected PN concentration.

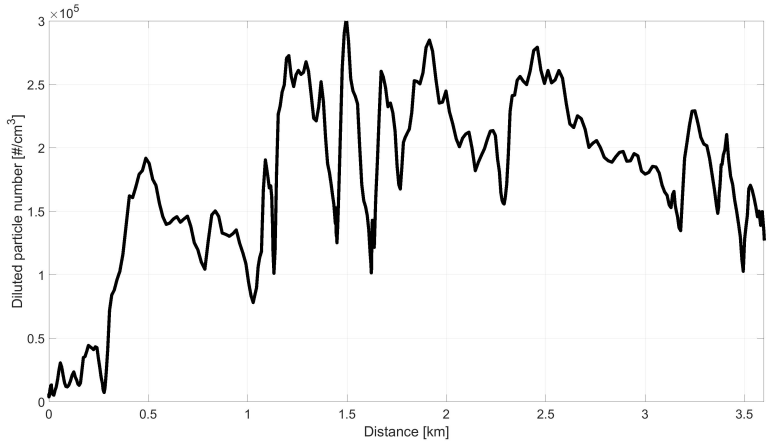

(a)

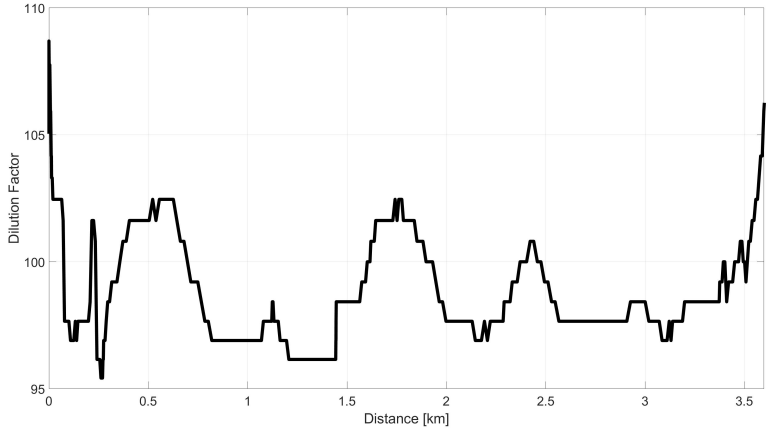

(b)

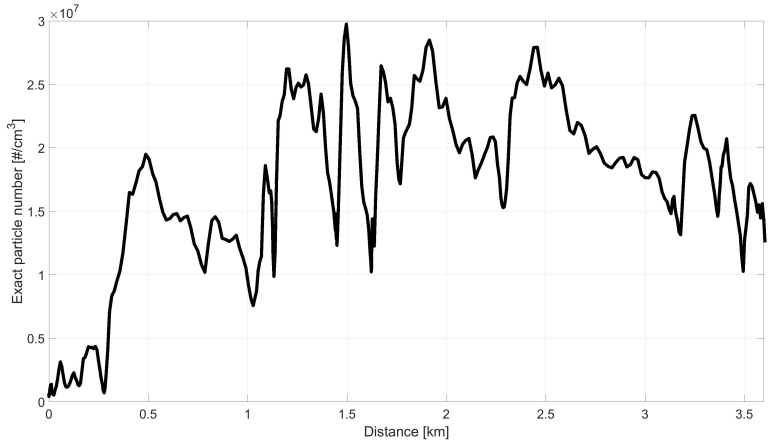

(c)

Figure 3.18: PN concentration for test CA.3 before and after applying dilution factor. (a) Diluted PN concentration (b) Dilution factor (c) Corrected PN concentration after applying dilution factor.

3.5 Experimental Uncertainity

No physical quantity can be measured with perfect certainty; there are always errors in any measurement. This means that if some quantity is measured then measurement repeats, the almost certainly different value the second time will be measured. This experiment is not an exception in this problem and definitely, there are some kinds of errors related to this research that should be considered and calculated.

Experimental error is the difference between a measurement and the true value or between two measured values. Experimental error, itself, is measured by its accuracy and precision. Accuracy measures how close a measured value is to the true value or accepted value. Since a true or accepted value for a physical quantity may be unknown, it is sometimes not possible to determine the accuracy of a measurement. Experimental errors, on the other hand, cannot be eliminated simply by repeating the experiment. There are two types of experimental errors: zeroth-order errors and random errors.

3.5.1 Random errors

Some common ways to describe accuracy and precision are significant figures, percent error, percent difference and mean and standard deviation. In this research, the mean and standard deviation method is applied to do the error analysis.

When a measurement is repeated several times, the measured values are grouped around some central value. This grouping or distribution can be described with two numbers: the mean, which measures the central value, and the standard deviation which describes the spread or deviation of the measured values about the mean.

For a set of N measured values for some quantity x, the mean of x is represented by

the symbol $\bar{x}$ and is calculated by the following formula:

$$\bar{x} = \frac{1}{N}\sum_{i=1}^{N} x_i = \frac{1}{N}(x_1 + x_2 + ... + x_{N-1} + x_N) \tag{3.8}$$

where x_i is the i-th measured value of x. The mean is the sum of the measured values divided by the number of measured values.

The standard deviation of the measured values is represented by the symbol σ_x and is given by the formula:

$$\sigma_x = \sqrt{\frac{1}{N-1}\sum_{i=1}^{N}(x_i - \bar{x})^2} \tag{3.9}$$

In this research to report experimental results the first standard deviation is used. So the format of my results is like this:

$$x = \bar{x} \pm \sigma_x \tag{3.10}$$

Here one sample of data error analysis is given to see how it works. One result that is provided in Chapter 4 is NOx sesnsor results at different temperatures. For example the result at ambient temperature of $-15°C$ is given in Table 3.12. In this table, the repeated tests for NOx is given at a certain temperature. As it is seen the value of emission factor changes in this test so it is important to do the error analysis described before to have confidence about the reported results. The mean $\bar{X} = 466$ and deviation $\sigma = 57$ for this result, so NOx emission factor for this test is $= 466 \pm 57$ mg/km.

Table 3.12: NOx emission factor for repeated tests at ambient temperature of $-15°C$. Test IDs are provided in Table 4.1

Test ID	**NOx Emission Factor (mg/km)**
(CA.1)	563
(CA.2)	448
(CA.3)	469
(CA.4)	438
(CA.5)	412
Mean	466
Standard Deviation	57

3.5.2 Zeroth-order error analysis

The error estimation has been described so far was related to the repeatability error relating to each set of tests. However each sensors that records emission values has its own error that should be considered.

The NOx sensor is an accurate fast responding sensor which the error of this sensor is reported less than 5 ppm in 500 ppm values [14] so the error of this sensor is about 1 percent. The CPC device is reported to have Concentration measurement precision within 5-10 percent [1] and GPS and OBD is 2 percent accurate [5]. These errors are considered as zeroth error. These values are shown in Table 3.13.

Table 3.13: Zeroth-order error for measured parameters of this research

Measured parameter	**Zeroth order error of the parameter**
NOx (ppm)	1 %
PN ($\#/cm^3$)	5-10 %
Mass air flow rate (g/s)	2 %
Distance (km)	2 %
Speed (km/h)	2 %

In addition to the error related with each device there are errors in the calculations and assumptions made in the process of data analysis which in know as internal error

that is described here for each set of data. According to section3.4 to convert the raw data received from each device to the analysed data some calculations are done on each set of data. These calculation itself has some sets of error that should be considered.

In this part the error that is correlated with the calculation done in each set of data will be discussed. These errors include the assumptions done for different variables during calculations and error that can happen in using each equation. This kind of error analysis is called zeroth order error analysis.

If values for the quantities X, Y, and Z, are measured with uncertainties dX, dY, and dZ, and the final result, R, is the sum or difference of these quantities, then the uncertainty δR is:

$$R = X + Y - Z \tag{3.11}$$

$$\delta R \approx \delta X + \delta Y + \delta Z \tag{3.12}$$

$$\delta R = \sqrt{(\delta X)^2 + (\delta Y)^2 + (\delta Z)^2} \tag{3.13}$$

In the same way as for sums and differences, also the result for the case of multiplication and division can be stated. According to [101] if the engineering equation has the form of Eq. 3.14:

$$\psi = a \prod_{i=1}^{m} x_i^{v_i} \tag{3.14}$$

In this case σ_y is considered as the calculation error of ψ and σ_i is the error of each parameter in ψ equation and will be calculated in Eq. 3.15:

$$\frac{\sigma_y}{y} = [\sum_{i=1}^{m} v_i^2 (\frac{\sigma i}{x_i})^2]^{\frac{1}{2}} \tag{3.15}$$

Using the method described in Eq. 3.14 and 3.15 NOx and PN emission factors errors are calculated in this research.

As a sample of error analysis calculation for one test of NOx is done here.

According to Eq. 3.4 NOx concentration (ppm), total molar mass ratio and exhuast flow rate (g/s), are parameteres that multiplied with each other and the NOx mass flow rate (mg/s) is calculated, thus in Eq. 3.15 these parameters should be considered.

As it is mentioned NOx sensor error is around 1 percent. The mass molar value by considering different combustion equations and different formulas for NOx(NO,NO_2,...) will change from 1.02 to 1.1 and the exhaust flow rate by considering both fuel rate and mass air flow rate will change maximum 2 percent. Finally by substitute these values in Eq. 3.15, the calculation error of NOx will be obtained in Eq. 3.18:

$$NOx(mg/s) = NOx(ppm) \times \frac{MW_{NO}}{MW_{exh}} \times \dot{m}_{exh} \tag{3.16}$$

$$\frac{\sigma NOx(mg/s)}{NOx(mg/s)} \approx \frac{\sigma NOx(ppm)}{NOx(ppm)} + \frac{\sigma MW}{MW} + \frac{\sigma \dot{m}_{exh}}{\dot{m}_{exh}} \tag{3.17}$$

$$\sigma NOx(mg/s) = NOx(mg/s).\sqrt{(\frac{\sigma NOx(ppm)}{NOx(ppm)})^2 + (\frac{\sigma MW}{MW})^2 + (\frac{\sigma \dot{m}_{exh}}{\dot{m}_{exh}})} \tag{3.18}$$

In these equations $\frac{MW_{NO}}{MW_{exh}}$ is considered as MW. According to Eq. 3.18 the error in NOx calculation is 8 percent

The same process for error calculation of PN conversion to #/km is done and the result shows that the error in PN calculation is 19 percent.

Chapter 4

Results

In this research, RDE tests are done by using in-house built PEMS system to study the effect of ambient temperature, vehicle speed and driving behaviour on NOx and particle emissions of a light-duty GDI engine vehicle.

The results are divivded into three sections of (a) effects of ambient temperature, (b)effects of vehicle speed, and (c) effects of driving behaviour on NOx and particulate emissions.

Table 4.1 provides a summary of all tests at different conditions. PN data is only available for limited number of cases as the CPC sensor, heated line, and dilution system required high power input which was limited by the available generator.

Table 4.1: The information for the test categories of ambient temperature, constant speed, and driving behaviour done in this research

Test Category	Date	Test ID.	Ambient T ($^{\circ}C$) $\pm 4^{\circ}C$	Route	NOx	PN
Amb. Temp.	March 8	CA.1	-15	A	✓	✓
	March 8	CA.2	-15	A	✓	✓
	March 8	CA.3	-15	A	✓	✓
	March 8	CA.4	-15	A	✓	✓
	March 8	CA.5	-15	A	✓	✓
	March 8	CA.6	-15	A	✓	✓
	April 14	MA.1	+5	A	✓	✓
	April 14	MA.2	+5	A	✓	✓
	April 14	MA.3	+5	A	✓	✓
	April 14	MA.4	+5	A	✓	✓
	April 14	MA.5	+5	A	✓	✓
	April 14	MA.6	+5	A	✓	-
	April 14	MA.7	+5	A	✓	-
	April 14	MA.8	+5	A	✓	-
	April 14	MA.9	+5	A	✓	-
	April 14	MA.10	+5	A	✓	-
	April 14	MA.11	+5	A	✓	-
	April 14	MA.12	+5	A	✓	-
	April 14	MA.13	+5	A	✓	-
	April 14	MA.14	+5	A	✓	-
	April 14	MA.15	+5	A	✓	-
	April 14	MA.16	+5	A	✓	-
	April 14	MA.17	+5	A	✓	-
	April 14	MA.18	+5	A	✓	-
	April 14	MA.19	+5	A	✓	-
	April 14	MA.20	+5	A	✓	-
	June 2	WA.1	+15	A	✓	-
	June 2	WA.2	+15	A	✓	-
	June 2	WA.3	+15	A	✓	-
	June 2	WA.4	+15	A	✓	-
	June 2	WA.5	+15	A	✓	-
Const. Speed	May 1	SS.1	+10	B	✓	-
	May 1	SS.2	+10	B	✓	-
Drive Behav.	May 1	DB.1	+10	C	✓	-
	May 1	DB.2	+10	C	✓	-

4.1 Effect of ambient temperature on NOx and PN emissions

Three sets of ambient test at $-15°C$, $+5°C$, $+15°C$ were performed and are summarized in Table 4.1. As the tests were conducted during a full day of experimentation, with a maximum ambient temperature variation of $4°C$ from the average as indicated in Table 4.1.

4.1.1 Emission concentration variation over the drive cycle

In this section, the result for the repeated tests for the ambient temperature variation tests is provided. In this part, the tests are done in different ambient temperatures to investigate the impact of temperature on exhaust emissions.

The NOx and PN emissions and speed vs. distance at $-15°C$ ambient temperature are shown in Figure 4.1. Four selected tests are shown which are CA.1, CA.2, CA.3, CA.4 (see Table 4.1).

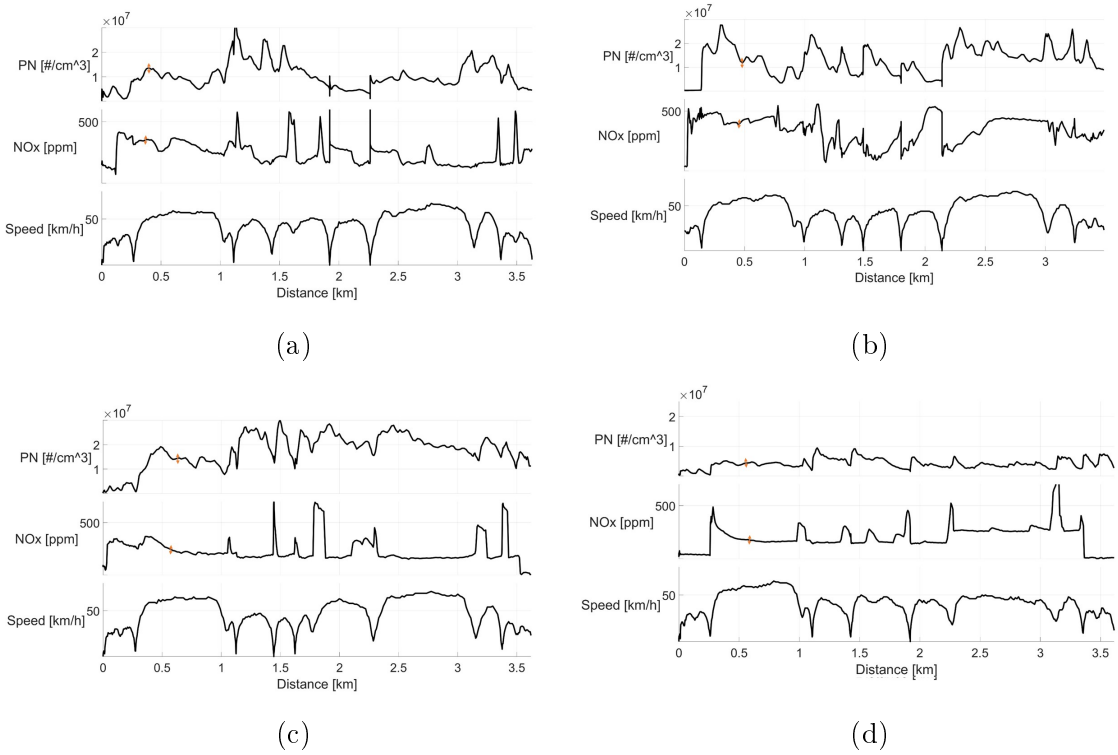

Figure 4.1: Exhaust NOx and PN concentrations versus distance for (a)CA.1, (b)CA.2, (c)CA.3, and (d)CA.4 of cold ambient temperature at $-15°C$. Test IDs are in Table 4.1

Based on the data in Figure 4.1 for the ambient temperature of $-15°C$, the emission concentration was converted to emission mass flow rate and integrated over distance to obtain emission factors in mass per unit distance.

The emission factors of the tested vehicle was obtained at $(466 \pm 57) mg/km$ for NOx and $(1.59 \pm 1) \times 10^{11} \#/km$ for PN.

During the sharp decelerations, fuel cut-off is expected but at some times, in this plot a NOx spike happens. Looking at the OBD data for fuel cut-off can explain this however OBD installed in this vehicle does not provide any fuel data. This spike during fuel cut-off may be because of time difference between devices and also transient response related to the dynamic of NOx sensor.

Also the transient response relating to the dynamic of NOx sensor is important here.

The response time of NOx sensor is less than 1 second. This dynamic of sensor is important when there is a peak in the plot. As the plot shows the measured value of NOx sensor, this may differ from the exact engine NOx emission. The peaks in the plot can be sharper in the exact engin NOx emission. The engine model can give this exact amount of NOx by considering the time constant τ and first order engine model. The NOx and PN emission and speed vs. distance at $+5°C$ is shown in Figure 4.2. Four selected tests are shown which are MA.1, MA.2, MA.3, MA.4- see Table 4.1.

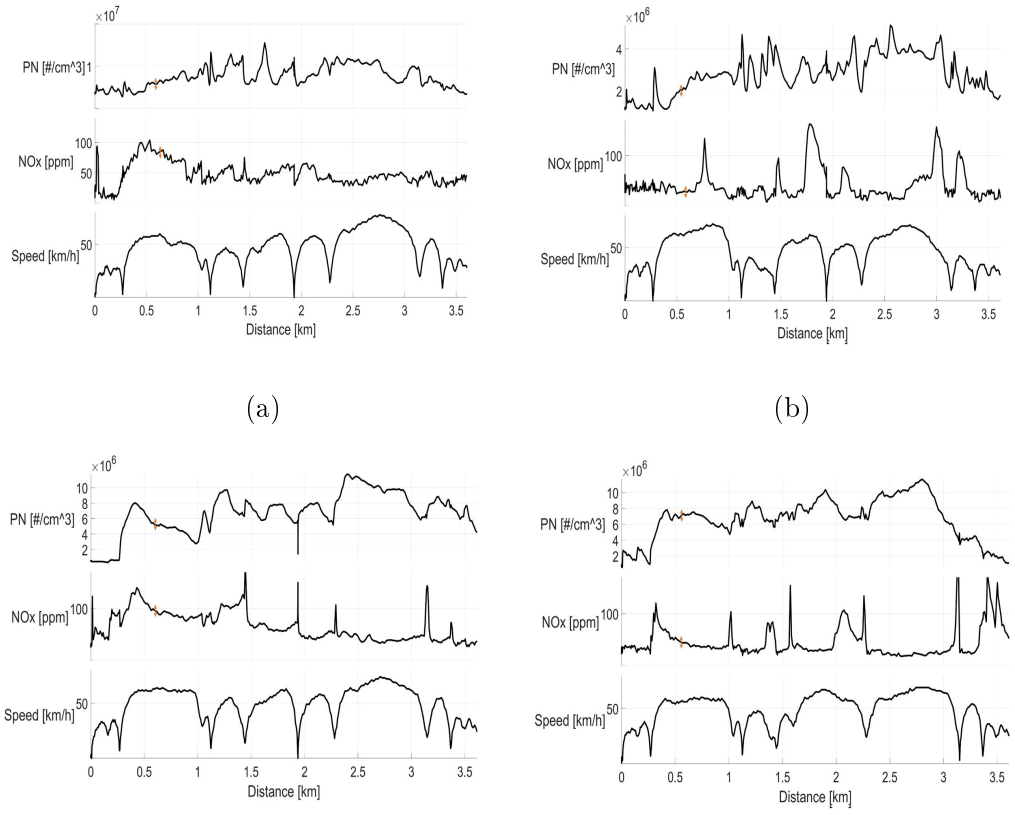

Figure 4.2: Exhaust NOx and PN concentrations versus distance for (a)MA.1, (b)MA.2, (c)MA.3, and (d)MA.4 of mild ambient temperature at $+5°C$. Test IDs are in Table 4.1

Based on provided data on Figure 4.2 for ambient temperature of $+5°C$, the emis-

sion concentration was again converted to emission mass flow rate and integrated over distance to obtain emission factors in mass per unit distance.

The emission factors of the tested was obtained at $(67 \pm 9)(mg/km)$ for NOx and $(6.8 \pm 2.4) \times 10^{10}(\#/km)$ for PN.

The NOx emission and speed vs. distance in at $+15°C$ is shown in Figure 4.3. Four selected tests are shown which are WA.1, WA.2, WA.3, WA.4- see Table 4.1.

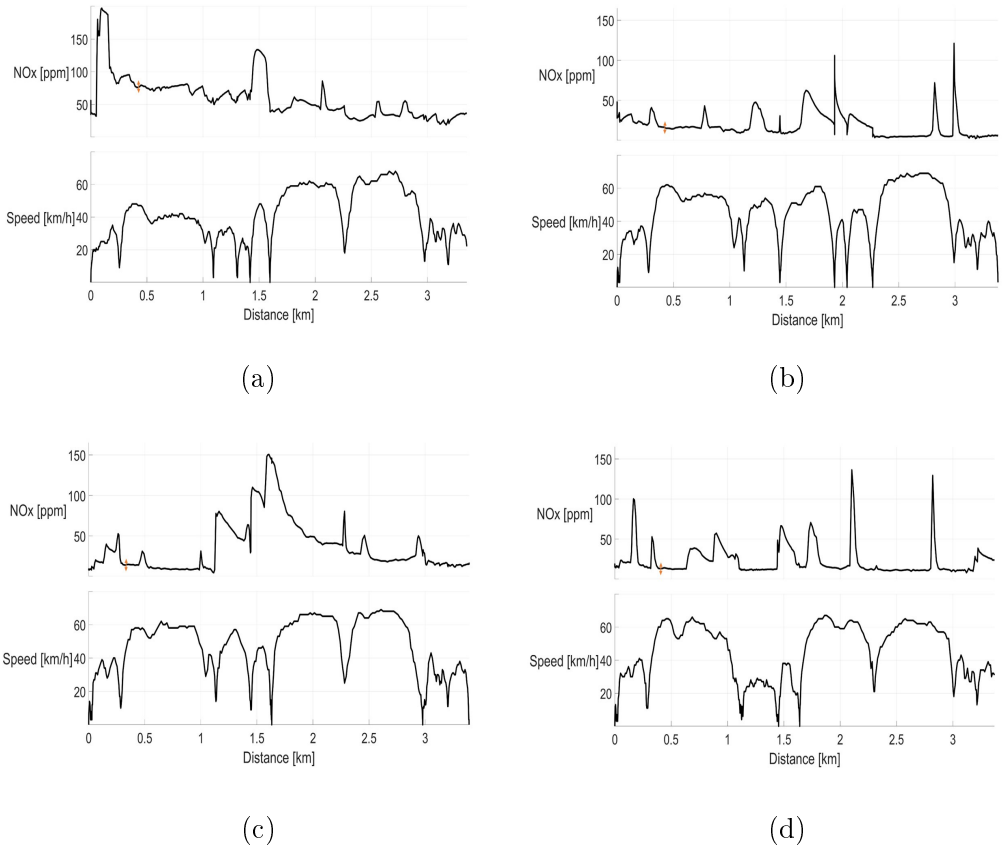

Figure 4.3: Exhaust NOx concentrations versus distance for (a)WA.1, (b)WA.2, (c)WA.3, and (d)WA.4 of warm ambient temperature at $+15°C$. Test IDs are in Table 4.1

Note that according to Table 4.1 Pn measurement was not done for the rest of experimentations particularly at ambient temperature of $+15°C$, due to power supply

problems for the heated line and the air compressor.

The NOx emission factor of the tested vehicle was obtained at $(56 \pm 7)(mg/km)$.

To compare the NOx and PN emission data collected during cold and warm ambient temperature tests the first test at each temperature is selected and both are plotted. These tests are tests CA.1, MA.1, WA.1 (see Table 4.1). The ambient temperature variation are shown in Figure 4.4.

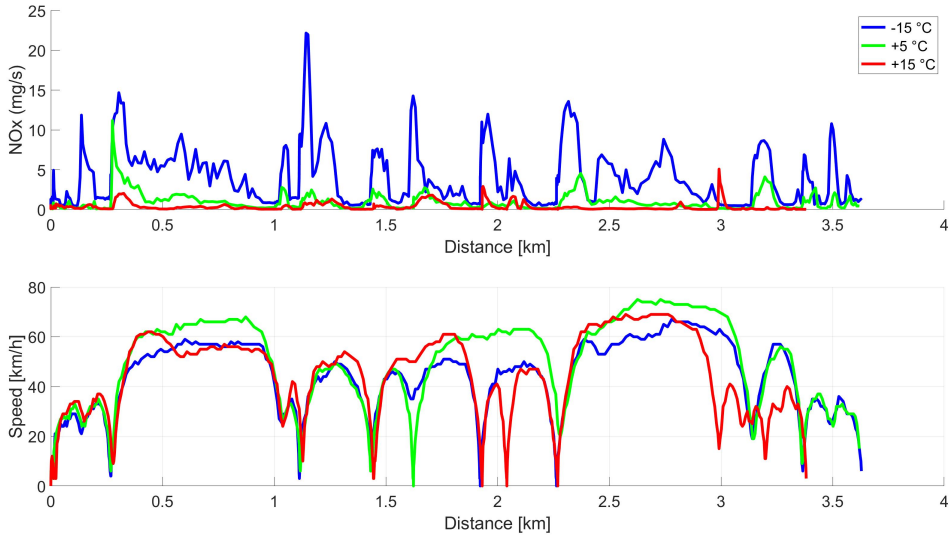

Figure 4.4: A comparison of NOx mass flow rate for three cases test at cold ambient (CA.1), mild ambient (MA.1), warm ambient (WA.1) above; corresponding speed below. Test IDs are in Table 4.1

Note that same drive cycle were drive for CA.1, MA.1, WA.1 as shown in Figure 4.4. Despite similar driving cycle, NOx mass flow rate variation over the travelled distance increased with reduced ambient temperature. The PN emission and speed versus distance for $-15°C$ and $+5°C$ ambient temperatures are compared in Figure 4.5 with identical driving cycles.

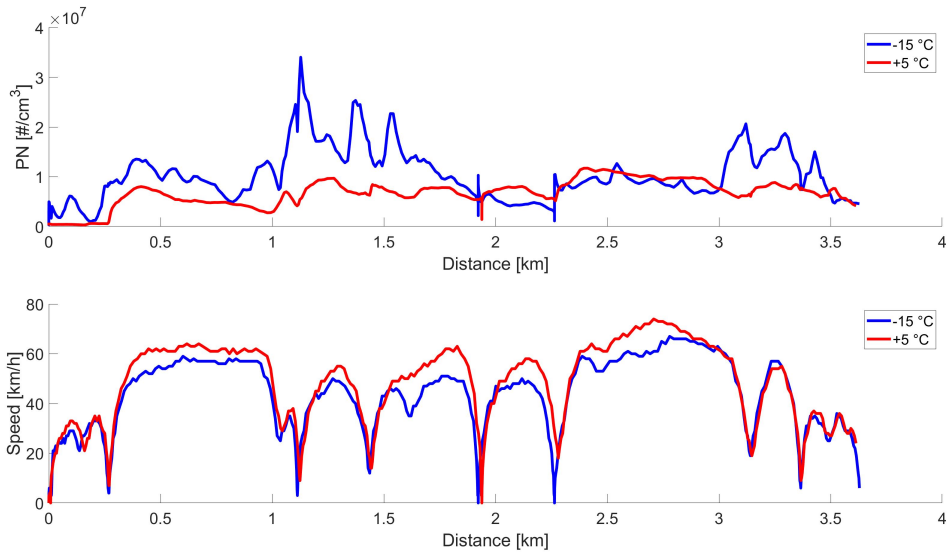

Figure 4.5: A comparison of PN concentration for two cases of test at cold ambient (CA.1), mild ambient (MA.1) above and correspondent speed below. Test IDs are in Table 4.1

According to Figure 4.5 for the same driving cycles for test cases of CA.1 and MA.1 the values for PN emissions were considerably higher for the cold climate test. Figure 4.6 shows variation of cumulative NOx over distance for three cases of CA.1, MA.1, WA.1. Figure 4.6a plots the cumulative NOx absolute value over one representation driving cycle which is for CA.1 while Figure 4.6b shows the normalized values.

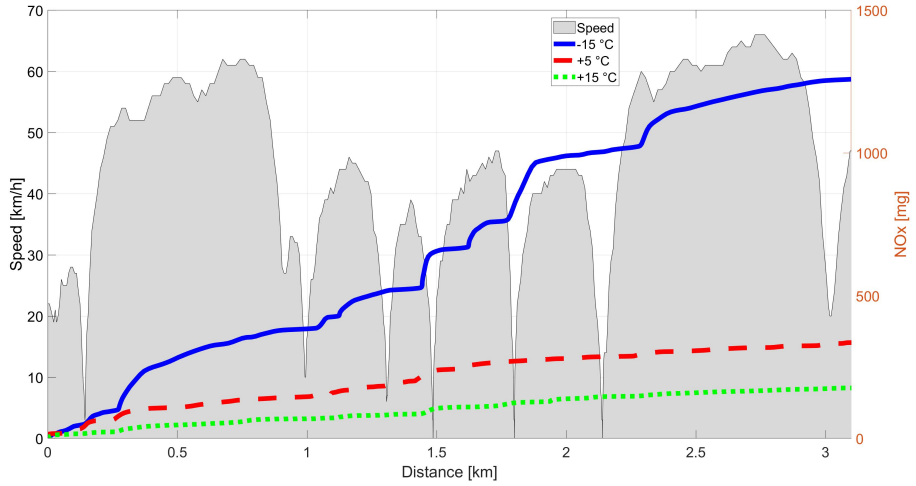

(a)

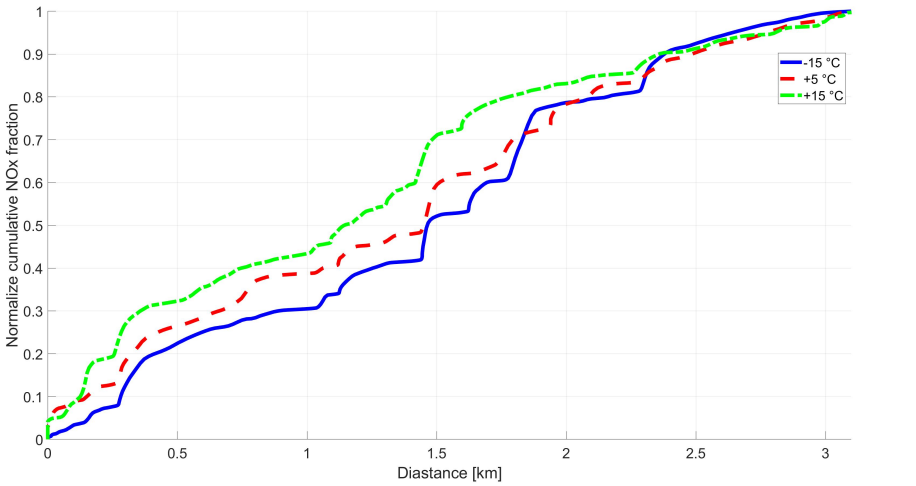

(b)

Figure 4.6: Cumulative NOx mass flow rate emission comparison for the three cases of test at cold ambient (CA.1), mild ambient (MA.1), warm ambient (WA.1). (a) cumulative NOx mass flow rate comparison with drivng cycle in grey (b) Normalized cumulative values for correspondent tests. Test IDs are in Table 4.1

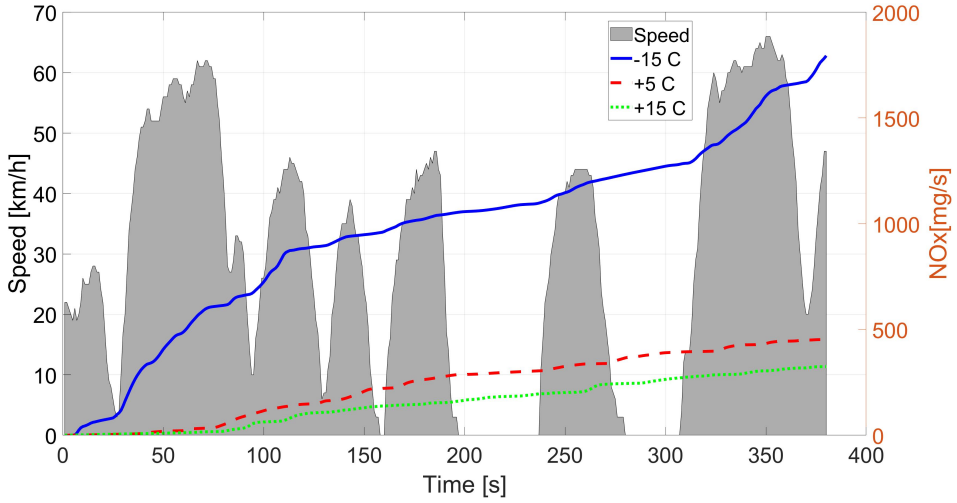

Figure 4.7: Cumulative NOx mass flow rate emission comparison for the three cases of test at cold ambient (CA.2), mild ambient (MA.2), warm ambient (WA.2). Cumulative NOx mass flow rate comparison with drivng cycle in grey. Test IDs are in Table 4.1

As NOx formation is time-based, Figure 4.7 shows variation of cumulative NOx over time for three cases of CA.2, MA.2, WA.2. In this plot same as the plot versus distance the pattern is repeated and NOx acts similar in cold, mild and warm ambient temperature.

Figure 4.8 shows variation of cumulative PN over distance for two cases of CA.1, MA.1. Figure 4.8a is the absolute value with one representation driving cycle which is for CA.1 and Figure 4.8b shows the normalized values.

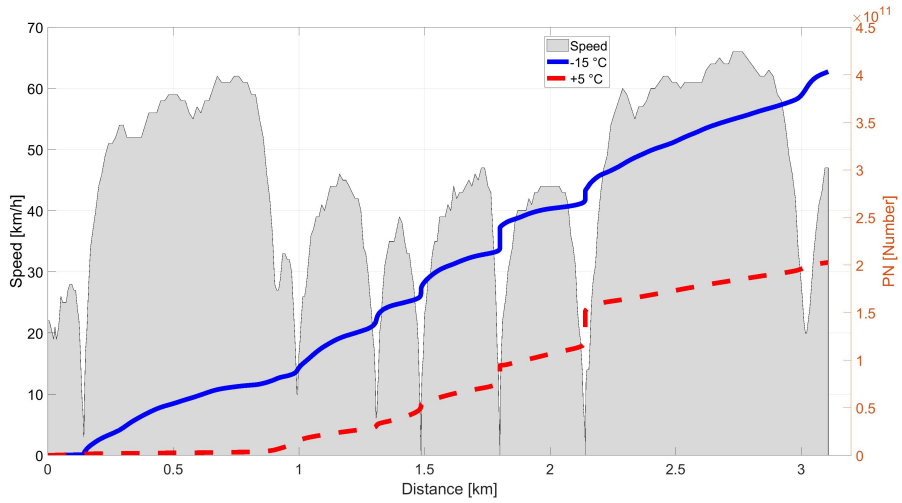

(a)

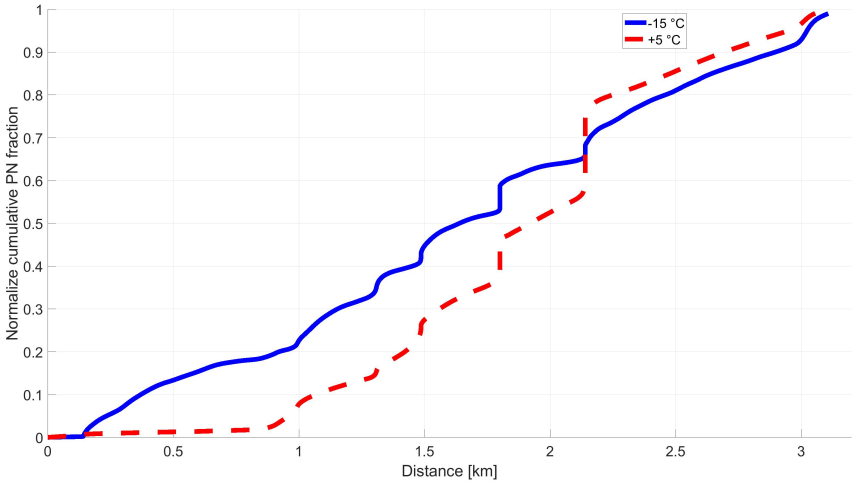

(b)

Figure 4.8: Cumulative PN number emission comparison for the two cases of test at cold ambient (CA.1), mild ambient (MA.1). (a) cumulative PN number comparison with driving cycle in grey (b) Normalized cumulative values for correspondent tests. Test IDs are in Table 4.1

Alternative depiction of NOx emission for different temperatures, shown in Figure 4.6. The cumulative NOx emission for $-15°C$, $+5°C$, $+15°C$ versus time is shown. In this figure the driving cycle is shown in gray color and the cumulative NOx emission is shown in different blue ($-15°C$), red($+5°C$) and green($+15°C$) colors.

The cumulative PN emission and speed profile versus time is shown in Figure 4.8. In this figure the driving cycle is shown in gray color and the cumulative NOx emission is shown in blue ($-15°C$), red($+5°C$) and green($+15°C$) colors.

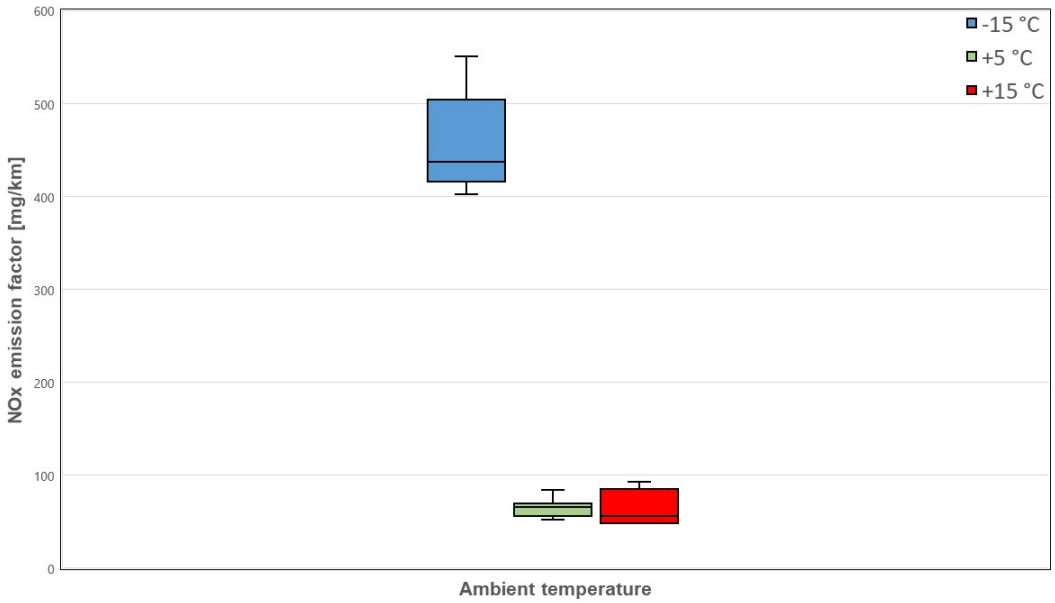

Figure 4.9: A comparison of NOx emission factor for all tests at cold ambient $-15°C$, mild ambient $+5°C$, warm ambient temperature $+15°$.

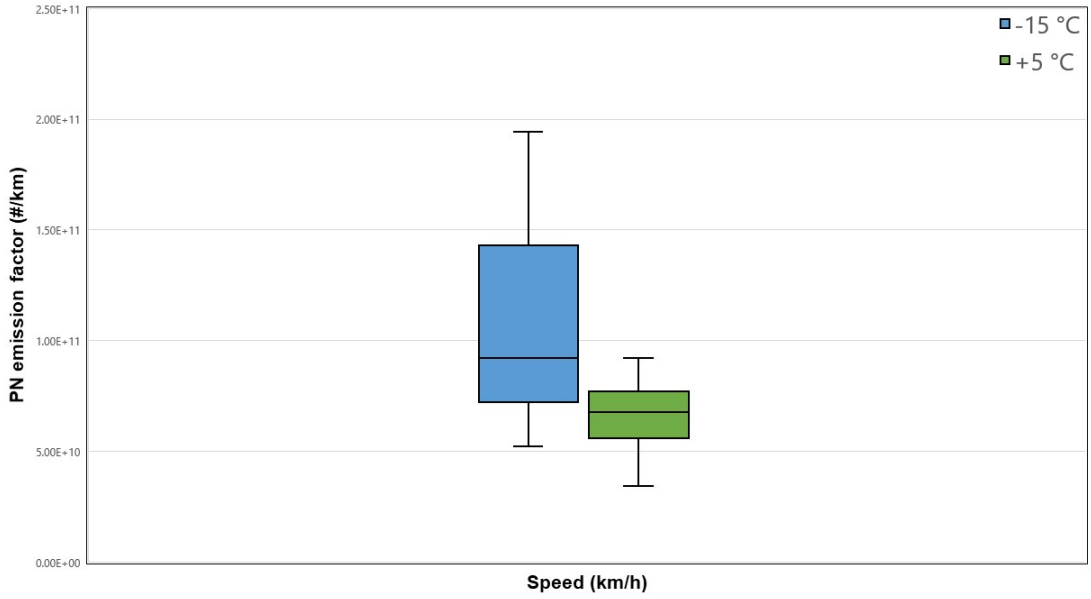

Figure 4.10: A comparison of PN emission factor for all tests at cold ambient $-15°C$, mild ambient $+5°C$.

Table 4.2 provides the average values of the NOx and PN emission factors at various ambient temperatures relates to Figure 4.9 and 4.10.

Table 4.2: Average NOx and PN emission factors.

Ambient Temperature ($°C$)	**NOx Emission Factor (mg/km)**	**PN Emission Factor (#/km)**
-15	466 ± 57	$(1.59 \pm 1) \times 10^{11}$
$+5$	67 ± 9	$(6.8 \pm 2.4) \times 10^{10}$
$+15$	56 ± 7	-

No emission factor regulation is available for $-15°C$ ambient for NOx and PN, so the values are compared with factors available in standard emission regulations and emission models noting the fact that all testing parameters such as driving cycle are different.

The NOx emission limit for US EPA Tier 2 for gasoline LDV for the model year 2008 (the same model year of the tested vehicle) is 65 mg/km [102]. While the NOx

emission factor at an ambient temperature of $+15°C$ was within emission regulation limits (despite ageing catalyst, different ambient temperature, and different driving cycle compared to standard testing procedure), it was measured slightly higher at $+5°C$ ambient temperature and 7.1 times higher than emission regulation at $-15°C$. Although the Tier regulation needs test in designated route and specific conditions, this comparison only made to have a sense about these emission factor numbers at different temperatures.

Increased NOx can be attributed to many factors such as vehicle age, mileage, ageing of TWC and possible lack of proper maintenance. However, in the same emission regulation, conformity of 1.1 over the age of the vehicle is allowed. The much larger value of NOx reported in this study comes from real-world driving instead of standard cycle driving and extreme cold ambient of $-15°C$ which is not tested in any standard test procedure.

Despite not a true cold start, one possible reason that causes this effect is the impact of low temperature on the catalyst converter [103]. In the vehicle, a three-way catalytic converter is an exhaust emission control device used to simultaneously reduce NOx, CO, and HC that reduces toxic gases and pollutants in exhaust gas from stoichiometric internal combustion engines into less-toxic pollutants by catalyzing a redox reaction (an oxidation and a reduction reaction)[104].

When the catalytic converter does not reach its minimum operating temperature requirement or light-off temperature[105], this leads to a poor reduction of emissions until the light-off temperature is reached. As the catalyst temperature was not measured in this study, it can only be observed through the measured data that at the cold climate of $-15°C$ it seems the temperature in the catalyst did not reach the light off temperature until much later in the cycle compared to the warmer tests.

A vehicle operates in cold weather conditions when the engine block and the catalyst substrate are at temperatures substantially below their respective normal operating

temperatures. Generally at cold temperatures friction is higher and the catalyst is inactive [106]. Together, these two factors contribute to higher tailpipe emissions. For example, if the catalyst temperature is less than $+270°C$, the emission conversion efficiency is less than 50 percent [107].

The NOx emission factor of the current study at $+5°C$ is in the range that at emission regulation limit of the same vehicle at the time of production. As can be seen, the age and mileage of this vehicle do not have a considerable impact on the emission of this vehicle and it is still in the range of emission regulation. All these data show that a tested vehicle that has a lower emission factor than emission regulation in warm weather but this rapidly degrades at $-15°C$. It is assumed that in cold weather the catalyst light-off is an important issue that affects the number of emissions.

Mobile source emission models have equations or correction factors for the cold start of the vehicles. As an example, the well-known US EPA mobile emission factor model provides such data. The model is called MOVES and the latest version is 2014b. MOVES2014b provides NOx cold-start vehicle emission of 1.2 g at $-17°C$ and 0.1 g at $+24°C$ [108]. Assuming a linear relation this is equal to a 26.8 mg increase of NOx cold start emission per each degree C of ambient temperature reduction. Although the NOx emission factor reported in this research is different from the cold start, the NOx emission factor does follow a similar trend. Here the RDE NOx emission factor increases 14 mg/km per each degree C of ambient temperature reduction as seen in Figure 4.9.

In [49], NOx emission of a Euro 6 vehicle at $-7°C$ tested over standard European cycle was reported. Accoring to the comprehensive literature review this is the coldest temperature repeated for a NOx emission measurement test done on gasoline engine using RDE. The results reported higher emissions of CO, NOx, and solid PN when vehicles were tested at $-7°C$ compared to $+23°C$. It was reported that NOx emission from gasoline vehicles at $-7°C$ were on average 1.7 times [0.8 to 4.6 times] higher

than at $+23°C$, CO_2 emissions were on average 30% higher at $-7°C$ than at $+23°C$, and GDI's solid PN emissions increased 1.6 to 2.8 times from $+23°C$ to $-7°C$. Also in [109], it is reported that NOx emissions are 7 times higher at $-5°C$(700 mg/km) than at $+23°C$ (100 mg/km) for diesel engine.

Figure 4.6 shows the variation of cumulative and normalize NOx over distance for three cases of NOx test at different ambient temperatures. This plot shows the cumulative value of NOx emission at $-15°C$ is 4.5 times higher than the value of $+15°C$, however, the normalized value of NOx shows a higher slope of the line for the test at $+15°C$. As it is shown in Figure 4.6 at the beginning of the test at $+15°C$, the NOx emission immediately goes up and the line has a big slope, after that the slope decreases and continues with the almost same amount, whereas this does not happen for the test at $-15°C$ at the beginning of the test and it happens after a long time at the end of the test. This shows that in the warm ambient temperature test catalyst activates after a short amount of time although it takes much longer time for the catalyst to be activated in cold weather conditions.

US EPA emission regulation does not have a PN emission limit value for any gasoline engine. The use of PN limit values in emission regulations around the world has started in 2016 by putting limit values for diesel engines (in addition to particulate mass) and GDI engines. Euro6 emission standard limit for GDI engine is 6×10^{11} #/km tested in the standard driving cycle on a chassis dynamometer at normal ambient temperature. As such a comparison of values obtained in this research comparison with Euro6 emission, regulation is only done for trend analysis.

The PN emission factor results were obtained at the cold ambient temperature of $-15°C$ at $(1.59 \pm 1) \times 10^{11}$ #/km. The value is 2.3 times higher than PN emission factors at an ambient temperature of $+5°C$ at $(6.8 \pm 2.4) \times 10^{10}$ #/km.

Same as NOx increased PN is contributed to many factors such as vehicle age, mileage, and possible lack of proper maintenance. However, the larger value of PN reported

in this study comes from real-world driving instead of standard cycle driving and extreme cold ambient of $-15°C$ which is not tested in any standard test procedure. Figure 4.8 shows the variation of cumulative and normalized PN over distance for two cases of PN test at different ambient temperatures. This plot shows the cumulative value of PN emission at $-15°C$ is 2 times higher than the value of $+5°C$. The normalized value of PN in Figure 4.8 does not act in the same way that happens to NOx to have a higher slope at the beginning of the test at warm temperature test. The reason is that the three-way catalyst does not affect PN and during the beginning of the test the normalized value of PN at $+5°C$ is lower than the value at $-15°C$. Additionally, it proves the previous discussion on NOx that the higher slope at the beginning of warm temperature test, shows that in the warm ambient temperature test catalyst activates after a short amount of time although it takes much longer time for the catalyst to be activated in cold weather conditions.

In [49] PN emission of a Euro 6 vehicle at $-7°C$ tested over standard European cycle was reported. It was reported that PN emission from gasoline vehicles at $-7°C$ was 2 to 6 times higher than at $+23°C$. PN emissions were low for the tested diesel vehicles, being approximately 2 orders of magnitude lower than those from gasoline vehicles. This indicates the good performance of the current diesel particle filter (DPF) technologies. The higher PN emissions from the diesel vehicles at cold temperature could be because of semi-volatile material is not oxidated as the catalytic converters have not yet reached the light-off temperature.

In [48] it is shown that the PN emission factors increased as the ambient temperature decreased from $+30°C$ to $-7°C$ for both the GDI and PFI vehicles. The average solid PN emission factors of the GDI vehicle over the WLTC at $-7°C$ were 1.8 to 2.0 times those at $+30°C$.

Figure 4.9 and 4.10 shows the averaged NOx and PN emission factor for all tests. A linear regression interpolation of Figure 4.9 data for NOx predicts increase of 14

mg/km per each degree C decrease of ambient temperature from $+15°C$ to $-15°C$. This includes all engine emissions of start, driving and constant warm-up period.

A similar analysis for PN shows an increase of PN emission factor of 3.5×10^9 per each degree C decrease of ambient temperature.

The correction factor described above are based on very limited experiments but the trend seems to make sense and they provide correction factors that have not been reported before.

4.2 Effect of vehicle speed on NOx emissions

Tests are designed to study the effect of speed on the NOx emission as the NOx emission is related to the speed of the vehicle. However, for real driving emissions are found to decrease when travel speeds increase. Both emissions and fuel consumption are at a minimum at constant speeds of 60-80 km/h. Emissions at low travel speeds were found to be relatively high due to the changes in the speed at speeds in city streets[110].

4.2.1 NOx emission for the steady speed test

Here, the vehicle is tested on the highway which is shown in route B (as described in section 3.2.1)and vehicle cruise control is used to hold a constant speed. In this test the engine is fully warmed up. The NOx results for constant speed driving conditions are provided here. The plots are shown versus distance and the difference between emission at different constant speeds can be seen in Figure 4.11.

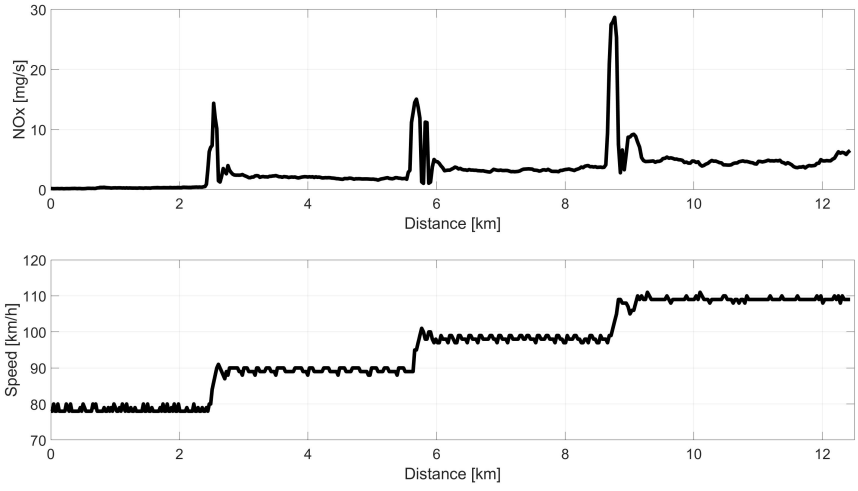

Figure 4.11: Exhaust NOx mass flow rate versus distance for constant speed test SS.1 above and correspondent speed below. Test IDs are in Table 4.1

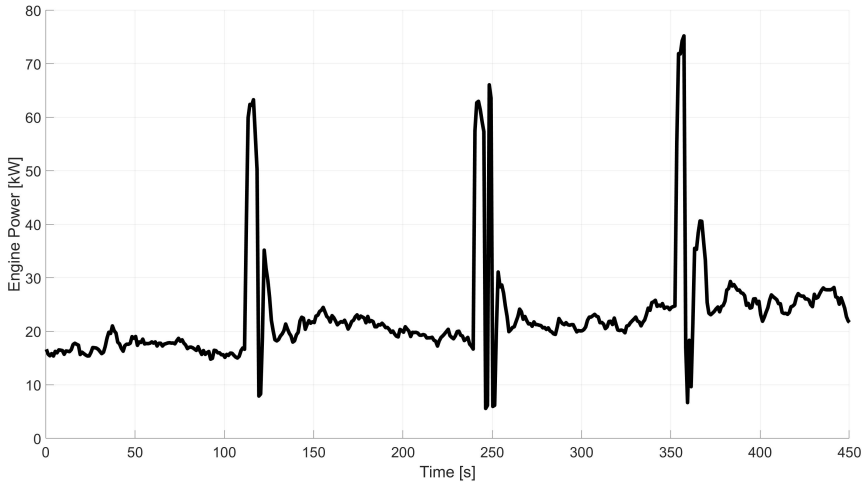

Figure 4.12: Engine power versus time for constant speed test SS.1 for speeds (80,90,100,110)km/h. Test IDs are in Table 4.1.

The NOx emission and speed versus distance for different speeds of 80(km/h), 90(km/h), 100(km/h), 110(km/h) are shown in Figure 4.11. The NOx emission factors for this test are $(35 \pm 7) mg/km$ for 80(km/h), $(98 \pm 12) mg/km$ for 90(km/h), $(174 \pm 9) mg/km$ for 100(km/h), $(232 \pm 24) mg/km$ for 110(km/h) and the emission factor regulation for NOx according to EPA Tier 2 is 65(mg/s).

Some peaks with much higher values than other parts of the plot can be seen in Figure 4.11. The reason for those peaks shown is the transition between two speeds. Forgoing from one speed to the other it is necessary to accelerate. This will be done by opening the throttle and using more fuel which leads to the jump in the emission.

4.2.2 Comparison of NOx emission results for different speeds

To make a comparison between the NOx emission data collected during different constant speeds, the cumulative NOx emission result with the driving cycle in grey area is shown in Figure 4.13. This result for different constant speeds is done in the same driving route (Route B) and at the same ambient temperature

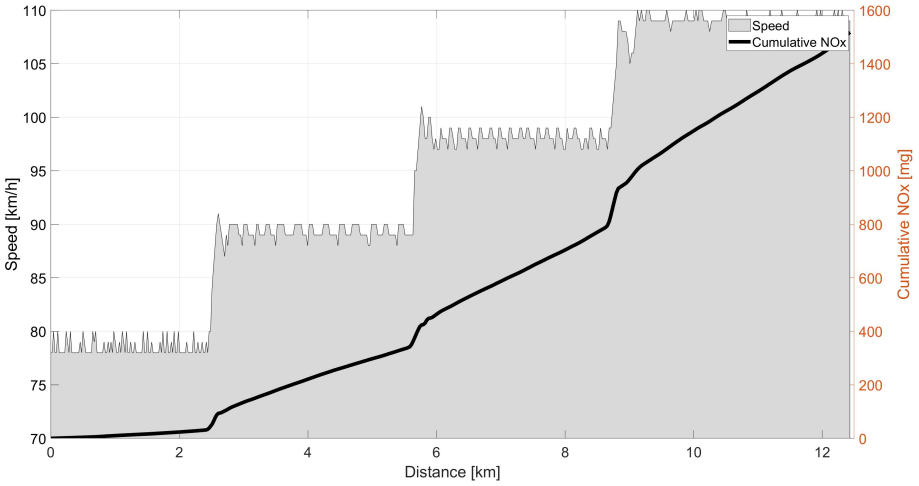

(a)

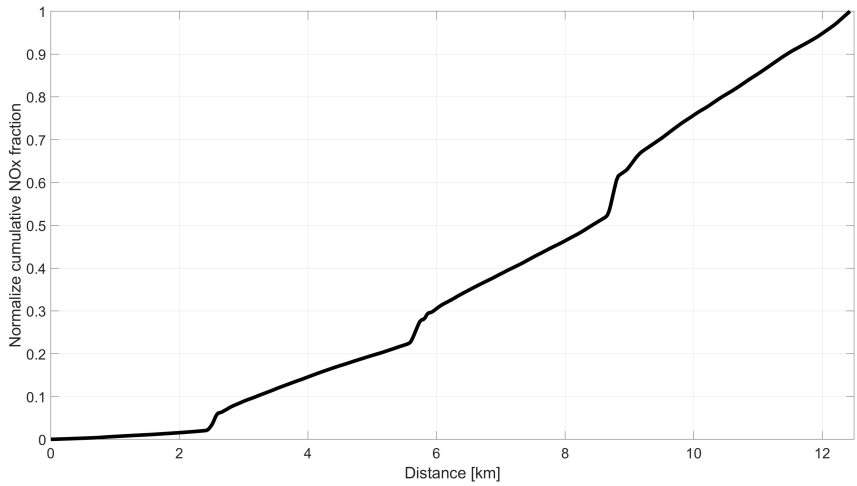

(b)

Figure 4.13: Cumulative NOx mass flow rate emission comparison for the one case of steady speed test(SS.1) for speeds (80,90,100,110)km/h. (a) cumulative NOx mass flow rate comparison with driving cycle in grey (b) Normalized cumulative values for correspondent tests. Test IDs are in Table 4.1

In Figure 4.13 the cumulative and normalize values of NOx for different speeds are shown and as it can be seen the slope of NOx for each speed is different from others and as the speed increases this slope goes up. The slope of the lines increases from 0.7 for 80 km/h to 4 for 110 km/h which means 5.7 times increase when the

speed changes from 80 km/h to 110 km/h.

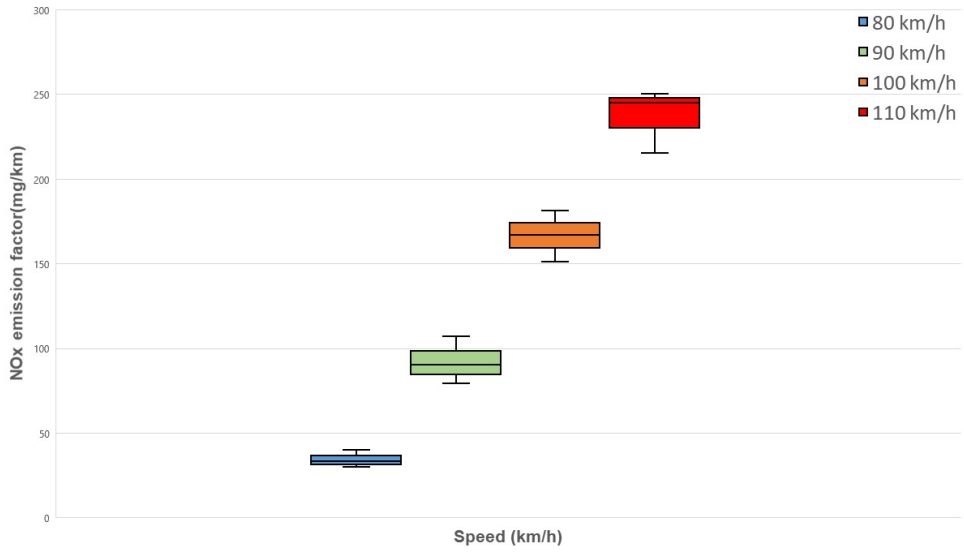

Figure 4.14: A comparison of NOx emission factors in term of mh/km for all steady speed tests (SS.1,SS.2) for speeds (80,90,100,110)km/h

It is expected that increased speed results in aerodynamic drag increasing as the square of speed. As NOx is directly related to vehicle power demand a 2nd-degree polynomial was fitted for NOx emission factors of Figure 4.14. The result shows the NOx emission changes with the speed as a second polynomial ratio of $0.0325V^2 + 0.595V$ over the speeds tested.

As the engine power and slope of the testing route affects the engine load and as a result impacts on NOx emission, so the engine power and NOx emission factor in g/kWh is calculated. In Figure 4.15 the engine power versus time for the constant speed test is shown.

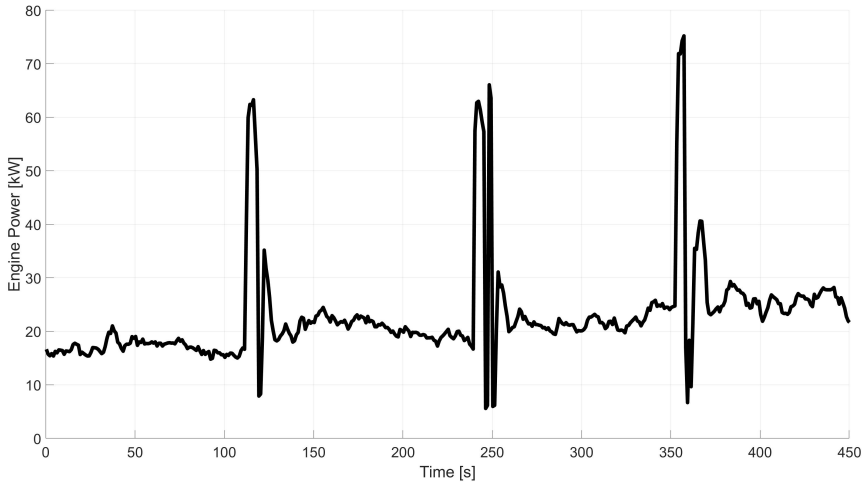

Figure 4.15: Engine power versus time for constant speed test SS.1 for speeds (80,90,100,110)km/h. Test IDs are in Table 4.1.

From Figure 4.15 the total kWh power of the engine during the highway test can be calculated. The total NOx emission is calculated from Figure 4.11, as:

$$Emissionfactor[g/kWh] = \frac{\int_{t1}^{t2} NOxemssion}{\int_{t1}^{t2} Enginepower} \tag{4.1}$$

Figure 4.16 shows the averaged NOx emission factor based on the engine power for all tests done for constant speeds of 80, 90, 100, and 110 km/h.

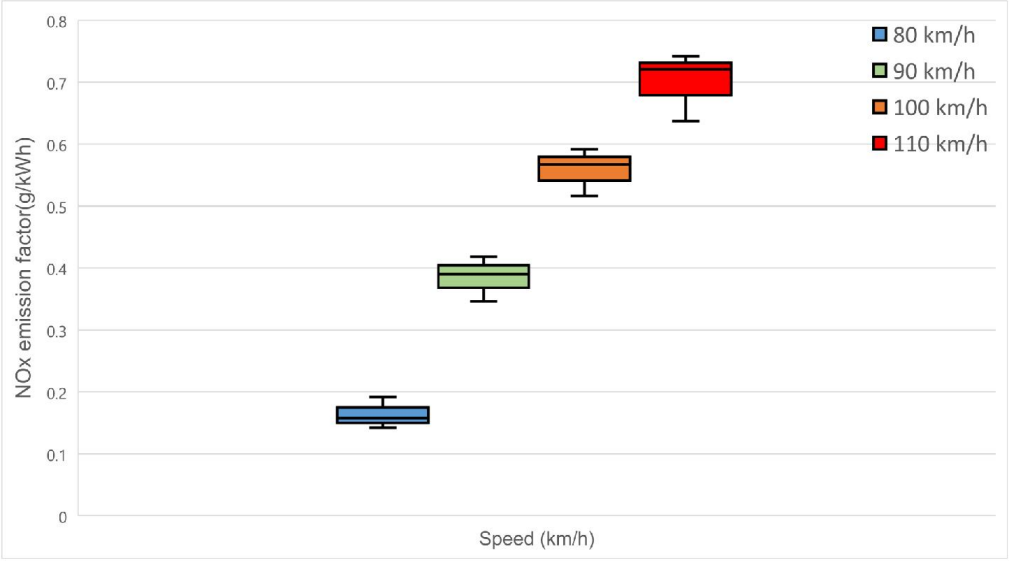

Figure 4.16: A comparison of NOx emission factors in term of g/kWh for all steady speed tests (SS.1,SS.2) for speeds (80,90,100,110)km/h

The NOx emission factors for this test are $(0.159 \pm 0.01)g/kWh$ for $80(km/h)$, $(0.394 \pm 0.03)g/kW$ for $90(km/h)$, $(0.558 \pm 0.04)g/kW$ for $100(km/h)$, and $(0.713 \pm 0.06)g/kW$ for $110(km/h)$.

The pattern of NOx emission factor in Figure 4.16 and 4.14 are similar, indicating the route conditions including road slope is not significant factor in these tests. The aerodynamic drag increase causes higher engine load and so NOx increases in higher speeds.

4.3 Effect of driving behaviour on NOx emissions

Factors that affect the number of emissions are the road condition and the driving style. The PEMS system gives us this opportunity to study these in real driving conditions. In this section, the effect of driving behaviour on emissions is investigated.

4.3.1 Methodology of Driving behaviour conditions definition

To study the effect of different driving behaviour on emissions it is required to define the different driving condition and then test each of them to see how emission changes during each situation.

There are kinematic conditions that driving behaviour can be defined based on. In a reference book of driving cycle for in the use of road measurement of road vehicle emission by TJ Barlow [6], these kinematic conditions are provided and will be used here. In Table 4.3 these parameters are given .

Different cycles and their properties are provided in [6] which can be used as a sample to compare driving behaviours used in this research with others. In Table **??** the properties of driving behaviour used in this research and New European Driving Cycle(NEDC) and EPA FTP-75 which are available in the reference are given [6].

Table 4.3: Kinematic driving behavior parameters[6]

Group	Parameter	Units
Distance related	Total distance	m
Time related	Total time	s
	Driving time	s
	Cruising time	s
	Drive time spent accelerating	s
	Drive time spent decelerating	s
	Time spent braking	s
	Standing time	s
	% of time driving	%
	% of cruising	%
	% of time accelerating	%
	% of time decelerating	%
	% of time braking	%
	% of time standing	%
Speed related	Average trip speed	km/h
	Average driving speed	km/h
	Standard deviation of speed	km/h
	Speed: 75th - 25th percentile	km/h
	Maximum speed	km/h
Acceleration related	Average acceleration	m/s^2
	Average positive acceleration	m/s^2
	Average negative acceleration	m/s^2
	Standard deviation of acceleration	m/s^2
	Standard dev. of positive acceleration	m/s^2
	Acceleration: 75th - 25th percentile	m/s^2
	Number of accelerations	
	Number of accelerations per km	/km
Stop related	Number of stops	
	Number of stops per km	/km
	Average stop duration	s
	Average distance between stops	m

The driving cycle for the driving behaviour tests ID DB.1, DB.2 are provided in Figure 4.17 and 4.18. The kinematic parameters of these two plots are calculated and shown in Table 4.4. In the same Table, kinematic parameters of two defined driving cycle of NEDC and FTP-75 are presented for comparison.

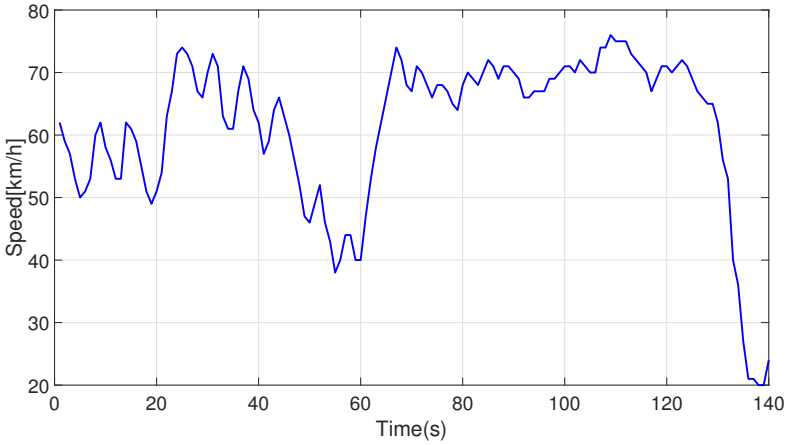

Figure 4.17: Driving cycle for the Driving behaviour type 1(Test ID DB.1)

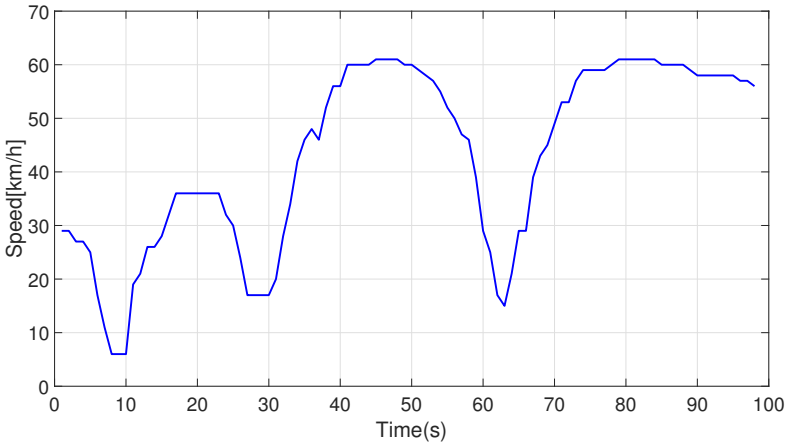

Figure 4.18: Driving cycle for the Driving behaviour type 2(Test ID DB.2)

Table 4.4: Kinematic parameters values for two defined driving behaviours and Extra-urban driving cycle values as a sample

Parameter	**Test ID DB.1**	**Test ID DB.2**	**NEDC**	**FTP-75**
Total driving time	141(s)	98(s)	1180(s)	1874(s)
Total driving distance	2.4(km)	1.2(km)	11(km)	17.8(km)
Average speed	61 (km/h)	43 (km/h)	42(km/h)	34(km/h)
Number of acceleration	32	8	31	61
% of time positive acceleration	36 %	27 %	23 %	36%
% of time negative acceleration	31 %	22 %	17 %	30 %
Average positive acceleration	2.92 $(\frac{m}{s^2})$	0.78 $(\frac{m}{s^2})$	0.53$(\frac{m}{s^2})$	0.42 $(\frac{m}{s^2})$
Average negative acceleration	-2.83 $(\frac{m}{s^2})$	-0.64 $(\frac{m}{s^2})$	-0.71 $(\frac{m}{s^2})$	-0.45 $(\frac{m}{s^2})$

The two driving conditions tested in this research are denoted aggressive driving behaviour (DB.1) and normal driving behaviour (DB.2). In DB.1 the driver has high acceleration/deceleration and drives aggressively. As it is shown in Table **??** the number and average of acceleration and deceleration for this type of driving behaviour are 4-5 times more than the second type which speed changes smoothly and avoid rough acceleration. These conditions can be also defined through the throttle position data that is available from the OBD device. In the throttle position results provided in Figure 4.19 it is shown how the instantaneous acceleration changes throttle position and causes more use of fuel.

The first driving behaviour is a driving condition that the acceleration is high, so the

throttle valve opens immediately with many large throttle peaks.

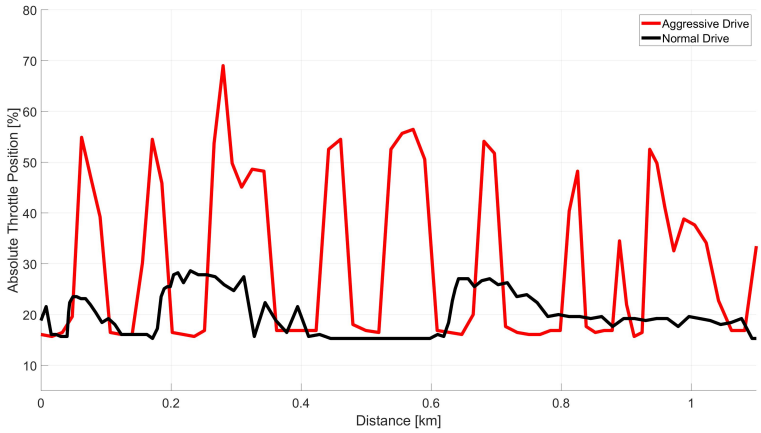

Figure 4.19: Comparison for the throttle position of the engine in the tests with driving behaviour type 1(DB.1) and 2(DB.2)

4.3.2 Effects of driving behaviour on NOx emission factors

The NOx results for two driving behaviour conditions described in the last section are provided here. In this test the engine is fully warmed up. The plots are shown versus distance and the difference between the emission of aggressive and normal driving behaviour can be seen.

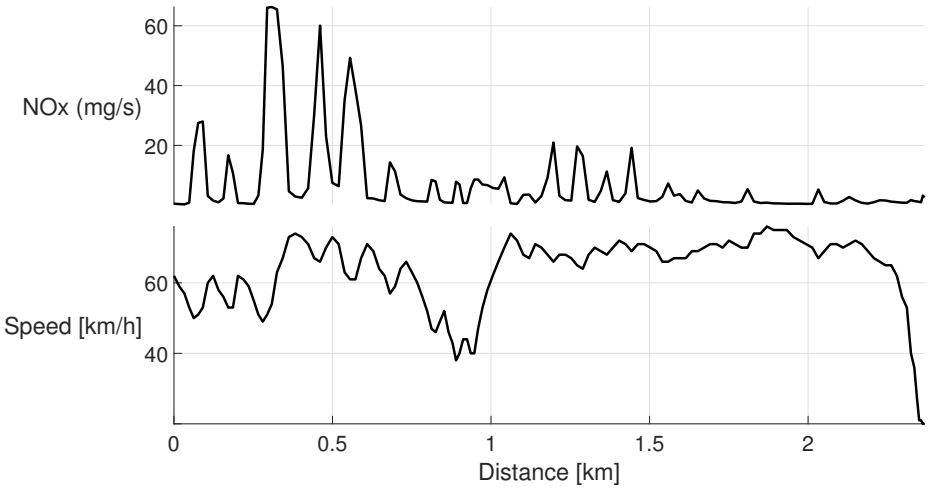

Figure 4.20: Exhaust NOx mass flow rate versus distance aggressive driving behaviour test DB.1 above and correspondent speed below. Test IDs are in Table 4.1

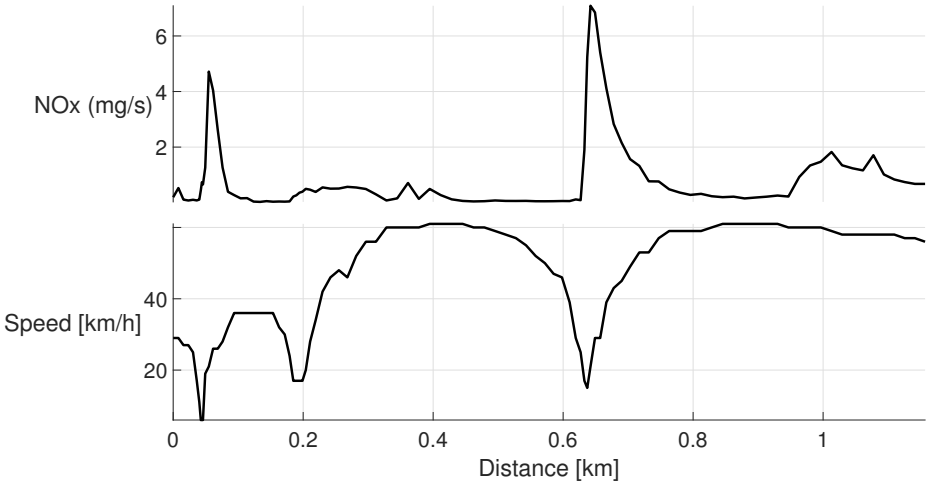

Figure 4.21: Exhaust NOx mass flow rate versus distance for normal driving behaviour test DB.2 above and correspondent speed below. Test IDs are in Table 4.1

The NOx emission and speed versus distance for aggressive and normal driving behaviour are shown in Figure 4.20and 4.21. The tests were done 2 times, the NOx emission factors for these tests are $(856)mg/km$ for aggressive driving behaviour and $(67)mg/km$ for normal driving behaviour. The reason for this high emission for aggressive driving behaviour is that high transient NOx emissions represent a large

number of total NOx emissions, although they are produced during a small percentage of driving time. These high NOx emissions could reduce emission factors by 30-82 percent[69]. The emission of high transient NOx emissions are related to characteristic speed modes of urban, rural and motorway sections, and are produced in a narrow engine speed range of transient engine conditions. In general, the probability of producing high instantaneous NOx emissions increases as the engine speed, the exhaust gas temperature or the vehicle speed is increased.

Also, it is shown that in normal driving behaviour NOx emission factor is in the range of emission in warm weather and passes emission regulation however it exceeds the regulation in aggressive driving which emphasizes the effect of high transient NOx emissions.

4.3.3 Comparison of NOx emissions for two cases of driving behaviour

To make a comparison between the NOx emission data collected during aggressive(DB.1) and normal(DB.2) driving behaviour tests, the tests from both driving behaviours are put in Figure 4.22 to show the difference of NOx mass flow rate emissions in these two tests. These tests are done in the same driving route (Route C) and at the same ambient temperature.

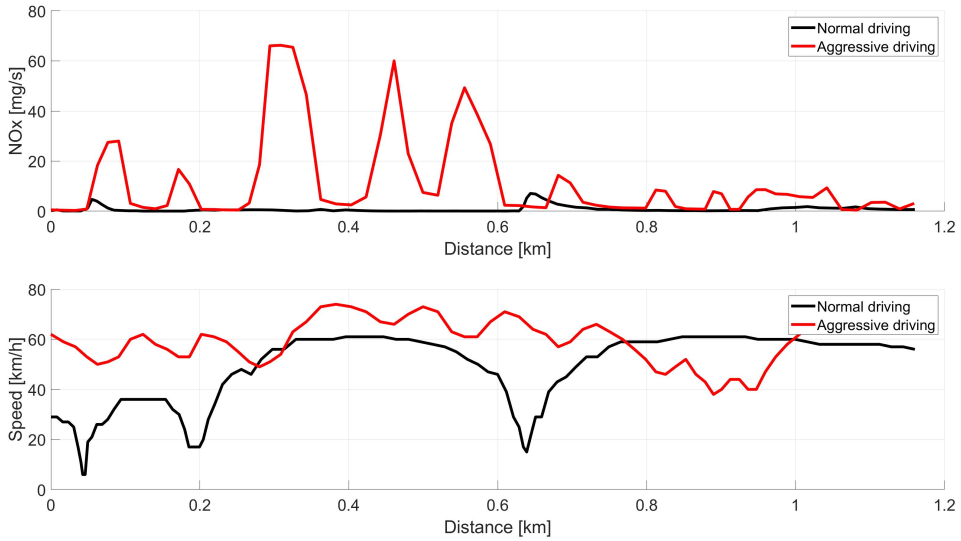

Figure 4.22: A comparison of NOx mass flow rate for two cases test in aggressive(DB.1) and normal driving behaviour (DB.2) above and correspondent speed below. Test IDs are in Table 4.1

The NOx emission and speed versus distance for aggressive and normal driving behaviour are shown in Figure 4.22 in the same plot to see the difference of NOx mass flow rate for two types of driving behaviour. The NOx emission factors for this test are $(856)mg/km$ for aggressive driving behaviour and $(67)mg/km$ for normal driving behaviour.

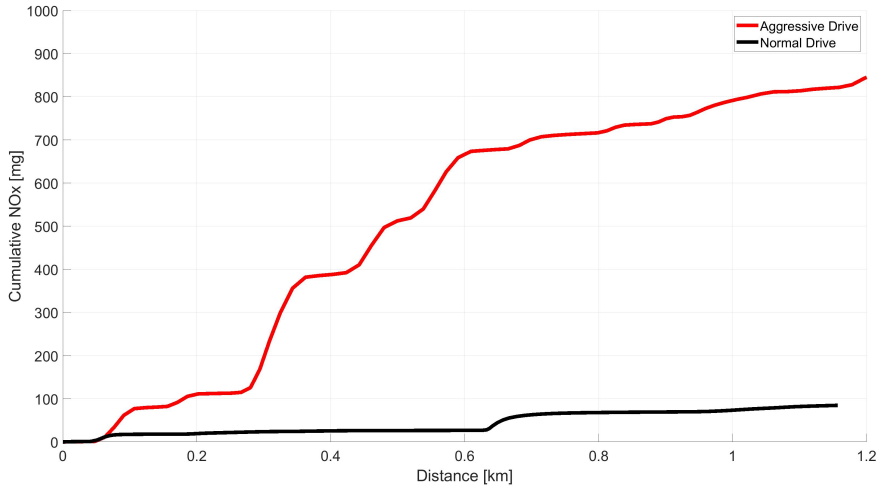

(a)

Figure 4.23: Cumulative NOx mass flow rate emission comparison for one case of driving behaviour test for agressive (DB.1) and normal(DB.2) driving behaviour. Test IDs are in Table 4.1

A comparison of NOx emission factor for the same driving route (Route C) and at the same ambient temperature shows an increase of NOx emissions by a factor of 12.7 for driving behaviour quantified by number of acceleration, averaage speed, and average positive and negative acceleration in Table 4.4.

Figure 4.23 shows cumulative and normalize NOx mass flow rate emission comparison for two different driving behaviour type DB.1 and DB.2. This shows a significant increase in NOx emission in driving behaviour with immediate acceleration and deceleration. This means a driving style with high values of average positive and negative acceleration leads to a high amount of emission which can go up to 12 times higher than a normal driving behaviour with a small amount of positive and negative acceleration.

The result has important implications for applications such as autonomous driving or using connected vehicles where driving behaviour between stop and starts and each intersections can be optimized.

Chapter 5

Conclusion

Conclusions and possible future work of this research are presented in this chapter.

5.1 Effects of ambient temperature on NOx and particulate emissions

The experimental results of this research show that the NOx emission factor of the Toyota Highlander model 2008 with a GDI engine and TWC in the exhaust (without GPF) for the test at $-15°C$ ambient temperature is at $(466 \pm 57) mg/km$ for NOx and $(1.59 \pm 1) \times 10^{11} \#/km$ for PN over an urban drive cycle A.

As there is no emission factor available for $-15°C$ ambient for NOx and PN, the values are compared with factors available in standard emission regulations and emission models noting the fact that all testing parameters such as driving cycle are different. The NOx emission limit for US EPA Tier 2 for LDV is at 65 mg/km. The NOx emission factor of the current study at $-15°C$ was 7.1 times higher than that of the emission regulation limit of the same vehicle at the time of production for this real urban driving cycle.

Increased NOx is attributed to many factors such as vehicle age, mileage, ageing

of TWC and possible lack of proper maintenance. However, in the same emission regulation, conformity of only 1.1 overage is allowed. The much larger value of NOx reported in this study comes from real-world driving instead of standard cycle driving and the cold ambient of $-15°C$ which is not tested in any standard test procedure. The results for NOx emission factor with the same vehicle and same driving cycle at $+5°C$ ambient temperature is $(67 \pm 9)(mg/km)$ for NOx and $(6.8 \pm 2.4) \times 10^{10}(\#/km)$ for PN. The PN value for the test at $-15°C$ is 2.3 times higher than PN emission factors at an ambient temperature of $+5°C$.

The results for the warm temperature test at an ambient temperature of $+15°C$ shows the NOx emission factor is $(56 \pm 7)(mg/km)$ for NOx which is within the Tier2 emission limit.

5.2 Effects of vehicle speed on NOx and particulate emission

The experimental results show the NOx emission factors for the constant speed test goes up quadratically with increasing speed as expected. The results show the emission factor of (35 ± 7) mg/km for 80 km/h, (98 ± 12) mg/km for 90 km/h, (174 ± 9) mg/km for 100 km/h, (232 ± 24) mg/km for 110 km/h. It is expected that increased speed affects engine specific power (engine torque) at the 2nd order polynomial ratio. As NOx is directly related to vehicle power demand a 2nd-degree polynomial was fitted for NOx emission factors. The result shows the NOx emission changes by speed with a second polynomial ratio of $0.0325V^2 + 0.595V$.

5.3 Effects of driving behaviour on the NOx and particulate number emission

Real-world driving NOx emission of the vehicle was measured using two types of driving behaviours quantified by the average positive acceleration of the vehicle on the same route.

A comparison of NOx emission factors for the same driving route and at the same ambient temperature shows an increase of NOx emissions by 12.7 folds for driving behaviour quantified by average positive acceleration. The NOx result indicates that the NOx emission factor increases from (67 ± 7) mg/km for normal driving behaviour to (856 ± 63) for aggressive driving behaviour. The average positive acceleration for the normal driving behaviour and aggressive driving behaviour were 0.78 $(\frac{m}{s^2})$ and 2.92 $(\frac{m}{s^2})$; respectively. This reinforces the idea that driver behaviour can be used to minimize fuel and emissions, particularly in an autonomous vehicle where traffic light information could be used to minimizing acceleration.

5.4 Future work

- Adding CO, HC, and CO_2 sensors to the NOx and particulate sensors used in this research, to would allow a more comprehensive comparison to measure emission factor of these gases.

- Implementing a more vehicle suitable and faster responding PEGASOR particle sensor in the Toyota Highlander car would allow an interesting comparison of the CPC and PEGASOR.

- More particle number data in both cold and warm weather to allow a further

comparison between warm and cold weather PN emission factors.

- Expanding the cold weather temperatures range, from $-15°C$ to $-30°C$ (the city of Edmonton experiences temperatures as cold as $-30°C$) to get a more accurate non-linear emission factor model.

- Testing vehicle for more speeds and more kinds of driving behaviour in urban conditions.

Bibliography

[1] Aerosol devices Inc. Magic™ cpc specifications. https://aerosoldevices.com/magic-cpc-specifications/, May 2020.

[2] Dekati di-1000 dilutor. https://www.dekati.com/products/dekati-diluter/, May 2020.

[3] Li-cor 850 manual. https://www.licor.com/documents/gz8gaf0ls5vhvpl52xtmyr8mfoh5kwe8, May 2020.

[4] ECM engine control and monitoring. NOx CANt specification. http://www.ecm-co.com/product.asp?ncant, May 2020.

[5] VEPEEK OBD specification. https://www.veepeak.com/product/obdcheck-ble/, May 2020.

[6] Tim J Barlow, S Latham, IS McCrae, and PG Boulter. A reference book of driving cycles for use in the measurement of road vehicle emissions. *TRL Published Project Report*, 2009.

[7] Naaqs 2019 report of air pollution. https://www.epa.gov/air-trends/air-quality-national-summary#air-quality-trends, May 2020.

[8] US Environmental Protection Agency. Fast facts on transportation greenhouse gas emissions.

[9] Ruixiong Zhang, Yuhang Wang, Charles Smeltzer, Hang Qu, William Koshak, and K Folkert Boersma. Comparing omi-based and epa aqs in situ no 2 trends: towards understanding surface no x emission changes. *Atmospheric Measurement Techniques*, 11(7):3955–3967, 2018.

[10] Jaye Ellis. Developments in canadian environmental law: self regulatory initiatives under the new canadian environmental protection act. *OPENAIRE*, 2002.

[11] Canadian Environmental and Sustainability Indicators. Air health trends.

[12] Jae C Jung and Elizabeth Sharon. The volkswagen emissions scandal and its aftermath. *Global Business and Organizational Excellence*, 38(4):6–15, 2019.

[13] Motor Vehicle Emission Simulator. User guide for MOVES2014. *US Environmental Protection Agency*, 2014.

[14] Masoud Aliramezani, Charles Robert Koch, Marc Secanell, Robert E Hayes, and Ron Patrick. An electrochemical model of an amperometric NOx sensor. *Sensors and Actuators B: Chemical*, 290:302–311, 2019.

[15] 2kw honda eu 20i generator. `https://scanhi.com.au/equipments/honda-generators/honda-inverter-generators/eu20i/`, May 2020.

[16] Frederica Perera. Pollution from fossil-fuel combustion is the leading environmental threat to global pediatric health and equity: solutions exist. *International journal of environmental research and public health*, 15(1):16, 2018.

[17] Edward Weiner. Urban transportation planning in the united states: history, policy, and practice. 2016.

[18] Eleanor Setton, Julian D Marshall, Michael Brauer, Kathryn R Lundquist, Perry Hystad, Peter Keller, and Denise Cloutier-Fisher. The impact of daily mobility on exposure to traffic-related air pollution and health effect estimates. *Journal of exposure science & environmental epidemiology*, 21(1):42–48, 2011.

[19] Greg Dotson. State authority to regulate mobile source greenhouse gas emissions, part i: History and current challenge. *Envtl. L. Rep. News & Analysis*, 49:11037, 2019.

[20] John Byrne, Kristen Hughes, Wilson Rickerson, and Lado Kurdgelashvili. American policy conflict in the greenhouse: Divergent trends in federal, regional, state, and local green energy and climate change policy. *Energy Policy*, 35(9):4555–4573, 2007.

[21] Imad A Khalek, Thomas L Bougher, Patrick M Merritt, and Barbara Zielinska. Regulated and unregulated emissions from highway heavy-duty diesel engines complying with us environmental protection agency 2007 emissions standards. *Journal of the Air & Waste Management Association*, 61(4):427–442, 2011.

[22] Mark Sellnau, Kevin Hoyer, Wayne Moore, Matthew Foster, James Sinnamon, and William Klemm. Advancement of gdci engine technology for us 2025 cafe and tier 3 emissions. Technical report, SAE Technical Paper, 2018.

[23] Anne E Smith. Technical comments on the regulatory impact analysis supporting epa's proposed rule for utility mact and revised nsps (76 fr 24976). *August*, 3:2011, 2011.

[24] Qingwen Song and George Zhu. Model-based closed-loop control of urea scr exhaust aftertreatment system for diesel engine. *SAE Transactions*, pages 102–110, 2002.

[25] Timothy Johnson. Vehicular emissions in review. *SAE International Journal of Engines*, 7(3):1207–1227, 2014.

[26] Magdi Khair, Jacques Lemaire, and Stefan Fischer. Integration of exhaust gas recirculation, selective catalytic reduction, diesel particulate filters, and fuel-borne catalyst for no x/pm reduction. *SAE transactions*, pages 1607–1613, 2000.

[27] Klaus Harth, Knut Wassermann, Mirko Arnold, Stephan Siemund, Attilio Siani, Thomas Schmitz, and Torsten Neubauer. Catalyzed gasoline particulate filters. integrated solutions for stringent emission control; katalysierte benzin partikelfilter. integrierte loesungen fuer strenge emissionsregulierungen. 2013.

[28] Georgios Fontaras, Nikiforos-Georgios Zacharof, and Biagio Ciuffo. Fuel consumption and co2 emissions from passenger cars in europe–laboratory versus real-world emissions. *Progress in Energy and Combustion Science*, 60:97–131, 2017.

[29] RS O'Driscoll, HM ApSimon, T Oxley, and N Molden. Portable emissions measurement system (PEMS) data for euro 6 diesel cars and comparison with emissions modelling. *J. Earth Sci. Geotech. Eng.*, 6:15–28, 2016.

[30] Nils Hooftman, Maarten Messagie, Joeri Van Mierlo, and Thierry Coosemans. A review of the european passenger car regulations–real driving emissions vs local air quality. *Renewable and Sustainable Energy Reviews*, 86:1–21, 2018.

[31] Hui He and Lingzhi Jin. A historical review of the us vehicle emission compliance program and emission recall cases. *White paper*, 2017.

[32] Bart Degraeuwe and Martin Weiss. Does the new european driving cycle

(NEDC) really fail to capture the nox emissions of diesel cars in europe? *Environmental pollution*, 222:234–241, 2017.

[33] Leo Alphonse Gerard Breton. Real-time on-road vehicle exhaust gas modular flowmeter and emissions reporting system, May 7 2002. US Patent 6,382,014.

[34] R Parloff. How VW paid 25 dollar billion for 'dieselgate'—and got off easy. *Fortune, Feb*, 6, 2018.

[35] Luann J Lynch, Cameron Cutro, and Elizabeth Bird. The volkswagen emissions scandal. 2016.

[36] Natasha Terry-Armstrong et al. The volkswagen scandal-the high cost of corporate deceit. *Busidate*, 24(1):9, 2016.

[37] EPA. Epa, california notify volkswagen of clean air act violations/carmaker allegedly used software that circumvents emissions testing for certain air pollutants. 2015.

[38] Eddie Cottle. The myth of a green economy and green jobs: What strategy for labour? *Rosa Luxemburgo Stiftung*, 2015.

[39] RJ Vermeulen and Willar Vonk. *On-road emission measurements with PEMS on a heavy-duty truck with a retrofit dual-fuel system, using diesel and CNG.* Delft: TNO, 2013.

[40] Xiaoliang Wang, John G Watson, Judith C Chow, Steven Gronstal, Steven D Kohl, et al. An efficient multipollutant system for measuring real-world emissions from stationary and mobile sources. *Aerosol and Air Quality Research*, 12(2):145–160, 2012.

[41] Jinyoung Ko, Jeonghun Son, Cha-Lee Myung, and Simsoo Park. Comparative study on low ambient temperature regulated/unregulated emissions characteristics of idling light-duty diesel vehicles at cold start and hot restart. *Fuel*, 233:620–631, 2018.

[42] M Clairotte, TW Adam, AA Zardini, U Manfredi, G Martini, A Krasenbrink, A Vicet, E Tournié, and C Astorga. Effects of low temperature on the cold start gaseous emissions from light duty vehicles fuelled by ethanol-blended gasoline. *Applied Energy*, 102:44–54, 2013.

[43] David Choi, Megan Beardsley, David Brzezinski, John Koupal, and James Warila. Moves sensitivity analysis: the impacts of temperature and humidity on emissions. In *US EPA–Proceedings from the 19th Annual International Emission Inventory Conference, Ann Arbor, MI*, 2010.

[44] Suriya Vallamsundar and Jie Lin. MOVES versus mobile: comparison of greenhouse gas and criterion pollutant emissions. *Transportation research record*, 2233(1):27–35, 2011.

[45] Hatem Abou-Senna, Essam Radwan, Kurt Westerlund, and C David Cooper. Using a traffic simulation model (VISSIM) with an emissions model (MOVES) to predict emissions from vehicles on a limited-access highway. *Journal of the Air & Waste Management Association*, 63(7):819–831, 2013.

[46] United States Environmental Protection Agency. MOVES2014a: Latest version of motor vehicle emission simulator (moves). 2018.

[47] Tingting Liao, Shan Wang, Jie Ai, Ke Gui, Bolong Duan, Qi Zhao, Xiao Zhang, Wanting Jiang, and Yang Sun. Heavy pollution episodes, transport pathways and potential sources of pm2. 5 during the winter of 2013 in chengdu (china). *Science of the Total Environment*, 584:1056–1065, 2017.

[48] Rencheng Zhu, Jingnan Hu, Xiaofeng Bao, Liqiang He, Yitu Lai, Lei Zu, Yufei Li, and Sheng Su. Tailpipe emissions from gasoline direct injection (gdi) and port fuel injection (pfi) vehicles at both low and high ambient temperatures. *Environmental Pollution*, 216:223–234, 2016.

[49] Ricardo Suarez-Bertoa and Covadonga Astorga. Impact of cold temperature on euro 6 passenger car emissions. *Environmental pollution*, 234:318–329, 2018.

[50] M Rafael, M Sanchez, V Mucino, J Cervantes, and A Lozano. Impact of driving styles on exhaust emissions and fuel economy from a heavy-duty truck: laboratory tests. *International Journal of Heavy Vehicle Systems*, 13(1-2):56–73, 2006.

[51] Zejian Deng, Duanfeng Chu, Chaozhong Wu, Yi He, and Jian Cui. Curve safe speed model considering driving style based on driver behaviour questionnaire. *Transportation research part F: traffic psychology and behaviour*, 65:536–547, 2019.

[52] Adriano Alessandrini, Fabio Orecchini, Fernando Ortenzi, and Federico Villatico Campbell. Drive-style emissions testing on the latest two honda hybrid technologies. *European Transport Research Review*, 1(2):57–66, 2009.

[53] Britt A Holmén and Debbie A Niemeier. Characterizing the effects of driver variability on real-world vehicle emissions. *Transportation Research Part D: Transport and Environment*, 3(2):117–128, 1998.

[54] Yuhan Huang, Elvin CY Ng, John L Zhou, Nic C Surawski, Edward FC Chan, and Guang Hong. Eco-driving technology for sustainable road transport: A review. *Renewable and Sustainable Energy Reviews*, 93:596–609, 2018.

[55] Bin Ran, Peter J Jin, David Boyce, Tony Z Qiu, and Yang Cheng. Perspectives on future transportation research: Impact of intelligent transportation system technologies on next-generation transportation modeling. *Journal of Intelligent Transportation Systems*, 16(4):226–242, 2012.

[56] Wei Xiong, ShuXian He, and Tony Z Qiu. Research on connected vehicle architecture based on dsrc technology. In *2017 4th international conference on transportation information and safety (ICTIS)*, pages 530–534. IEEE, 2017.

[57] Qing Li, Fengxiang Qiao, and Lei Yu. Vehicle emission implications of drivers' smart advisory system for traffic operations in work zones. *Journal of the Air & Waste Management Association*, 66(5):446–455, 2016.

[58] L Rubino, P Bonnel, R Hummel, A Krasenbrink, U Manfredi, and G De Santi. On-road emissions and fuel economy of light duty vehicles using pems: Chase-testing experiment. *SAE international Journal of Fuels and Lubricants*, 1(1):1454–1468, 2009.

[59] Martin Weiss, Pierre Bonnel, Rudolf Hummel, Urbano Manfredi, Rinaldo Colombo, Gaston Lanappe, Philippe Le Lijour, Mirco Sculati, et al. Analyzing on-road emissions of light-duty vehicles with portable emission measurement systems (pems). *JRC Scientific and Technical Reports, EUR*, 24697, 2011.

[60] José M Luján, Vicente Bermúdez, Vicente Dolz, and Javier Monsalve-Serrano. An assessment of the real-world driving gaseous emissions from a euro 6 light-duty diesel vehicle using a portable emissions measurement system (pems). *Atmospheric Environment*, 174:112–121, 2018.

[61] Barouch Giechaskiel, Theodoros Vlachos, Francesco Riccobono, Fausto Forni, Rinaldo Colombo, Francois Montigny, Philippe Le-Lijour, Massimo Carriero,

Pierre Bonnel, and Martin Weiss. Implementation of portable emissions measurement systems (pems) for the real-driving emissions (rde) regulation in europe. *JoVE (Journal of Visualized Experiments)*, (118):e54753, 2016.

[62] Ricardo Suarez-Bertoa, Tero Lähde, Jelica Pavlovic, Victor Valverde, Michael Clairotte, and Barouch Giechaskiel. Laboratory and on-road evaluation of a gpf-equipped gasoline vehicle. *Catalysts*, 9(8):678, 2019.

[63] Piotr Bielaczyc, Jerzy Merkisz, Jacek Pielecha, and Joseph Woodburn. Rde-compliant pems testing of a gasoline euro 6d-temp passenger car at two ambient temperatures with a focus on the cold start effect. Technical report, SAE Technical Paper, 2020.

[64] Abdulfatah Abdu Yusuf and Freddie L Inambao. Effect of cold start emissions from gasoline-fueled engines of light-duty vehicles at low and high ambient temperatures: recent trends. *Case Studies in Thermal Engineering*, 14:100417, 2019.

[65] Junhong Park, Jongtae Lee, Sunmoon Kim, Jeongsoo Kim, and Keunwhan Ahn. A study on the emission characteristics of korean light-duty vehicles in real-road driving conditions. *Transactions of the Korean Society of Automotive Engineers*, 21(6):123–134, 2013.

[66] Martin Weiss, Pierre Bonnel, Jörg Kühlwein, Alessio Provenza, Udo Lambrecht, Stefano Alessandrini, Massimo Carriero, Rinaldo Colombo, Fausto Forni, Gaston Lanappe, et al. Will euro 6 reduce the NOx emissions of new diesel cars?–insights from on-road tests with portable emissions measurement systems (pems). *Atmospheric Environment*, 62:657–665, 2012.

[67] Basil Daham, Hu Li, Gordon E Andrews, Karl Ropkins, James E Tate, and

Margaret C Bell. Comparison of real world emissions in urban driving for euro 1-4 vehicles using a pems. Technical report, SAE Technical Paper, 2009.

[68] John May, Dirk Bosteels, and Cecile Favre. An assessment of emissions from light-duty vehicles using pems and chassis dynamometer testing. *SAE International Journal of Engines*, 7(3):1326–1335, 2014.

[69] Zamir Mera, Natalia Fonseca, José-María López, and Jesús Casanova. Analysis of the high instantaneous NOx emissions from euro 6 diesel passenger cars under real driving conditions. *Applied Energy*, 242:1074–1089, 2019.

[70] Taewoo Lee, Jiyoung Kim, Junhong Park, Sangzin Jeon, Jongtae Lee, and Jeongsoo Kim. Influence of driving routes and seasonal conditions to real-driving NOx emissions from light diesel vehicles. *Transactions of the Korean Society of Automotive Engineers*, 22(1):148–156, 2014.

[71] Taewoo Lee, Junhong Park, Sangil Kwon, Jongtae Lee, and Jeongsoo Kim. Variability in operation-based NOx emission factors with different test routes, and its effects on the real-driving emissions of light diesel vehicles. *Science of the total environment*, 461:377–385, 2013.

[72] Wojciech Gis, Maciej Gis, and Jacek Pielecha. Evaluation of exhaust emissions in real driving emissions tests in different test route configurations. In *International Scientific Conference Transport of the 21st Century*, pages 143–153. Springer, 2019.

[73] Ricardo Suarez-Bertoa, Victor Valverde, Michael Clairotte, Jelica Pavlovic, Barouch Giechaskiel, Vicente Franco, Zlatko Kregar, and Covadonga Astorga. On-road emissions of passenger cars beyond the boundary conditions of the real-driving emissions test. *Environmental research*, 176:108572, 2019.

[74] Barouch Giechaskiel, Athanasios Mamakos, Joseph Woodburn, Andrzej Szczotka, and Piotr Bielaczyc. Evaluation of a 10 nm particle number portable emissions measurement system (pems). *Sensors*, 19(24):5531, 2019.

[75] A Kontses, G Triantafyllopoulos, L Ntziachristos, and Z Samaras. Particle number (pn) emissions from gasoline, diesel, lpg, cng and hybrid-electric light-duty vehicles under real-world driving conditions. *Atmospheric Environment*, 222:117126, 2020.

[76] Hwan S Chong, Sangil Kwon, Yunsung Lim, and Jongtae Lee. Real-world fuel consumption, gaseous pollutants, and co2 emission of light-duty diesel vehicles. *Sustainable Cities and Society*, 53:101925, 2020.

[77] Kangjin Kim, Wonyong Chung, Myungsoo Kim, Charyung Kim, Cha-Lee Myung, and Simsoo Park. Inspection of pn, co2, and regulated gaseous emissions characteristics from a gdi vehicle under various real-world vehicle test modes. *Energies*, 13(10):2581, 2020.

[78] Cavan McCaffery, Hanwei Zhu, Chengguo Li, Thomas D Durbin, Kent C Johnson, Heejung Jung, Rasto Brezny, Michael Geller, and Georgios Karavalakis. On-road gaseous and particulate emissions from gdi vehicles with and without gasoline particulate filters (gpfs) using portable emissions measurement systems (pems). *Science of The Total Environment*, 710:136366, 2020.

[79] Barouch Giechaskiel, Matthias Schwelberger, Christophe Delacroix, Massimo Marchetti, Marc Feijen, Klaus Prieger, Sven Andersson, and Hua Lu Karlsson. Experimental assessment of solid particle number portable emissions measurement systems (pems) for heavy-duty vehicles applications. *Journal of Aerosol Science*, 123:161–170, 2018.

[80] Lars Gidhagen, Christer Johansson, Joakim Langner, and VL Foltescu. Urban scale modeling of particle number concentration in stockholm. *Atmospheric Environment*, 39(9):1711–1725, 2005.

[81] Theodoros Grigoratos, Georgios Fontaras, Barouch Giechaskiel, and Nikiforos Zacharof. Real world emissions performance of heavy-duty euro vi diesel vehicles. *Atmospheric environment*, 201:348–359, 2019.

[82] Barouch Giechaskiel. Particle number emissions of a diesel vehicle during and between regeneration events. *Catalysts*, 10(5):587, 2020.

[83] Victor Valverde and Barouch Giechaskiel. Assessment of gaseous and particulate emissions of a euro 6d-temp diesel vehicle driven> 1300 km including six diesel particulate filter regenerations. *Atmosphere*, 11(6):645, 2020.

[84] Seokjoo Kwon, Sangil Kwon, Jongtae Lee, Seonil Oak, Youngho Seo, Sungwook Park, and Mun Soo Chon. Data evaluation methods for real driving emissions using portable emissions measurement system (pems). *Transactions of the Korean Society of Mechanical Engineers, B*, 39(12):965–973, 2015.

[85] Roberto A Varella, Marta V Faria, Pablo Mendoza-Villafuerte, Patrícia C Baptista, Luis Sousa, and Gonçalo O Duarte. Assessing the influence of boundary conditions, driving behavior and data analysis methods on real driving co2 and NOx emissions. *Science of the Total Environment*, 658:879–894, 2019.

[86] Shengli Wei, Tongyuan Ding, Shupei Zhang, Ping Tao, and Jie Chen. Analysis of vehicle co and NOx road emissions test based on pems. *Energy Sources, Part A: Recovery, Utilization, and Environmental Effects*, pages 1–15, 2020.

[87] Rosalind O'Driscoll, Marc EJ Stettler, Nick Molden, Tim Oxley, and Helen M ApSimon. Real world co2 and NOx emissions from 149 euro 5 and 6 diesel,

gasoline and hybrid passenger cars. *Science of the total environment*, 621:282–290, 2018.

[88] Dirk Bosteels. Real driving emissions and test cycle data from 4 modern european vehicles. In *IQPC 2nd International Conference Real Driving Emissions*, volume 18, 2014.

[89] Michael Giraldo and José I Huertas. Real emissions, driving patterns and fuel consumption of in-use diesel buses operating at high altitude. *Transportation Research Part D: Transport and Environment*, 77:21–36, 2019.

[90] Victor Valverde, Bernat Adrià Mora, Michaël Clairotte, Jelica Pavlovic, Ricardo Suarez-Bertoa, Barouch Giechaskiel, Covadonga Astorga-LLorens, and Georgios Fontaras. Emission factors derived from 13 euro 6b light-duty vehicles based on laboratory and on-road measurements. *Atmosphere*, 10(5):243, 2019.

[91] Barouch Giechaskiel, Simone Casadei, Michele Mazzini, Mario Sammarco, Gisella Montabone, Roberto Tonelli, Mauro Deana, Giovanni Costi, Francesco Di Tanno, Maria Vittoria Prati, et al. Inter-laboratory correlation exercise with portable emissions measurement systems (pems) on chassis dynamometers. *Applied Sciences*, 8(11):2275, 2018.

[92] B Giechaskiel, T Lahde, R Suarez-Bertoa, M Clairotte, T Grigoratos, A Zardini, A Perujo, and G Martini. Particle number measurements in the european legislation and future jrc activities. *Combustion Engines*, 57, 2018.

[93] Ricardo Suarez-Bertoa, Martin Pechout, Michal Vojtíšek, and Covadonga Astorga. Regulated and non-regulated emissions from euro 6 diesel, gasoline and cng vehicles under real-world driving conditions. *Atmosphere*, 11(2):204, 2020.

[94] Piotr Pajdowski, Joseph Woodburn, Piotr Bielaczyc, and Bartosz Puchałka. Development of rde/isc test methodology in light of euro 6d/vi emissions limits. *Combustion Engines*, 58, 2019.

[95] Barouch Giechaskiel, Pierre Bonnel, Adolfo Perujo, and Panagiota Dilara. Solid particle number (spn) portable emissions measurement systems (pems) in the european legislation: A review. *International Journal of Environmental Research and Public Health*, 16(23):4819, 2019.

[96] Barouch Giechaskiel, Tero Lähde, Sawan Gandi, Stefan Keller, Philipp Kreutziger, and Athanasios Mamakos. Assessment of 10-nm particle number (pn) portable emissions measurement systems (pems) for future regulations. *International Journal of Environmental Research and Public Health*, 17(11):3878, 2020.

[97] Pablo Mendoza-Villafuerte, Ricardo Suarez-Bertoa, Barouch Giechaskiel, Francesco Riccobono, Claudia Bulgheroni, Covadonga Astorga, and Adolfo Perujo. NOx, nh3, n2o and pn real driving emissions from a euro vi heavy-duty vehicle. impact of regulatory on-road test conditions on emissions. *Science of The Total Environment*, 609:546–555, 2017.

[98] Jacek Pielecha, Jerzy Merkisz, Karolina Kurtyka, and Kinga Skobiej. Cold start emissions of passenger cars with gasoline and diesel engines in real driving emissions tests. *Combustion Engines*, 58, 2019.

[99] Martin Weiss, Elena Paffumi, Michaël Clairotte, Yannis Drossinos, Theodoros Vlachos, Pierre Bonnel, and Barouch Giechaskiel. Including cold-start emissions in the real-driving emissions (rde) test procedure. *Publications Office of the European Union*, 2017.

[100] Time stamp synchronization. `https://www.mathworks.com/help/matlab/ref/timeseries.synchronize.html`, May 2020.

[101] Robert M Bethea and R Russell Rhinehart. *Applied engineering statistics*, volume 121. CRC Press, 1991.

[102] Epa emission regulation. `https://www.epa.gov/emission-standards-reference-guide/all-epa-emission-standards`, May 2020.

[103] Junhua Li, Huazhen Chang, Lei Ma, Jiming Hao, and Ralph T Yang. Low-temperature selective catalytic reduction of nox with nh3 over metal oxide and zeolite catalysts—a review. *Catalysis today*, 175(1):147–156, 2011.

[104] Christoph M Schär, Christopher H Onder, Hans P Geering, and M Elsener. Control of a urea scr catalytic converter system for a mobile heavy duty diesel engine. *SAE transactions*, pages 1180–1188, 2003.

[105] Jianbing Gao, Guohong Tian, Aldo Sorniotti, Ahu Ece Karci, and Raffaele Di Palo. Review of thermal management of catalytic converters to decrease engine emissions during cold start and warm up. *Applied Thermal Engineering*, 147:177–187, 2019.

[106] Jing Sun and N Sivashankar. Issues in cold start emission control for automotive ic engines. In *Proceedings of the 1998 American Control Conference. ACC (IEEE Cat. No. 98CH36207)*, volume 3, pages 1372–1376. IEEE, 1998.

[107] Stefano Sabatini, Irfan Kil, Joseph Dekar, Travis Hamilton, Jeff Wuttke, Michael A Smith, Mark A Hoffman, and Simona Onori. A new semi-empirical temperature model for the three way catalytic converter. *IFAC-PapersOnLine*, 48(15):434–440, 2015.

[108] Humidity MOVES2010 Highway Vehicle Temperature. Air conditioning, and inspection and maintenance adjustments. *US Environmental*, 2010.

[109] Jinyoung Ko, Dongyoung Jin, Wonwook Jang, Cha-Lee Myung, Sangil Kwon, and Simsoo Park. Comparative investigation of nox emission characteristics from a euro 6-compliant diesel passenger car over the nedc and wltc at various ambient temperatures. *Applied energy*, 187:652–662, 2017.

[110] Steen Solvang Jensen. Driving patterns and emissions from different types of roads. *Science of the total environment*, 169(1-3):123–128, 1995.

Appendices

APPENDIX A

Summary of Test Results

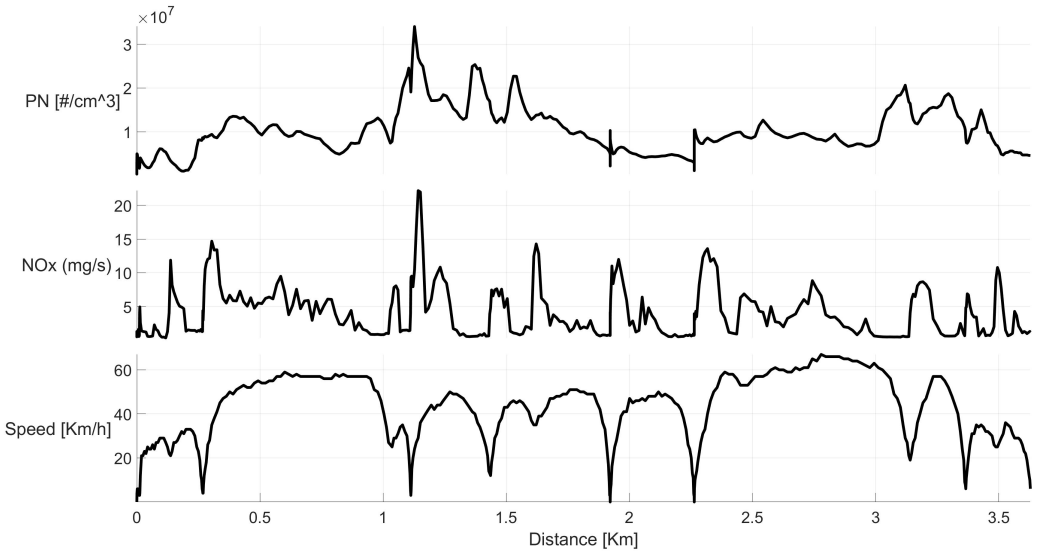

Figure 1: Ambient temperature test, temperature= -15 C, Route test A

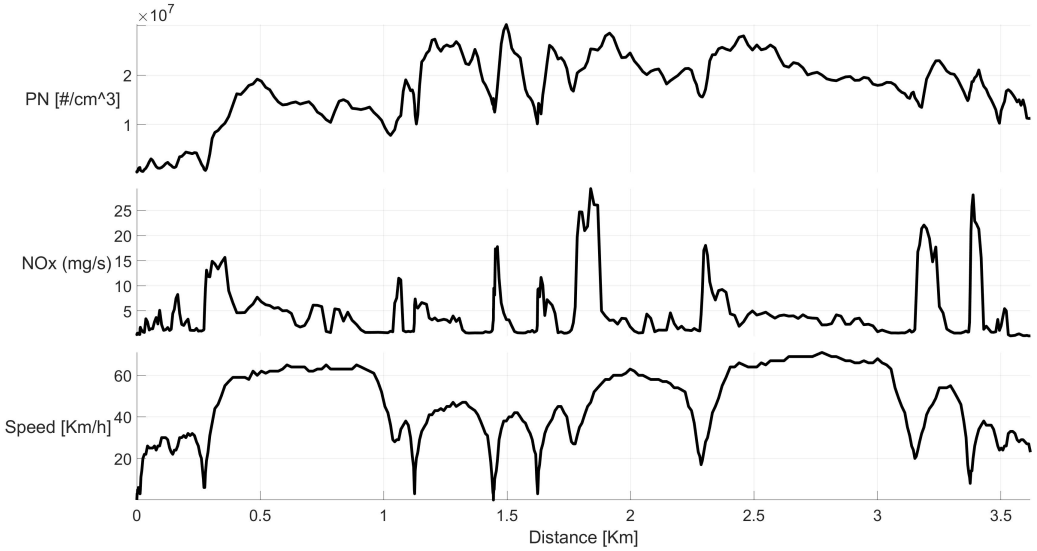

Figure 2: Ambient temperature test, temperature= -15 C, Route test A.

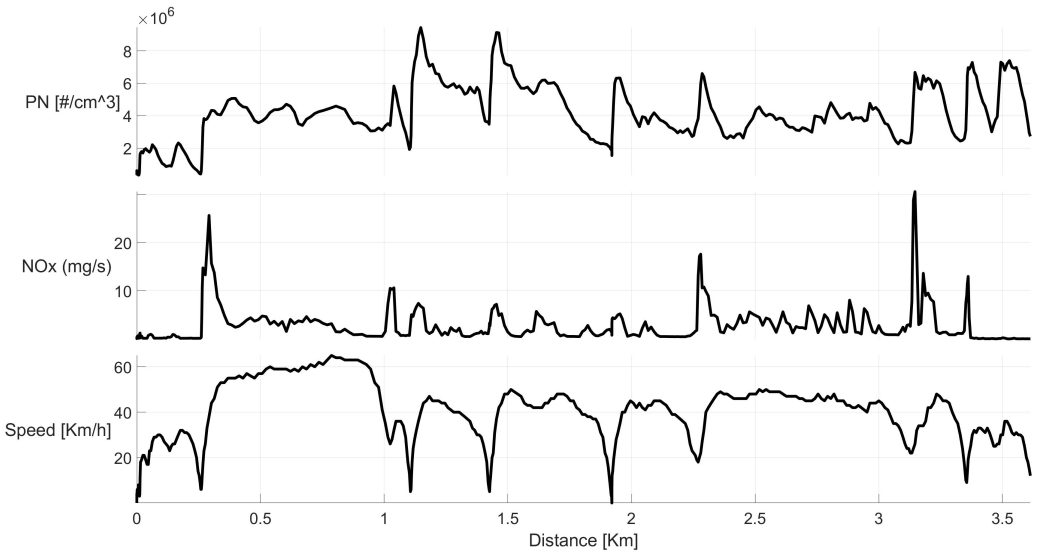

Figure 3: Ambient temperature test, temperature= -15 C, Route test A.

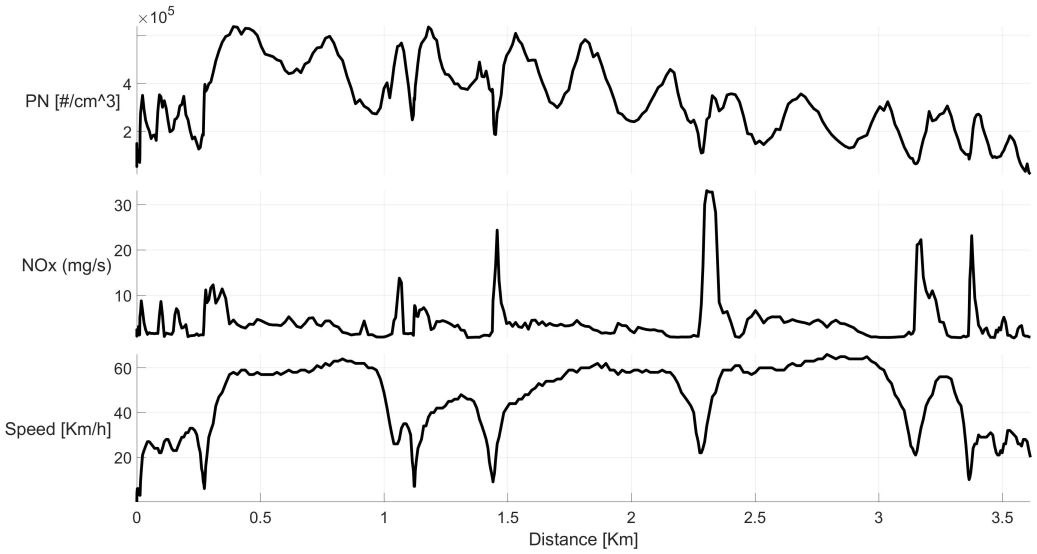

Figure 4: Ambient temperature test, temperature= -15 C, Route test A

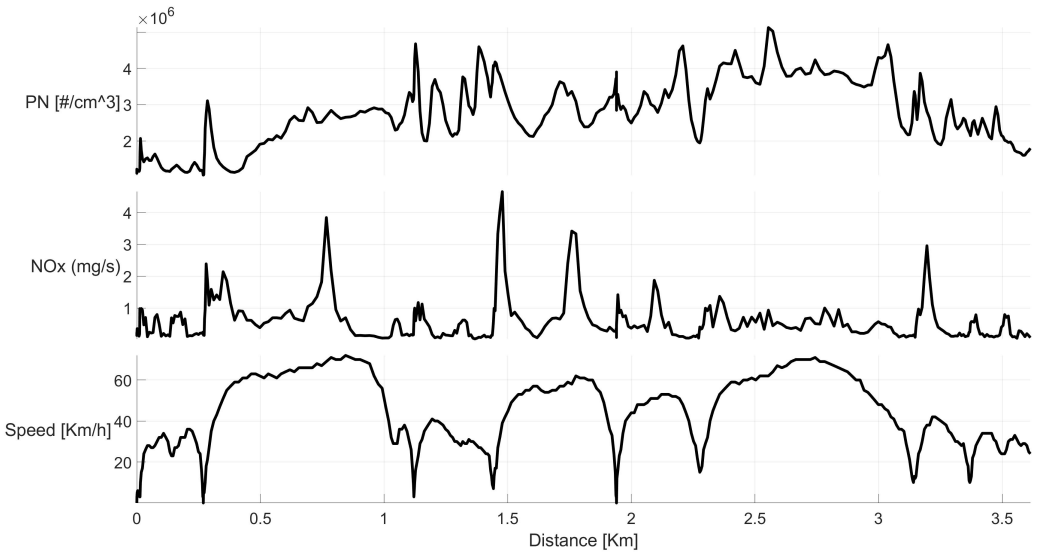

Figure 5: Ambient temperature test, temperature= +5 C, Route test A.

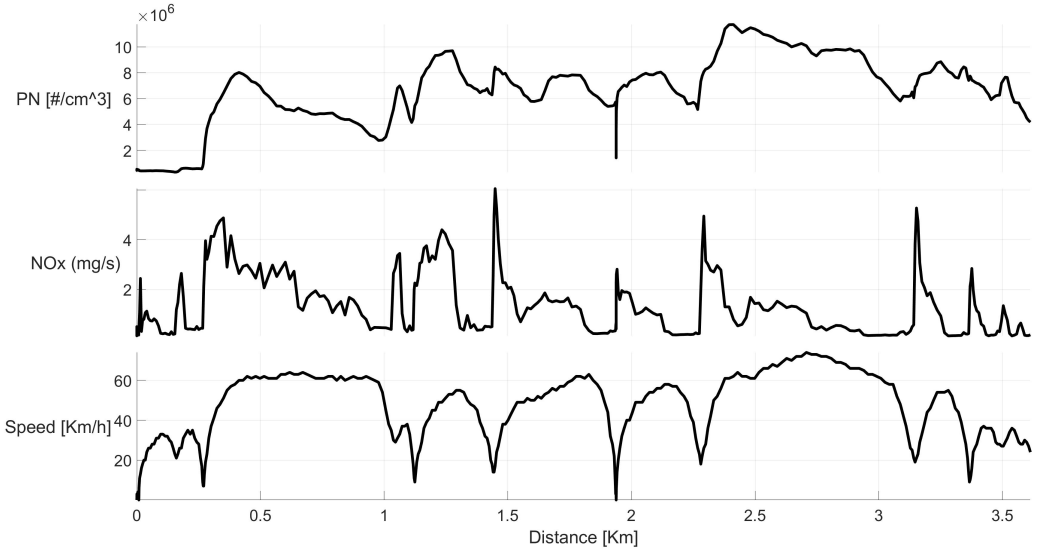

Figure 6: Ambient temperature test, temperature= +5 C, Route test A.

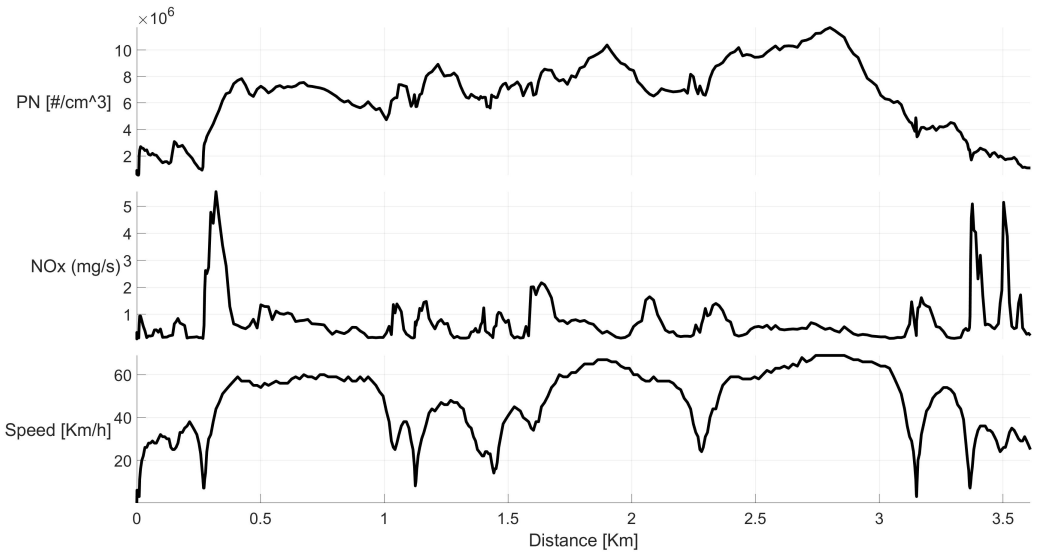

Figure 7: Ambient temperature test, temperature= +5 C, Route test A.

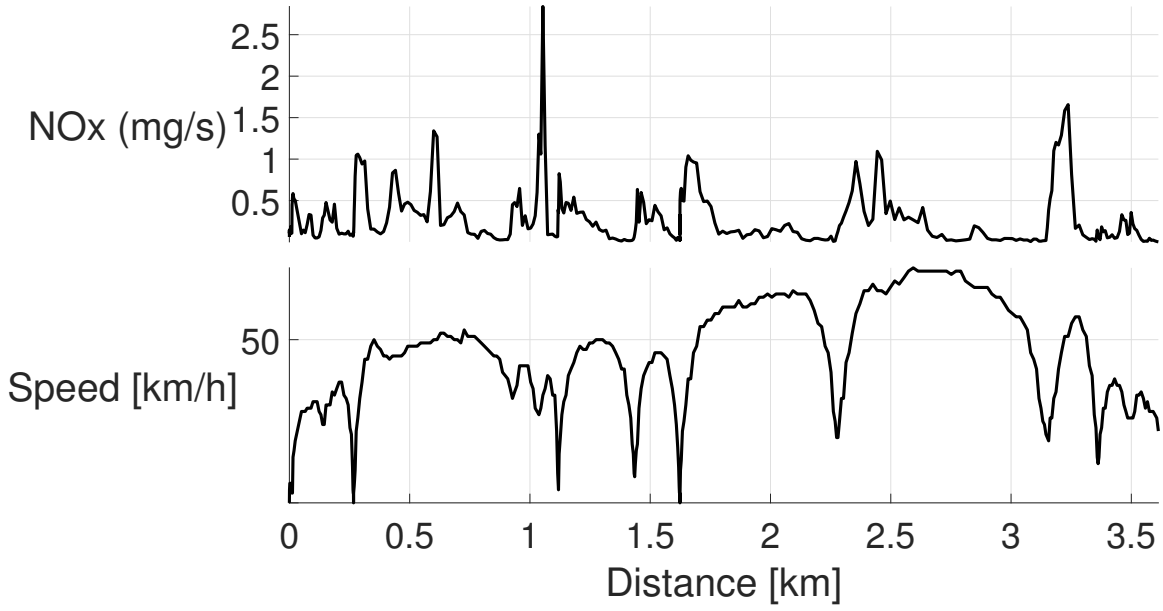

Figure 8: Ambient temperature test, temperature= +5 C, Route test A.

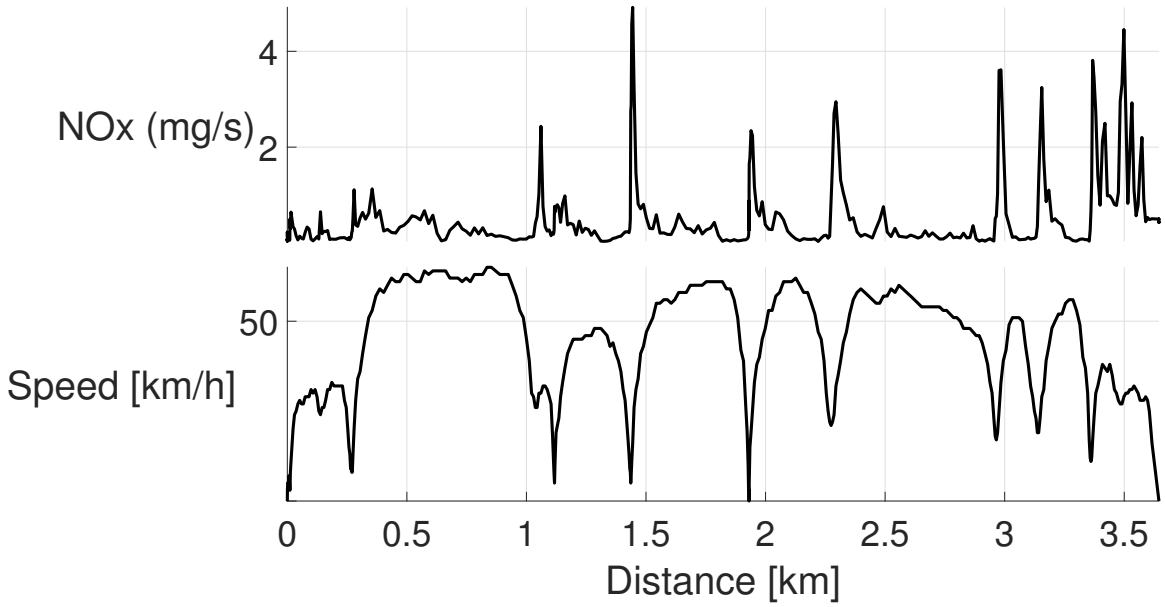

Figure 9: Ambient temperature test, temperature= +5 C, Route test A.

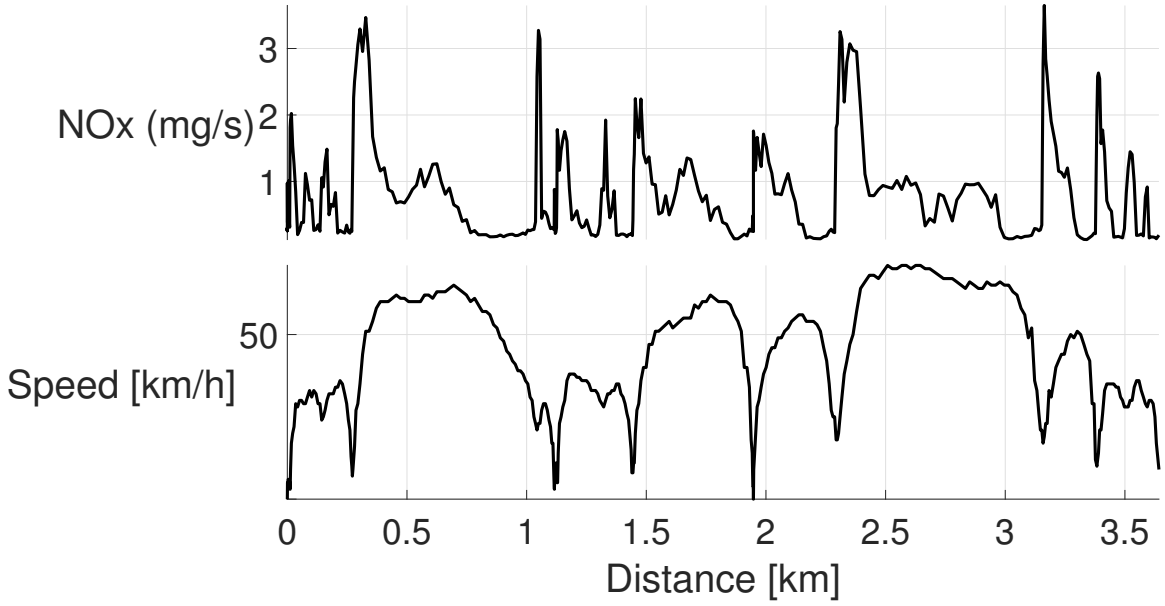

Figure 10: Ambient temperature test, temperature= +5 C, Route test A.

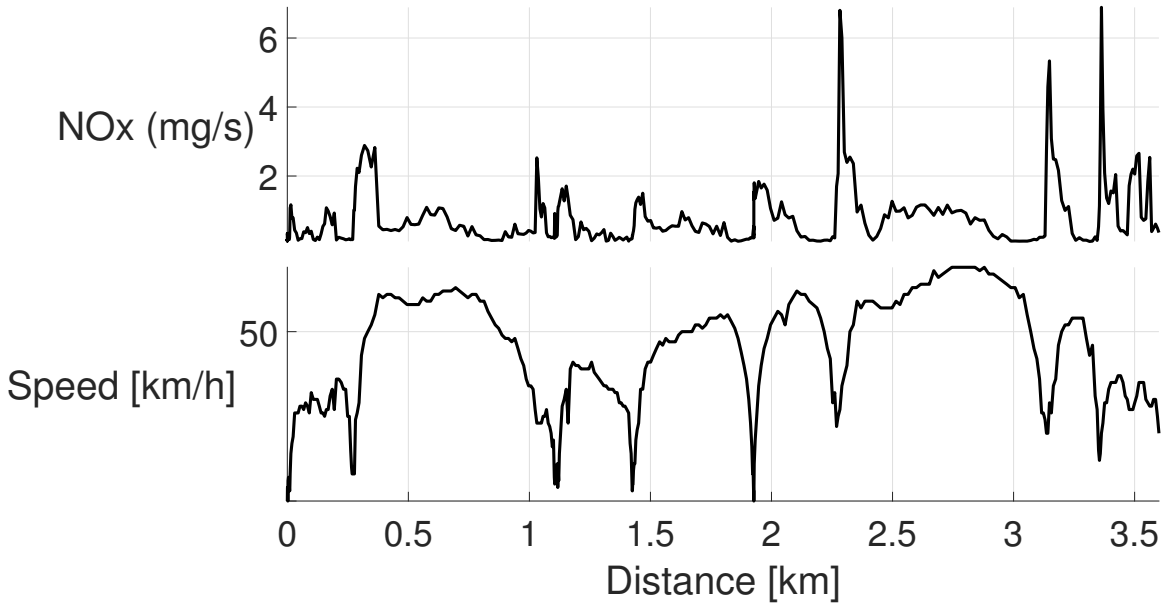

Figure 11: HAmbient temperature test, temperature= +5 C, Route test A, NOx emission factor= 78.27 (mg/km)

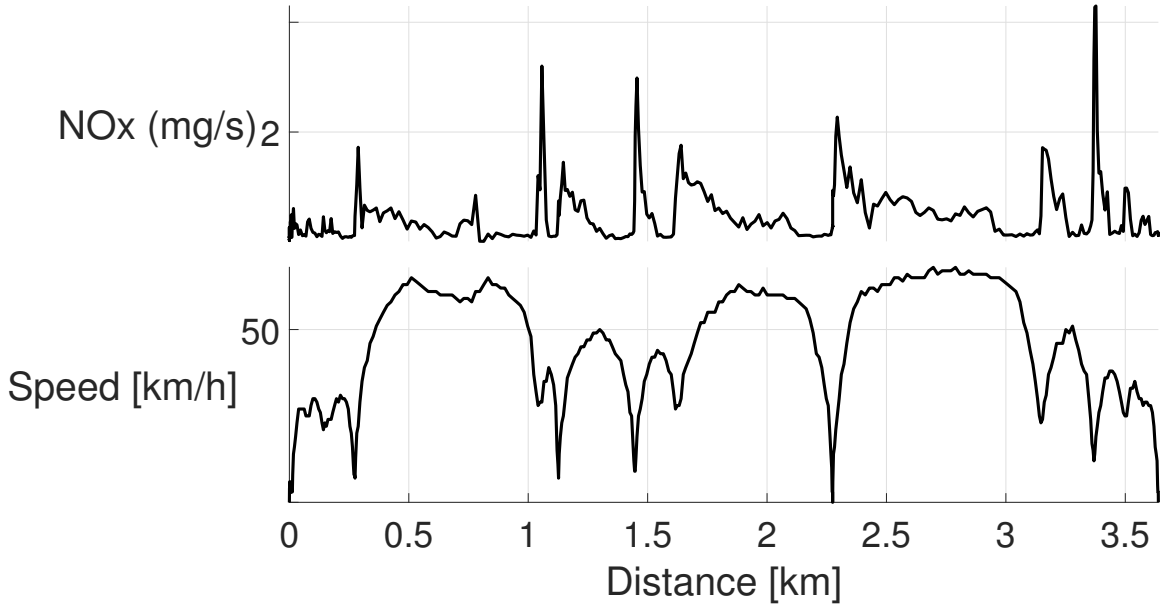

Figure 12: Ambient temperature test, temperature= +5 C, Route test A.

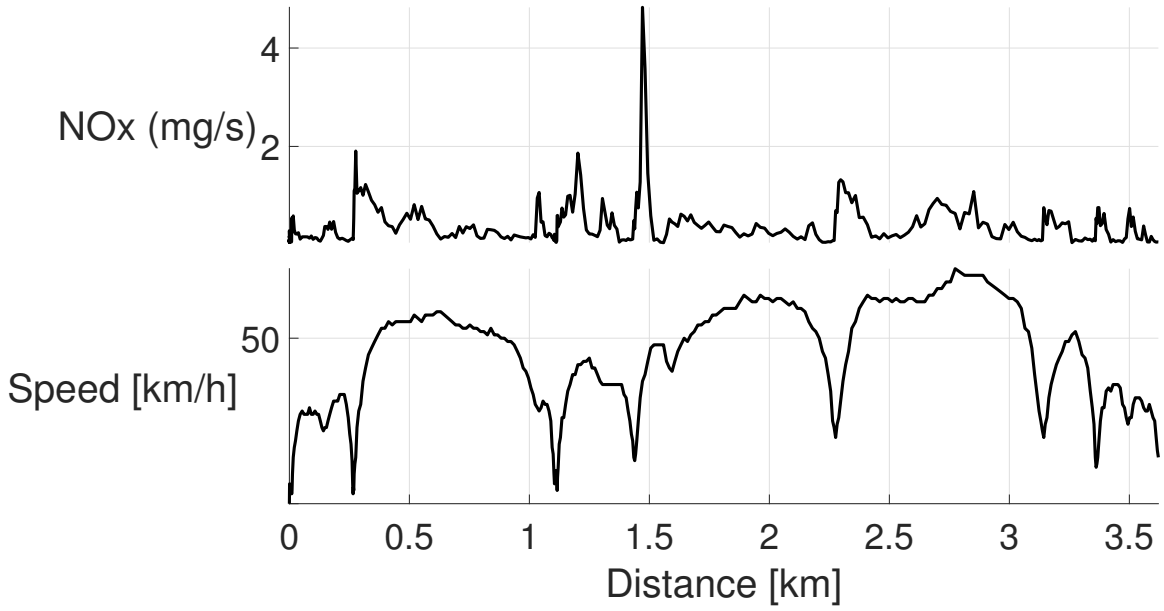

Figure 13: Ambient temperature test, temperature= +5 C, Route test A.

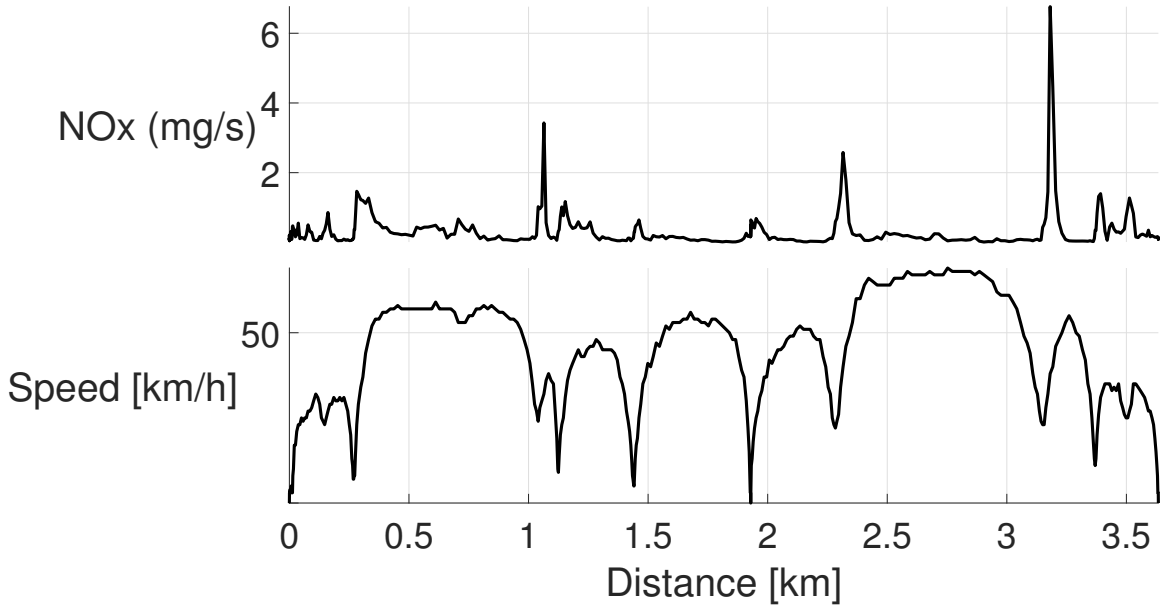

Figure 14: Ambient temperature test, temperature= +5 C, Route test A

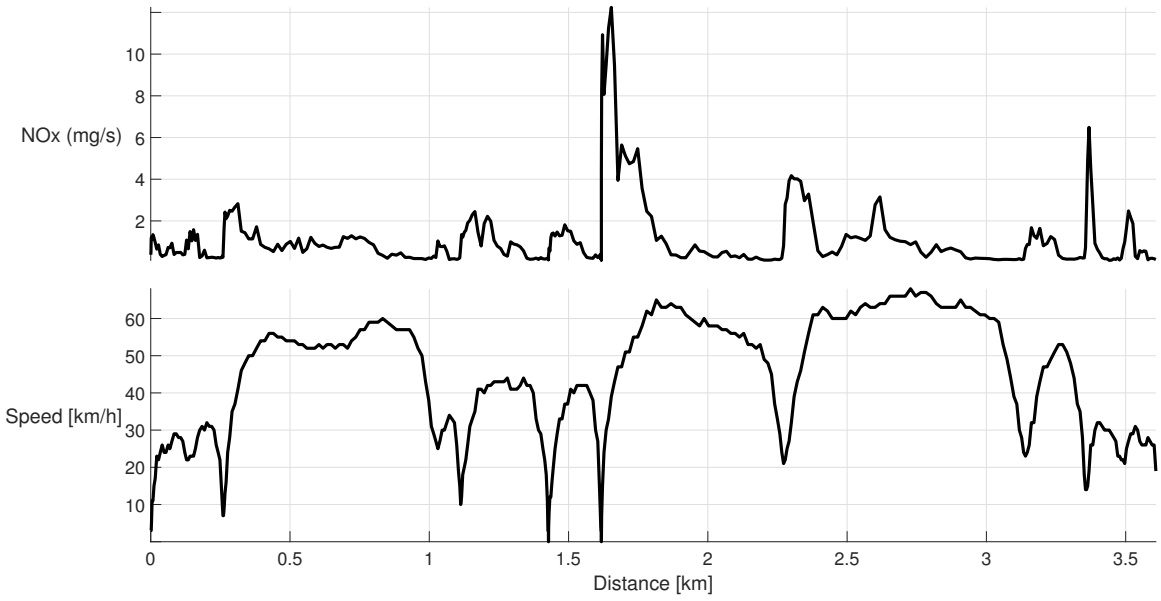

Figure 15: Ambient temperature test, temperature= +5 C, Route test A.

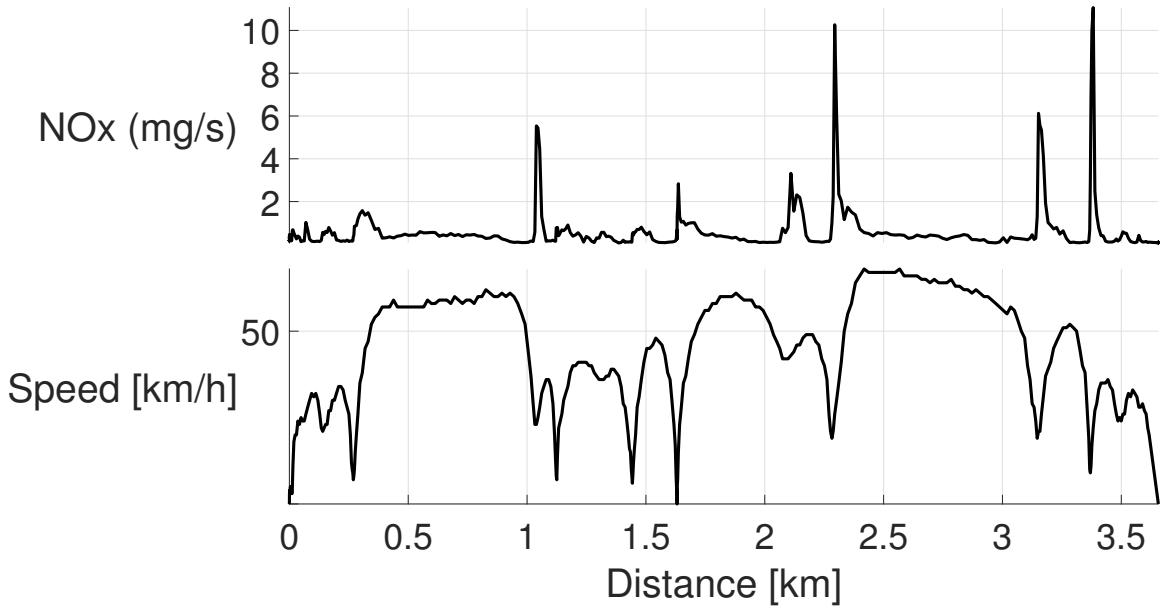

Figure 16: Ambient temperature test, temperature= +5 C, Route test A.

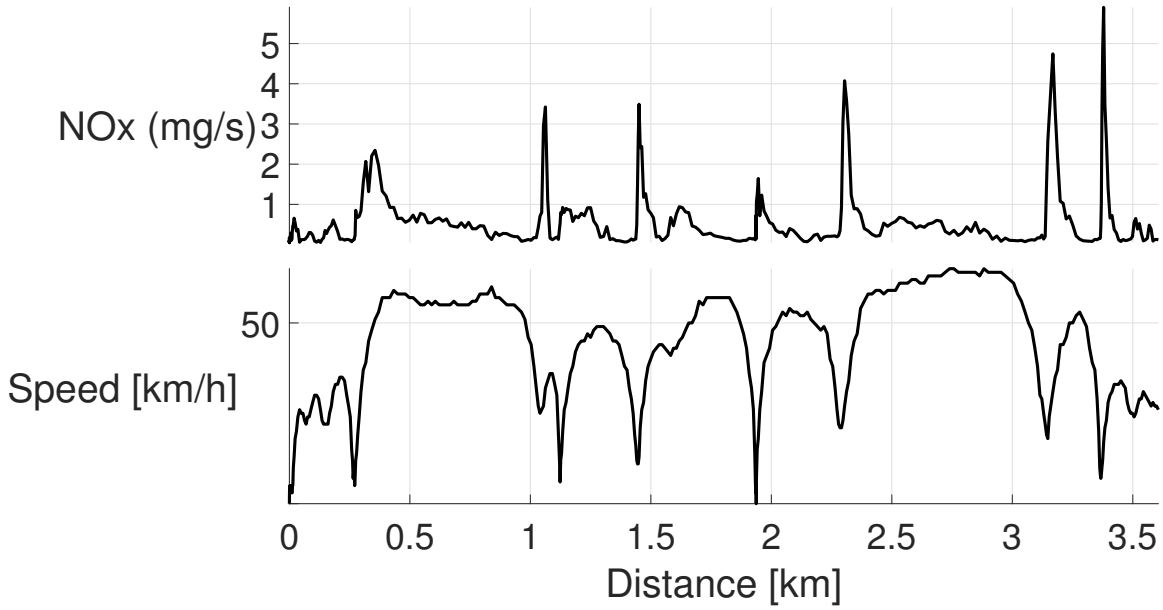

Figure 17: Ambient temperature test, temperature= +5 C, Route test A.

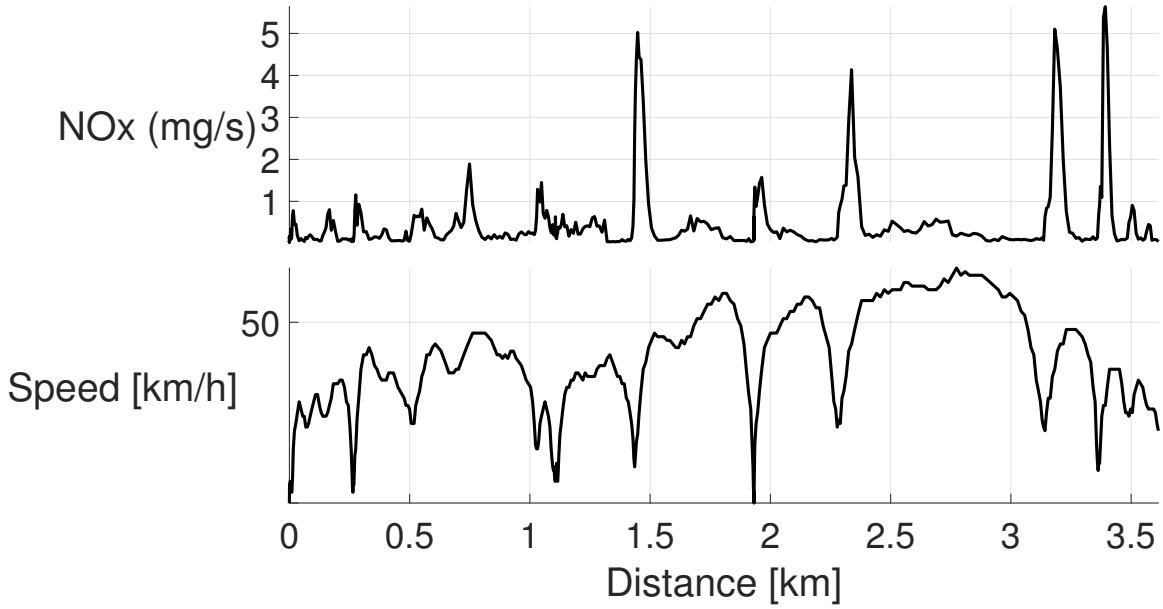

Figure 18: Ambient temperature test, temperature= +5 C, Route test A.

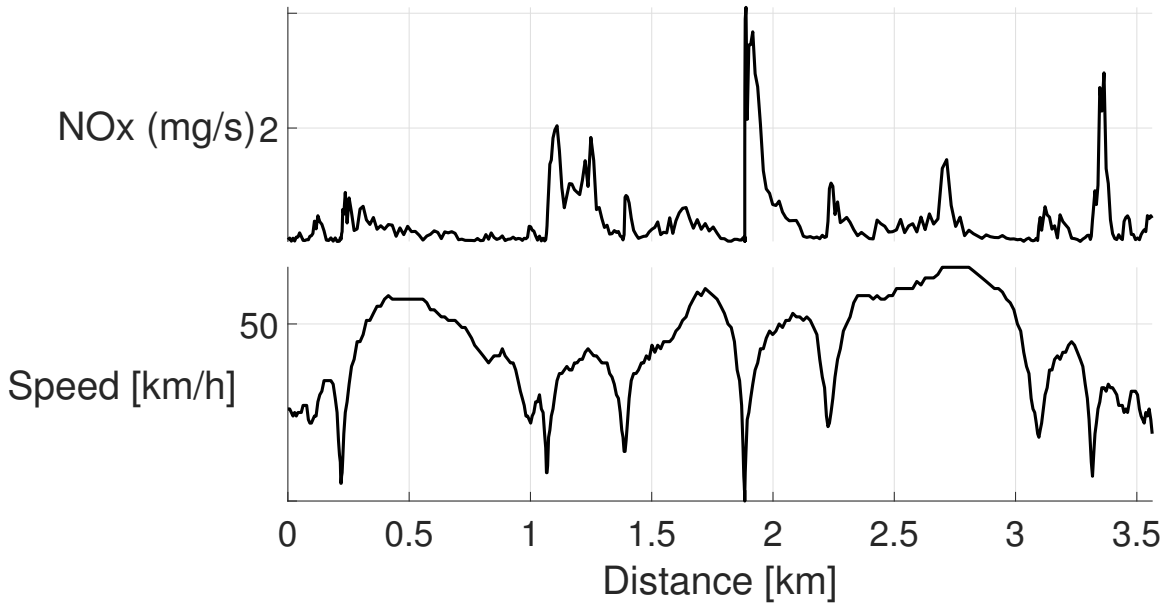

Figure 19: Ambient temperature test, temperature= +5 C, Route test A.

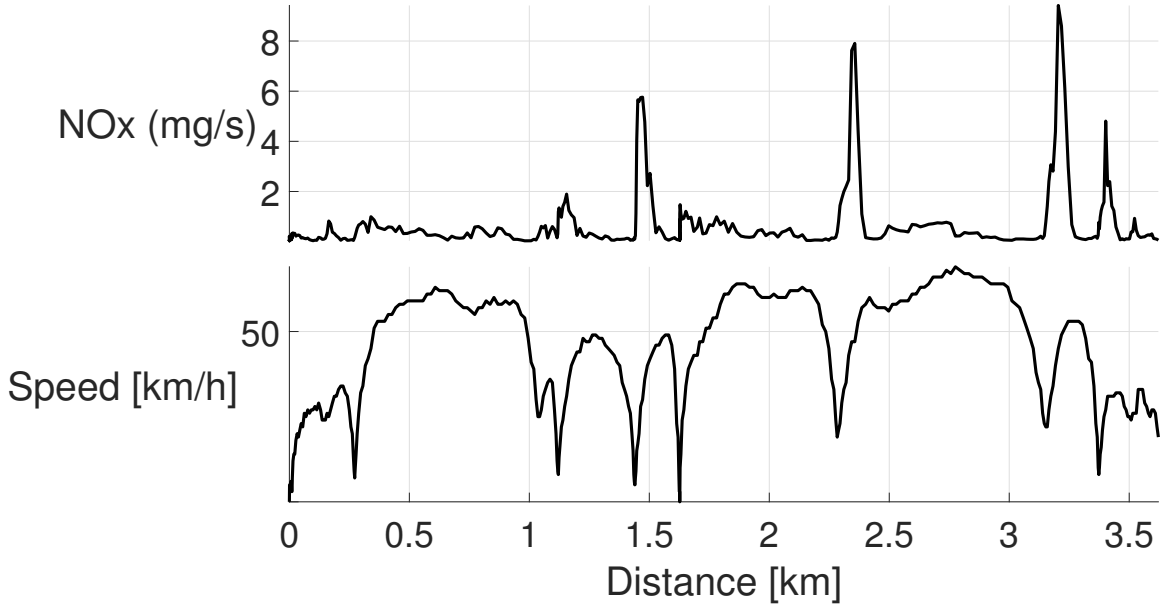

Figure 20: Ambient temperature test, temperature= +5 C, Route test A.

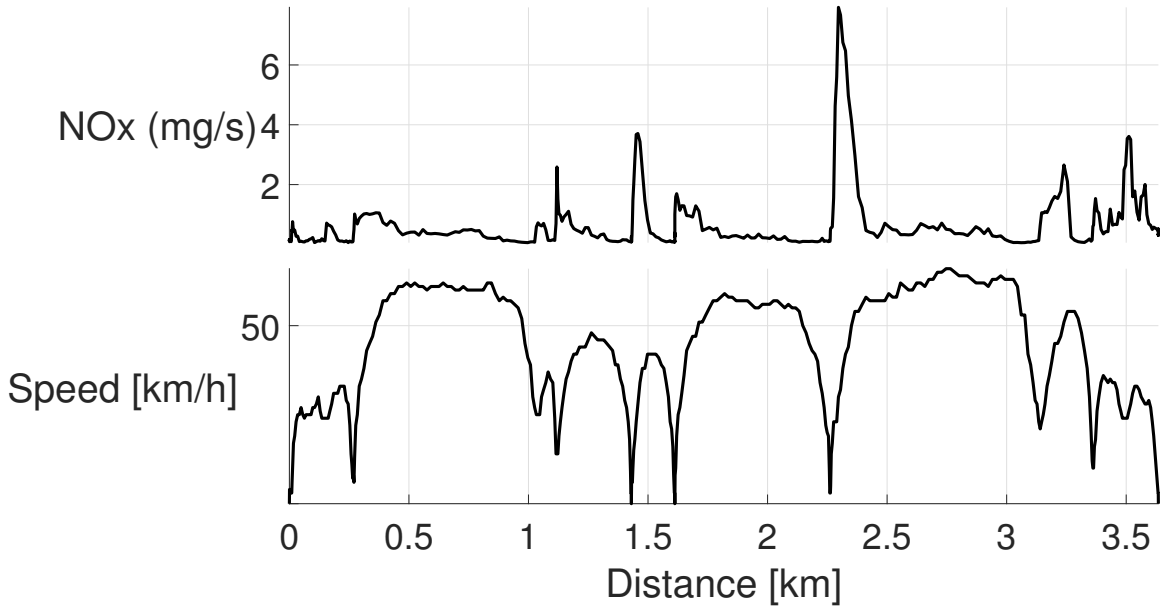

Figure 21: Ambient temperature test, temperature= +5 C, Route test A.

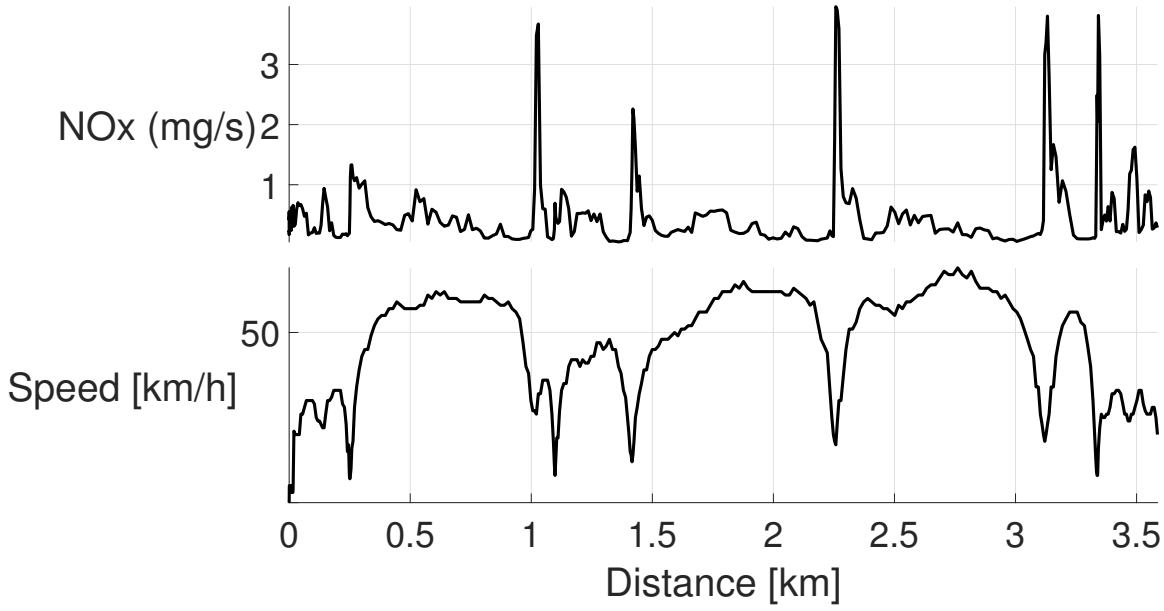

Figure 22: Ambient temperature test, temperature= +5 C, Route test A.

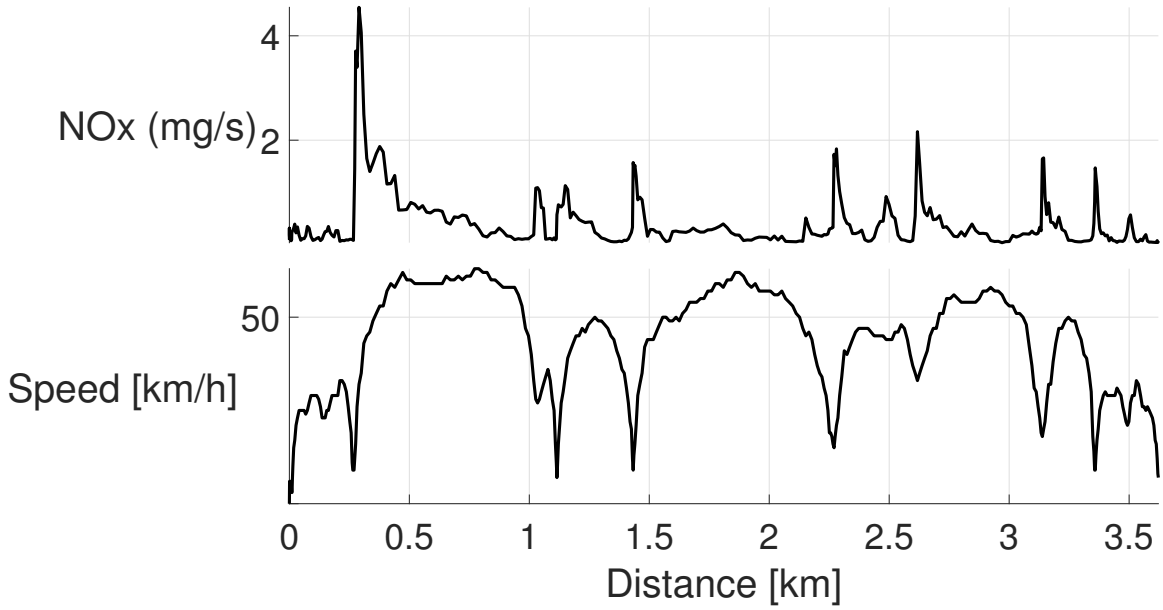

Figure 23: Ambient temperature test, temperature= +5 C, Route test A.

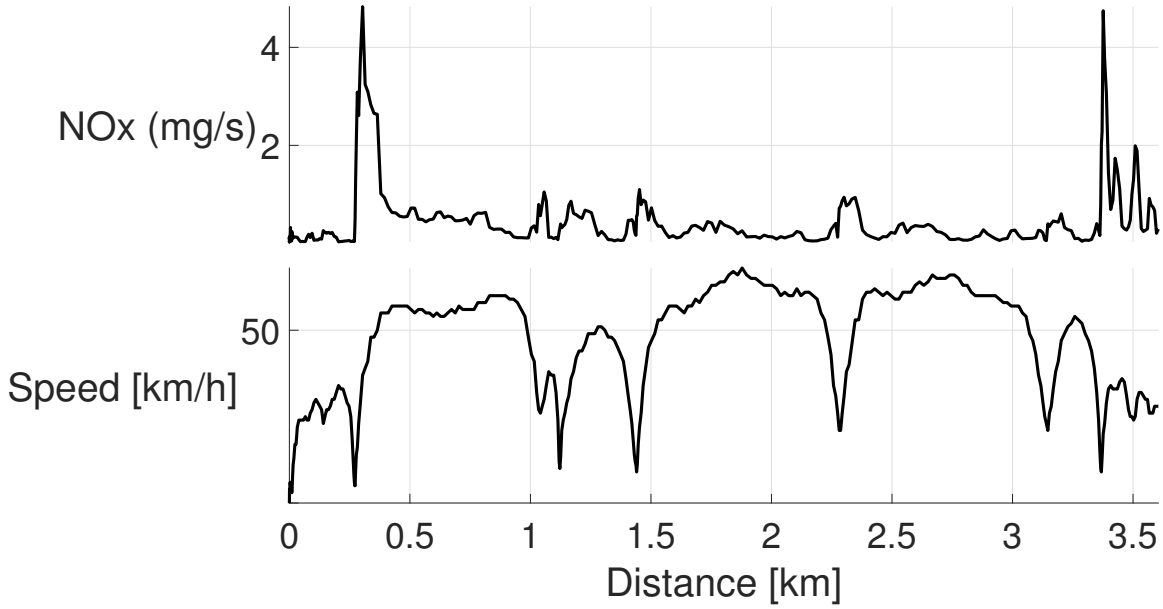

Figure 24: Ambient temperature test, temperature= +5 C, Route test A.

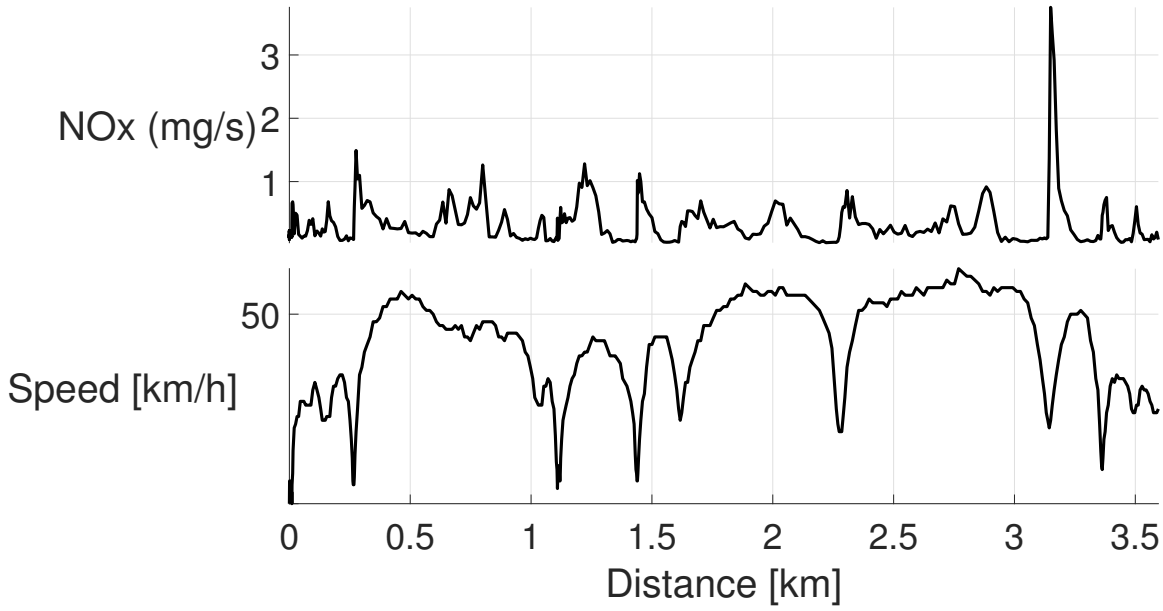

Figure 25: Ambient temperature test, temperature= +5 C, Route test A.

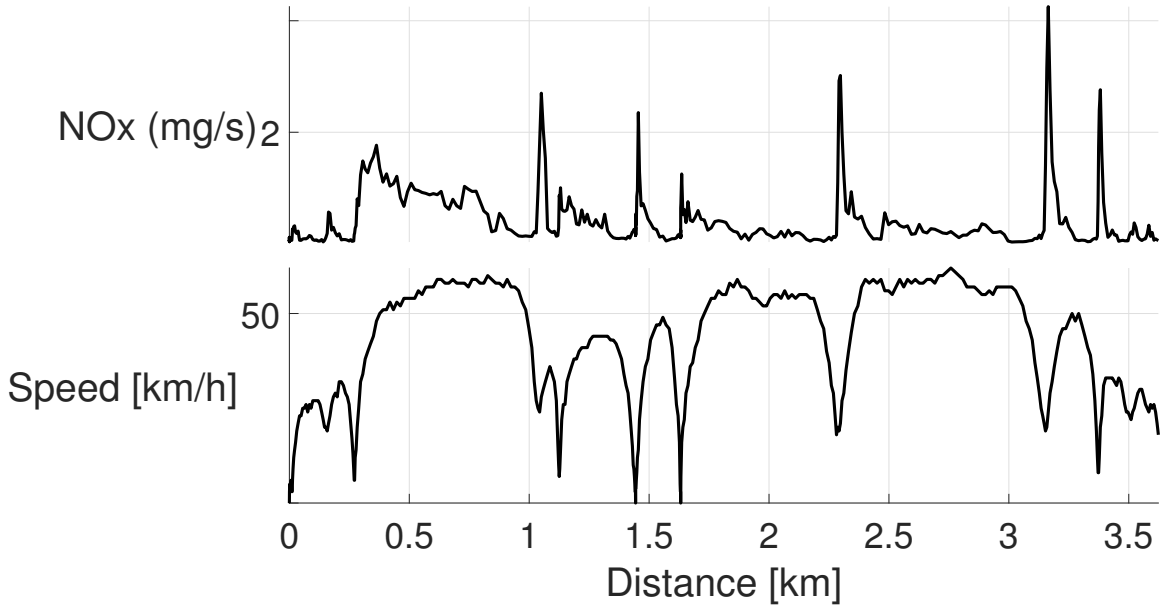

Figure 26: Ambient temperature test, temperature= +5 C, Route test A.

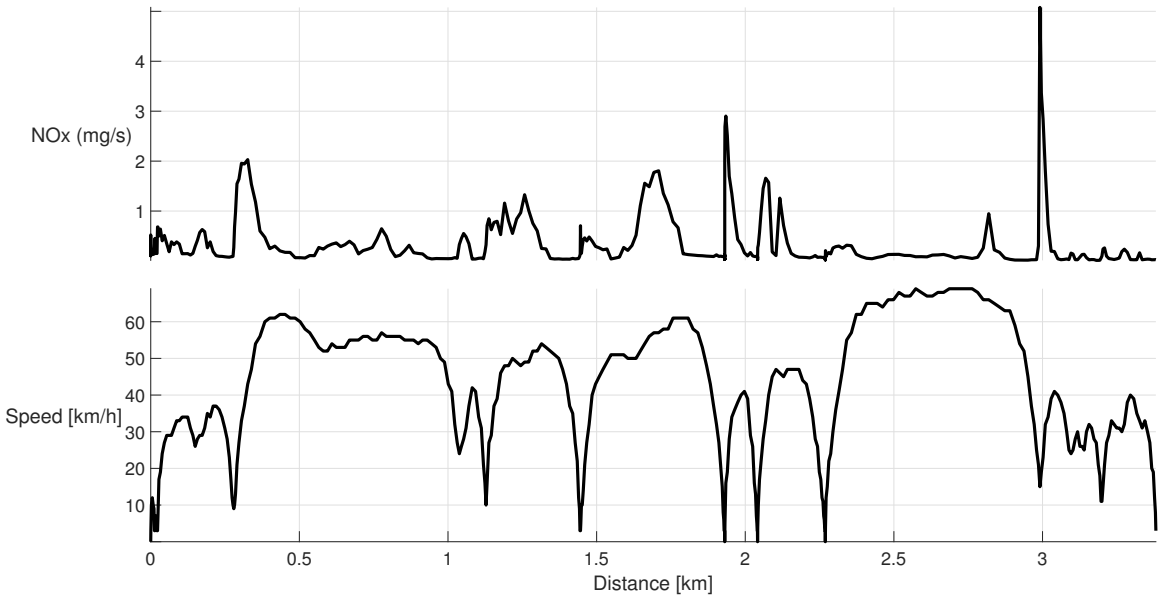

Figure 27: Ambient temperature test, temperature= +15 C, Route test A.

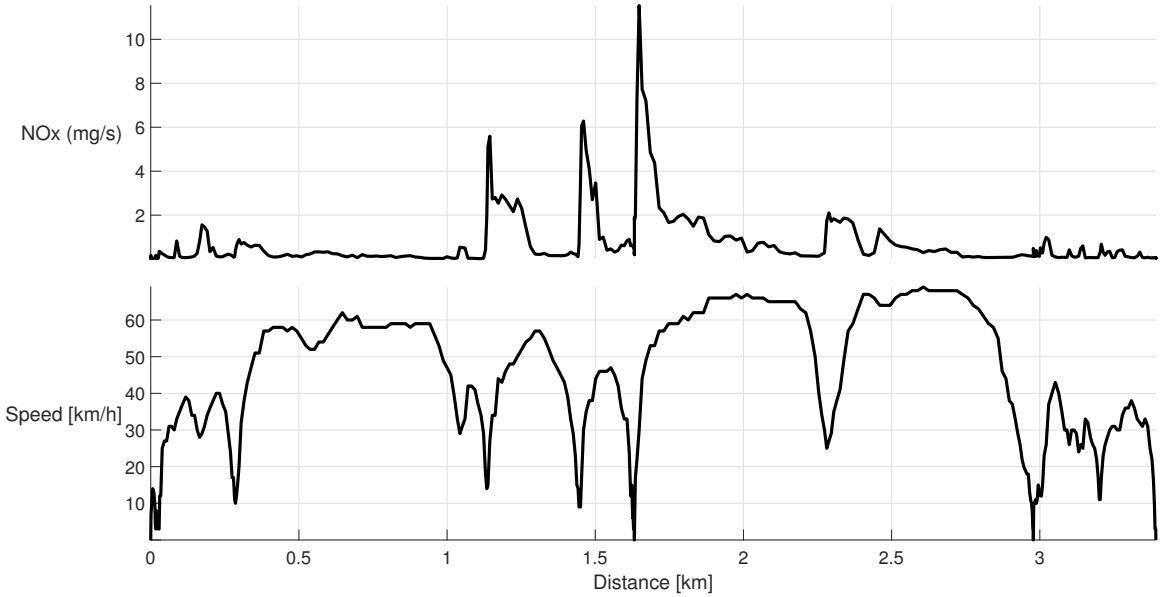

Figure 28: Ambient temperature test, temperature= +15 C, Route test A.

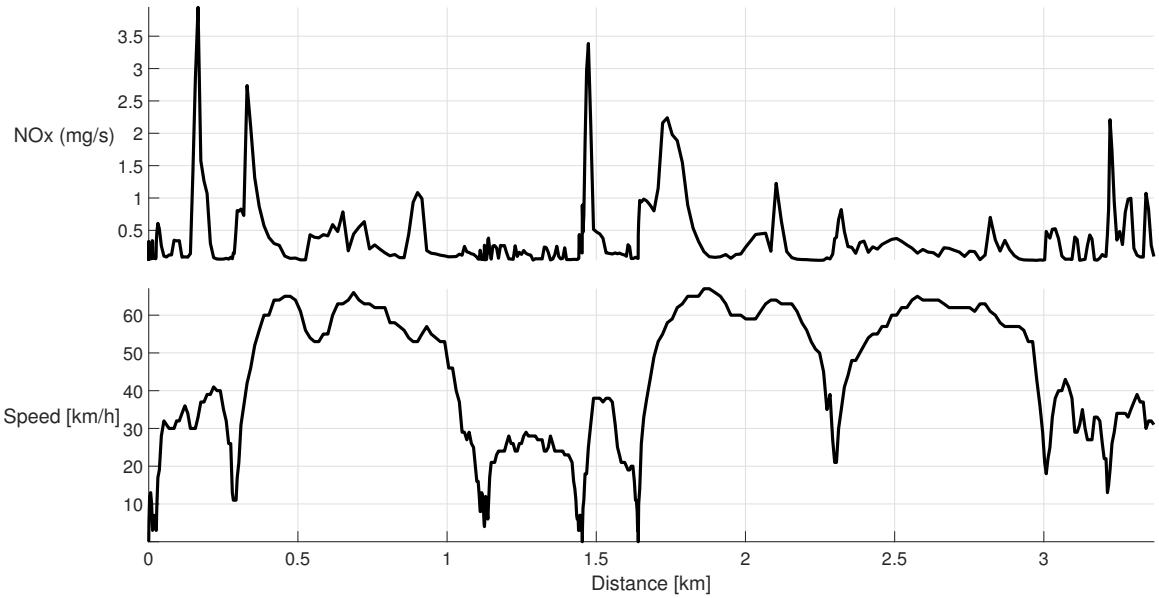

Figure 29: Ambient temperature test, temperature= +15 C, Route test A.

APPENDIX B

Code Summary

Pythone code for serial communication:

import serial

import io

import serial

ser = serial.Serial('/dev/ttyUSB0') # open serial port

print(ser.name) # check which port was really used

ser.write(b'hello') # write a string

ser.close() # close port

yourport = serial.Serial('COM7',115200) #xonxoff, #rtscts) #initiate/open por

yourport.flushInput() #this tells the serial port to clear the queue so that data doesn't overlap.

while True:

try:

print('k')

writer = csv.writer(f,delimiter=",")

Pythone code for converting .nmea file to .csv:

import pynmea2

msg = pynmea2.parse("GPGGA,184353.07,1929.045,S,02410.506,E,1,04,2.6,100.00,M,-33.9,M,,0000*6D")

print(msg)

path = 'C:'

files = ['191101SB002', '191101SB003','191101NB']

n = 0

```
for line in inputf:
n += 1
try:
msg = pynmea2.parse(line.strip())
if msg.data[1] == 'A':
outputf.write(str(msg.data[0]) + ,")
except Exception as e:
print(e,line)
pass
```

Matlab code for importing data:

```
opts = delimitedTextImportOptions("NumVariables", 16);
opts.DataLines = [8, Inf];
opts.Delimiter = ",";
opts.VariableNames = ["VarName1",..."];
opts.VariableTypes = ["double",...];
opts = setvaropts(opts, [1, 2, 4, 13, 14, 15], "TrimNonNumeric", true);
opts = setvaropts(opts, [1, 2, 4, 13, 14, 15], "ThousandsSeparator", ",");
opts.ExtraColumnsRule = "ignore";
opts.EmptyLineRule = "read";
opts.ImportErrorRule = "omitvar";
opts.MissingRule = "omitvar";
for i = [1 3 4]
nox = readtable(['C:test', num2str(i), '.csv'], opts);
end
```